

- D8.3 – Periodic Technical Report PART B M18

- VERSION -

VERSION	DATE
2	12/05/2022

- PROJECT INFORMATION -

GRANT AGREEMENT NUMBER	955930
PROJECT FULL TITLE	INNOVATIVE PHYSICAL/VIRTUAL SENSOR PLATFORM FOR BATTERY CELL
PROJECT ACRONYM	INSTABAT
START DATE OF THE PROJECT	01/09/2020
DURATION	3 years
CALL TOPIC	H2020-LC-BAT-13-2020
PROJECT WEBSITE	www.instabat.eu

- DELIVERABLE INFORMATION -

WP NO.	8
WP LEADER	CEA
CONTRIBUTING PARTNERS	CEA, BMW, CNRS, FAURECIA, IFAG, INSA Lyon, UAVR, VMI
NATURE	Periodic REPORT
PERIODIC REPORT	1 st
PERIOD COVER BY THE REPPORT	01/09/2020 – 30/04/2022
AUTHORS	Olivier RACCURT
CONTRIBUTORS	S. Genies, E. Villemin, C. Septet, O. Poncelet, S. Desousa-Nobre, V. Heiries, R. Franchi, A. Martin, D. Buzon, M. Priour, C. Gervillie, J.M. Tarascon, M. Nascimento, J. Pinto, J. Li, M. Schmuck, T. Roessler, Talal Khan Ali Zai, P. Karayaylali, B. Antunes, F. Bribiesca-Argomedo
CONTRACTUAL DEADLINE	30/04/2022
DELIVERY DATE TO EC	12/05/2022
DISSEMINATION LEVEL (PU/CO)	PU

- ACKNOWLEDGMENT -



This project has received funding from the European Union's Horizon 2020 research and innovation program under grant agreement No 955930.



CEA Deliverable reference	DEHT/LV/2022-038_ D8.3 – Periodic Technical Report PART B M18
---------------------------	---

Deliverable Review

Reviewer #1: F. Bribiesca-Argomedo		
Answer	Comments	Type*

1. Is the deliverable in accordance with		
1.1. The Description of actions?	<input checked="" type="checkbox"/> Yes <input type="checkbox"/> No	<input type="checkbox"/> M <input type="checkbox"/> m <input type="checkbox"/> a
2. Is the quality of the deliverable in a status		
2.1. That allows it to be sent to European Commission?	<input checked="" type="checkbox"/> Yes <input type="checkbox"/> No	<input type="checkbox"/> M <input type="checkbox"/> m <input type="checkbox"/> a
2.2. That needs improvement of the writing by the originator of the deliverable?	<input type="checkbox"/> Yes <input checked="" type="checkbox"/> No	<input type="checkbox"/> M <input type="checkbox"/> m <input type="checkbox"/> a
2.3. That needs further work by the Partners responsible for the deliverable?	<input type="checkbox"/> Yes <input checked="" type="checkbox"/> No	<input type="checkbox"/> M <input type="checkbox"/> m <input type="checkbox"/> a

Reviewer #2: M. Reytier		
Answer	Comments	Type*

3. Is the deliverable in accordance with		
3.1. The Description of actions?	<input checked="" type="checkbox"/> Yes <input type="checkbox"/> No	<input type="checkbox"/> M <input type="checkbox"/> m <input type="checkbox"/> a
4. Is the quality of the deliverable in a status		
4.1. That allows it to be sent to European Commission?	<input checked="" type="checkbox"/> Yes <input type="checkbox"/> No	<input type="checkbox"/> M <input type="checkbox"/> m <input type="checkbox"/> a
4.2. That needs improvement of the writing by the originator of the deliverable?	<input type="checkbox"/> Yes <input checked="" type="checkbox"/> No	<input type="checkbox"/> M <input type="checkbox"/> m <input type="checkbox"/> a
4.3. That needs further work by the Partners responsible for the deliverable?	<input type="checkbox"/> Yes <input checked="" type="checkbox"/> No	<input type="checkbox"/> M <input type="checkbox"/> m <input type="checkbox"/> a

* Type of comments: M = Major comment; m = minor comment; a = advice

- ABSTRACT/SHORT SUMMARY -

Summary for publication

Summary of the context and overall objectives of the project

The increased use of batteries requires their improvement in terms of safety as well as quality, reliability and life (QRL). The EU-funded INSTABAT project aims to observe in operando essential parameters of a Li-ion battery cell to provide higher accuracy states of charge, health, power, energy and safety (SoX) cell indicators. This will improve the batteries' safety and Quality, Reliability and Life (QRL). The project will develop a solution of smart sensing technologies and functionalities integrated into a battery cell. This solution will be able to perform reliable monitoring of key parameters, correlate the evolution of these parameters to the physicochemical degradation phenomena taking place at the battery cell's core and improve the battery's functional performance and safety. This ambition is aligned to the Battery 2030+ roadmap¹.

To achieve this goal, INSTABAT will develop a proof of concept of smart sensing technologies and functionalities, integrated into a battery cell and capable of:

- performing reliable in operando monitoring (time- and space-resolved) of key parameters (temperature and heat flow; pressure; strain; Li+ concentration and distribution; CO₂ concentration; “absolute” impedance, potential and polarisation) by means of:
 - (i) four embedded physical sensors (optical fibres with Fiber Bragg Grating and luminescence probes, reference electrode and photo-acoustic gas sensor),
 - (ii) two virtual sensors (based on reduced electro-chemical and thermal models),
- correlating the evolution of these parameters with the physico-chemical degradation phenomena occurring at the heart of the battery cell,
- improving the battery functional performance and safety, thanks to enhanced BMS algorithms providing in real-time higher accuracy SoX cell indicators (taking the measured and estimated parameters into consideration).

The main results will be: (1) a proof of concept of a multi-sensor platform (cell prototype equipped with physical/virtual sensors, and associated BMS algorithms providing SoX cell indicators in real time); (2) demonstration of higher accuracy for SoX cell indicators; (3) demonstration of improvement of cell functional performance and safety through two use cases for EV applications; (4) techno-economic feasibility study (manufacturability, adaptability to other cell technologies...).

INSTABAT smart cells will open new horizons to improve cell use and performances (e.g. by reducing ageing, allowing the decrease of safety margins, triggering self-healing, facilitating second life, etc.).

Work performed from the beginning of the project & main results

During the first period of the project several of objectives were achieved. Physical sensors development has progressed according to the initial workplan. The definition of requirements for smart batteries and for integration of the sensors into the cell was completed (WP1) and compiled in deliverable D1.1. and D1.2.

The development of four of the 5 physical sensors was achieved in the WP2: two optical fiber sensors for temperature and one optical fiber sensor for pressure measurement, photoacoustic sensor for CO₂ measurement and embedded reference electrode. A Li ion luminescent probe was developed and validated on the electrolyte and open the way for the development of the Li ion sensor. The compatibility of these sensors with the cell environment was validated and the insertion of fiber-optic sensors and reference electrode sensors was successful as were the tests in cycling conditions. We have demonstrated the capability of these sensors to measure the desired physical parameters inside the cell. The evaluation of accuracy, resolution, sensitivity, response time, frequency/speed of acquisition has been done for these sensors and a proof of concept of *in-operando* measurement in cycling condition was achieved during this first period. Currently, only the FBG sensor, the OF-lumT sensor and the reference electrode are at a sufficient stage of development to adapt to the battery environment and be integrated without affecting electrochemical performance. However, the optical sensor and reference electrode already provide valuable information for the understanding of chemical degradation phenomena.

1 <https://battery2030.eu/research/roadmap/>

Development of the Electrochemical virtual sensor has advanced as planned (D4.1) and initial validation against COMSOL model by CEA (D4.2) is underway with very positive preliminary results. The next phase will consist of adapting the model to the experimental data for the cell used in the project and develop some indicators necessary for the BMS operation. Electrochemical virtual sensors are fully parametrizable for varying resolution. Accuracy characterisation underway, good preliminary results. Development of reduced electrochemical model and E-BASE algorithm considering computation time restrictions and modularity in the resolution for the real-time implementation, as well as C code generation and compilation for integration into the real-time platform. First (preliminary) comparisons underway for SoC in simple scenarios for single temperature point and adequate initialization using the electrochemical model (E-BASE) seem to be within the 0.5% of the reference model (CEA 1D+1D electrode model).

A first version of the multi-physics instrumentation platform was developed in WP5 to exploit the sensors signal in real time. A first demonstration of the INSTABAT lab-on-cell concept was achieved with an instrumented cell with RE and Optical fiber Luminescence Temperature sensors in cycling condition at high loading (up to 3C and 4D). Within BIGMAP², an experimental portfolio of complementary techniques is developed towards the implementation of a multimodal and multiscale characterisation platform. *In-operando* synchrotron experiments were realised and analysed according to BIGMAP standards and protocols on INSTABAT pouch cells instrumented with different types of sensors. The spatially resolved real-time structural data obtained by X-rays diffraction (phase transitions, strain, local lithiation mechanism) will be cross-correlated to the various sensing data (temperature, local electrode potential), allowing monitoring the potential perturbations of reaction mechanisms due to sensor integration and to correlate micro-to-macro scale performance related to parameter variations along cycling. During this experiment we have validated the following steps:

- The instrumentation of cells with 2 sensors (OF LUM-T and RE).
- The cell performance was not modified by the integration of the sensors.
- The setup for, data acquisition and real-time treatment is functional with these 2 sensors
- The measurement of the internal cell parameters with sensors (Temperature, Electrochemistry).
- The local impact of sensors on the cell functioning can be characterised with operando XRD measurements.

Progress beyond the state of the art, expected results and potential impact

New non-invasive integrated sensors based on optical fiber, reference electrode and photo-acoustic technologies will be improved/developed and will allow to know in real time the evolution of internal battery key parameters. Virtual sensors, based on improved electro-chemical and thermal reduced models, will bring complementary data allowing a more comprehensive monitoring of the cell. BMS algorithms connecting the outputs of the physical/virtual sensors to battery physics-based models will also be developed to enable an optimised management of battery cells. The consortium also intends to correlate the evolution of physical parameters to cell physico-chemical degradation mechanisms to develop advanced responsive BMS that can significantly optimise the cell performance, lifetime and safety margins associated with cell usage. These correlations will also bring a much better knowledge of the cell in operando internal state, opening opportunities for innovation.

In addition, INSTABAT will innovate by assessing the: (1) number of sensors / measurement points needed and their best positioning to provide measurements with the highest possible quality; (2) impact of the measurements provided by the physical sensors on the accuracy of the virtual sensors; (3) benefits of each physical sensor and measured parameter on the accuracy of the SoX indicators to suggest the best trade-off between the number of physical measures and model accuracy. The gain in accuracy will also be related to the sensors cost, their potential disturbance of the cell functioning and to the manufacturing difficulties.

INSTABAT will contribute to an improvement of performance and strongly force the development of sustainable battery storage solutions for Li-ion batteries at a more competitive price. The “lab-on-a-cell” approach will be used to develop a new generation of Li-ion and post-Li-ion batteries in the future, which is aligned with the objectives of the Work Programme. Moreover, INSTABAT will contribute to a successful mass introduction of batteries for mobility, allowing for substantial improvements leading to an ultra-high performance. The INSTABAT project is also well aligned with the specific impacts set out in the call LC-BAT-13.

TABLE OF CONTENTS

SUMMARY FOR PUBLICATION	3
SUMMARY OF THE CONTEXT AND OVERALL OBJECTIVES OF THE PROJECT	3
WORK PERFORMED FROM THE BEGINNING OF THE PROJECT & MAIN RESULTS.....	3
PROGRESS BEYOND THE STATE OF THE ART, EXPECTED RESULTS AND POTENTIAL IMPACT	4
TABLE OF CONTENTS	5
PERIODIC TECHNICAL REPORT – PART B.....	7
1 EXPLANATION OF THE WORK CARRIED OUT BY THE BENEFICIARIES AND OVERVIEW OF THE PROGRESS.....	7
1.1 OBJECTIVES	7
1.2 EXPLANATION OF THE WORK CARRIED PER WP.....	11
WP1 - DEFINITION OF REQUIREMENT.....	11
WP2 - DEVELOPMENT OF PHYSICAL SENSORS	15
WP3 - CORRELATION BETWEEN MEASURED/ESTIMATED PARAMETERS AND PHYSICO-CHEMICAL DEGRADATION PHENOMENA OCCURRING IN THE BATTERY CELL.....	37
WP4 - DEVELOPMENT OF VIRTUAL SENSORS AND BMS SOX INDICATORS ALGORITHMS.....	56
WP5 - PROOF OF CONCEPT MULTI-SENSOR PLATFORM.....	62
WP6 - TECHNO-ECONOMIC FEASIBILITY, ADAPTABILITY TO OTHER CELL MARKETS AND ENVIRONMENTAL CONSIDERATIONS....	69
WP7 - DISSEMINATION, COMMUNICATION AND EXPLOITATION	71
WP8 - PROJECT MANAGEMENT	77
1.3 IMPACT	83
1.3.1 GENERAL IMPACTS	83
1.3.2 IMPACT ON THE PROJECT PARTNERS	86
2 UPDATE PLAN OF THE EXPLOITATION AND DISSEMINATION RESULTS.....	88
3 UPDATE OF DATA MANAGEMENT PLAN	89
4 FELLOW-UP OF RECOMMENDATIONS AND COMMENTS FROM PREVIOUS REVIEW(S)	90
5 DEVIATION FROM ANNEX 1 AND ANNEX 2.....	91
5.1 TASKS	91
5.2 USE RESOURCES.....	92
5.2.1 CEA.....	92
5.2.2 BMW GROUP	93
5.2.3 CNRS	93
5.2.4 IFAG	93
5.2.5 FAURECIA.....	94
5.2.6 INSA LYON.....	95
5.2.7 UAVR.....	96



PERIODIC TECHNICAL REPORT – PART B

1 Explanation of the work carried out by the beneficiaries and overview of the progress

1.1 Objectives

INSTABAT will deliver a **proof of concept of a multi-sensor platform (“lab-on-a-cell”)**, capable of monitoring simultaneously multiple battery key parameters and of correlating them with battery cell physico-chemical degradation processes. The Battery Management System (BMS) will receive in real-time the output data from the physical/virtual sensors of the platform, enabling the delivery of very accurate SoX cell indicators (States of Charge, Health, Power, Energy and Safety). The benefits of the improved accuracy of the SoX will be demonstrated via two critical uses cases: cycling at extreme conditions and high-power charging for EV applications.

Objective 1:

Perform time- and space-resolved measurements of battery cell critical parameters (Temperature and heat flow; pressure; strain; Li⁺ concentration; CO₂ concentration; “absolute” potential, impedance and polarization) by means of embedded physical sensors (WP2)

Progress towards fulfilling objective 1:

Physical sensors development has progressed according to the initial workplan. We have demonstrated the operation of sensors technologies (OF/FBG, OF/LumT, RE) and progress to the development of OF/LumL by demonstrated the operation of Li⁺ optical probe in the electrolyte. Insertion of 3 of physical sensors OF/FBG, OF/LumT and RE was demonstrate on full cell and tested in cycling condition. We have demonstrated the capability of sensors to measures physical parameters (T, heat flow, “absolute” potential, impedance and polarization). The progress of work to fulfilling the objective 1 is on track.

Key performances indicators related to the objective 1:

KPI 1: Demonstration of prototypes of sensing technologies at TRL 4 for OF/FBG, TRL 3/4 for RE, TRL 3 for OF/LumT and OF/LumL and TRL 3/4 for PA

We have demonstrated that physical sensors are functional in the cell environment. Some of them could be tested in the cells. Each sensor has been developed and tested in representative environment to explore their capability to detect the physical parameters.

KPI 2: Time- and space-resolved in operando measurements according to table in section 1.4.2 for accuracy, resolution, sensitivity, response time, frequency/speed of acquisition and sensor stability over cell lifetime

OF/FBG, OF/LumT and RE have been inserted into the cells and tested under cycling conditions. We have demonstrated the capability of theses sensors to measure the physical parameter inside the cell. The evaluation of accuracy, resolution, sensitivity, response time, frequency/speed of acquisition has been done for these sensors and a proof of concept of operando measurement in cycling condition was achieve during this first period. The accuracy and detection limit of PAS-CO₂ sensors was evaluated in N₂ atmosphere and will be tested in the cell atmosphere in the future work when the integration rules have been resolved. The OFLumL for the Li⁺ is not fully operational, only optical probe was developed with good sensitivity in carbonate medium. The next step is to insert this probe on the optical fiber to develop the OFLum.

KPI 3: No cross-sensitivity between measured parameters (e.g. decorrelated measurements for temperature, pressure and strain for OF/FBG)

The development of new OF/FBG sensors technology based on panda fiber was performed during the first period. The results were demonstrating the possibility to have a decorrelated measurement of temperature and pressure or strain. We have demonstrated for the multi-instrumented cells with RE and OF/LumT there is no cross interaction between the two sensors.

KPI 4: No degradation of cell performance and safety due to sensor individual integration (e.g. linked to chemical reactivity, thermal aspects or geometrical disturbance)

For this objective, the number and duration of test with instrumented cell is too low to answer at this stage of the project. However, some of electrochemistry test with instrumented cells (with OF/FBG, OF/LumT and RE) have been done without degradation of the cell performances. Aging tests will be carried out during the second period of the project. From these results, that we can conclude to the impact of sensors to the cell degradation.

Objective 2:
Perform time- and space-resolved estimations of battery cell critical parameters (Temperature and heat flow; Li+ concentration and distribution; “absolute” potential and polarization) by means of virtual sensors (**WP4**)

Progress towards fulfilling objective 2:

Development of Electrochemical virtual sensor has advanced as planned (D4.1 submitted) and initial validation against COMSOL model by CEA (D4.2) is underway with very positive preliminary results. The next phase will consist of adapting the model to the experimental data for the cell used in the project and develop some indicators necessary for the BMS operation.

Key performances indicators related to the objective 2:

KPI 5: Demonstration of virtual sensors derived from physical-based electro-chemical and thermal reduced models at TRL 3/4 for both E-BASE and T-BASE

Development of Electrochemical virtual sensor has advanced as planned (D4.1 submitted) and initial validation against COMSOL model by CEA (D4.2) is underway with very positive preliminary results. The next phase will consist of adapting the model to the experimental data for the cell used in the project and develop some indicators necessary for the BMS operation. Development of thermal virtual sensor underway

KPI 6: Time- and space-resolved real-time estimations according to table in section 1.4.2 for accuracy and resolution

Electrochemical virtual sensor fully parametrizable for varying resolution. Accuracy characterization underway, good preliminary results (see section detailing Task 4.2 below).

Objective 3:
Establish correlation between (1) cell physico-chemical degradation phenomena and (2) in operando measurements/ estimations (**WP3**)

Progress towards fulfilling objective 3:

The ageing campaign with instrumented cell will be started during the second period of the project. The results from these ageing tests will be used to establish a correlation between cell physico-chemical degradation phenomena and (2) in operando measurements/ estimations.

Key performances indicators related to the objective 3:

KPI 7: Correlations of thermal signature (from OF/FBG, OF/LumT, T-BASE); pressure and strain (from OF/FBG); CO₂ concentration (from PA); Li⁺ concentration (from OF/LumL, E-BASE); and absolute electro-chemical potential (from RE, E-BASE), each with at least one cell physico-chemical degradation phenomena

This correlation between the measurement of the internal parameters of the cell and the degradation phenomena will be possible when the aging test will be done during the second period of the project (WP3)

Objective 4:

Provide in real-time, via INSTABAT multisensory platform, (1) simultaneous monitoring of multiple battery key parameters (Temperature and heat flow; pressure; strain; Li⁺ concentration and distribution; CO₂ concentration; “absolute” impedance; potential; polarization) and (2) accurate SoX cell indicators (**WP5**)

Progress towards fulfilling objective 4:

Development of reduced electrochemical model and E-BASE algorithm considering computation time restrictions and modularity in the resolution for real-time implementation, as well as C code generation and compilation for integration into real-time platform.

Key performances indicators related to the objective 4:

KPI 8: Demonstration of multi-sensor platform (“lab-on-a-cell”) at TRL 3 (with at least 3 out of 4 physical sensors; 2 virtual sensors; data post-processing and logging; BMS on compact stand-alone prototyping unit)

Development of reduced electrochemical model and E-BASE algorithm considering computation time restrictions and modularity in the resolution for real-time implementation, as well as C code generation and compilation for integration into real-time platform.

KPI 9: No degradation of cell performance due to integration of physical sensors all together

This KPI will be evaluated during the second period of the project. We have already shown no degradation of cell performance at initial stage with the integration of two of physical sensors (RE and OF/LumT).

Objective 5:

Demonstrate improved performance of BMS algorithms (1) integrating measured/estimated parameters (2) based on fine electro-chemical and thermal modelling of the battery cell (**WP4**)

Progress towards fulfilling objective 5:

This objective will be achieved during the second period of the project.

Key performances indicators related to the objective 5:

KPI 10: High fidelity reproduction of cell electro-chemical and thermal behaviour using numerical simulation models:

- 1D+1D electrode model: < SoA6 (5% error for electrode potential; <20% error for lithium concentration throughout the thickness of the electrode at different Crates and extreme temperatures)
- p3D electro-thermal cell model: < SoA (5% error for cell voltage at different Crates and temperatures; <5% error for temperature gradient)
- 3D thermal cell model: < SoA (5% for the absolute maximum temperature, temperature gradient and hot spot locations)

First (preliminary) comparisons underway for SoC in simple scenarios for single temperature point using reduced electrochemical model (E-BASE) seem to be within the 0.5% of the reference model (CEA 1D+1D electrode model).

KPI 11: Demonstration of improved accuracy of BMS SoX7 indicators algorithms:

- State of Charge (SoC): 0.5% accuracy over the whole temperature range (SoA:3%)
- State of Power (SoP): 2% accuracy over the whole temperature range (SoA: 10%)
- 2% accuracy for estimation time horizon of the maximum available power, as compared to the measured one (SoA: 10%)
- State of Energy (SoE): 2% accuracy over the whole temperature range (SoA: 5%)
- State of Safety (SoS) indicator allowing the cell temperature extrapolation and providing safety margin value to predict thermal runaway

Objective 6:

Demonstrate improvement of cell functional performance and safety through two use cases for EV applications (WP3, WP4, WP5)

Progress towards fulfilling objective 6:

This objective will be achieved during the second period of the project.

Key performances indicators related to the objective 6:

KPI 12: Higher estimated performance for cycling at extreme conditions: increase operational temperature window by >10%; characterise impact of measurement/estimation of temperature on cell ageing

This KPI will be evaluated during the second period of the project.

KPI 13: Optimised plans for high-power charging, while still ensuring safety: 10% less time for high-power charging from SoC 10% to 80% by utilising sensor data output compared to conventional fast charging; high-power utilising sensor data output leads to 5% less ageing compared to conventional high-power charging

This KPI will be evaluated during the second period of the project.

Objective 7:

Carry out an industrial study for a multi-sensor platform; assess manufacturability and techno-economic feasibility, including adaptability to other cell technologies and use cases; provide environmental assessment, focusing on traceability, second life and recyclability (WP6)

Progress towards fulfilling objective 7:

This objective will be achieved during the second period of the project.

Objective 8:

Collaborate with other EU H2020 projects, in particular contribute to the large-scale research initiative on future Battery Technology, under the umbrella of the successful LC-BAT-15 consortium (WP7)

Progress towards fulfilling objective 8:

Collaboration with other EU H2020 project was already effective through the participation of the Battery2030+ initiative. Collaborative work was already started at different stages in communication and dissemination activities, experimental work and exchange and share the progress of INSTABAT work.

1.2 Explanation of the work carried per WP

WP1 - Definition of requirement

Work package number	1	Leader	IFAG						
Work package title	Definition of requirements								
Short name of participant	BMW	VMI	CNRS	CEA	FAURECIA	UAVR	INSA	IFAG	
Person	months	per	6	8.5	0.5	0.5	0.5	0.5	3.5
participant									
Start month	M1			End month			M6		

Objectives

The main objectives of WP1 are to:

- Translate the goals defined in INSTABAT objectives into sets of requirements, according to the current knowledge;
- Adjust the requirements to the special needs of the selected cell;
- Correlate these requirements to the developments assessed as feasible within the consortium and the project runtime;
- Use the results obtained in WP1 as an input for the other technical WPs;
- Involve all the consortium partners in the definition of requirements, taking advantage of their technical expertise in the field.

Highlights of most significant results

For an alignment between all partners on the definition of requirements, a kick-off conference call was organized by WP1 leader IFAG for October 16, 2020. Between October 2020 and end of February 2021, biweekly phone conferences with a good participation by all partners took place.

As a result of these discussions, deliverable D1.1 with an encompassing definition of requirements for smart batteries was completed and submitted by BMW on March 08, 2021, with about one month delay.

Similarly, deliverable D1.2 with a complete description of the requirements for integration of the sensors into the cell was completed and submitted by VMI on February 26, 2021, right on target.

With the submission of these deliverables, milestone M1 “Smart cell requirements broken down at each WP level” was reached on March 08, 2021, with only eight days delay.

Summary of progress towards objectives and details for each task

TASK 1.1 DEFINITION OF REQUIREMENTS FOR SMART BATTERIES, BROKEN DOWN AT BMS AND PHYSICAL/VIRTUAL SENSORS LEVEL

(Leader: BMW; Participants: All (M1-M5))

In extended, detailed discussions between all partners, the requirements for smart batteries were agreed on and documented in a deliverable report (D1.1) by BMW, the task leader for T1.1. For details about the requirements, please refer to this report, only an excerpt is given here.

Deliverable D1.1 states the following overarching requirements for full battery electric vehicles (BEVs) and plug-in hybrid electric vehicles (PHEVs) used for passenger vehicle applications:

- The detection or anticipation of safety-critical states and ageing mechanisms, so that countermeasures can be taken to avoid battery critical events, or at least to be able to send a timely warning signal.
- The development of adaptive “state-of-charge” (SoC), “state-of-health” (SoH) and “state-of-power” (SoP) estimators, which allows reliable performance in different environmental conditions and over the whole battery lifetime including second life application.
- Sensor-based battery operational strategies, which for example, improve fast charging and provide an adaptive “depth-of-discharge” (DoD) performance range larger than the standard range with fixed limits.

#	Requirements	Validation	Requirement Context	Priority	WP1	WP2	WP3	WP4	WP5
3	C-Rate capability: 0.3C charge/0.5C discharge continuous		Cell specifications	high					
4	Sensor must be fully functional in the following temperature ranges: Temperature range test chamber for storage: -40°C to +80°C. Temperature range test chamber for cycling tests: -25°C to +55°C. Max. Temperature of the cell core: chemistry-dependent, approx. + 80°C; Max. Temperature of cell housing: chemistry-dependent, approx. + 60 °C; Max. Temperature of cell terminal: chemistry-dependent, approx. + 70 °C	Sensor can be tested in dummy cells without active cell chemistry in the full temperature range.	Environmental condition	medium		x			x
10	Cell state of charge (SoC) must be able to be determined with a frequency of 0.1 Hz and an accuracy of 2%.	Applying a driving cycle (provided by BMW) at defined temperatures [for example 40 °C, 25 °C, 10 °C and 0 °C, -10 °C]. The cycle is stopped at certain time and the cell is discharged with a defined current (e.g. 1/ 3C) until the end-of-discharge voltage is reached. The external temperature in climatic chamber remains the same during the driving cycle and the discharge. The reference state of charge can be compared with the estimated state of charge determined by the algorithm.	BMS Functions / Use case	high				x	x
19	Cell external short circuit must be detected and communicated within 50 ms during operation	External short circuit test: The detection and communication of the short circuit event must take place within 50ms.	Safety	low			x		x
24	Sensor signals should be brought together at a central point on the cell for further evaluation	Evaluation through implementation	Demonstrator	high		x	x		x
27	Extended cycle life and calendaring life for sensor cells and electric and electronic component are required. for example, 5000 cycle life and 20 years calendaring life till battery end of service (cell dependent, therefore the definition is open)		second life application	medium					

Figure 1. Excerpt from the main table in deliverable D1.1, with functional requirements in six contexts

As documented in the detailed main table in deliverable D1.1 (see Excerpt in Figure 1), a total of 27 functional requirements in the six contexts “cell specifications”, “environmental condition”, “BMS functions / use case”, “safety”, “demonstrator”, and “second life application” were identified, each with a method for validation, a priority, and an assignment of relevance to the work packages. As one example (see Figure 1) in the category “BMS functions / use case”, requirement #10 “Cell state of charge (SoC) must be able to be determined with a frequency of 0.1 Hz and an accuracy of 2%” was given a high priority, is associated with WP5 and WP6 and will be validated in the following manner: “Applying a driving cycle (provided by BMW) at defined temperatures [for example 40°C, 25°C, 10°C and 0°C, -10°C]. The cycle is stopped at certain time and the cell is discharged with a defined current (e.g. 1/ 3C) until the end-of-discharge voltage is reached. The external temperature in climatic chamber remains the same during the driving cycle and the discharge. The reference state of charge can be compared with the estimated state of charge determined by the algorithm.”

In a second table in deliverable D1.1, the correlation of the requirements to the six physical / virtual sensors considered in INSTABAT is provided. For instance, the luminescence sensor will contribute to the determination of the cell SoC by providing information about the Li-ion concentration.

For additional information and more details, please refer to the deliverable report D1.1.

TASK 1.2 DEFINITION OF REQUIREMENTS FOR INTEGRATION OF SENSORS INTO THE CELLS

(Leader: VMI; Participants: All) (M1-M6)

The same discussions as for T1.1 were used to work out the requirements for the integration of sensors into the cells between all partners, documented in a deliverable report (D1.2) by VMI, the task leader for T1.2. Again, details about the requirements can be found in this report, only an excerpt is given here.

As documented in deliverable D1.2, a total of 17 requirements were identified in the five categories “mechanical”, “electrical”, “environmental”, “lifetime” and “safety”. In addition, concrete tests and the corresponding passing criteria were specified for the cells with integrated sensors. For both, requirements and test results, hard exclusion criteria were defined. As one example in the category “mechanical”, Figure 2 shows the cross-section in z-direction of a sector of the stack for a tentative INSTABAT Prototype Cell for two hypIGMAP sensors, a cylindrical sensor (left) and a reference electrode (right). For this type of integration, the following hard exclusion criteria were defined:

- Sensors with a larger cross-section in the z-direction than 2 times the electrode diameter (~250µm).
- Safety-critical deposition of lithium at locations where the sensors are integrated into the stack.
- The integration of the Multi-Sensor platform increases the safety hazard level to > 4.

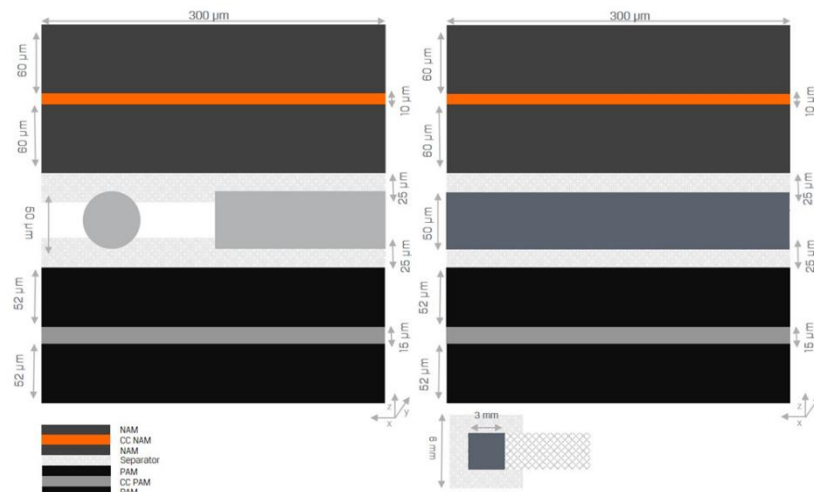


Figure 2. Cross-section in z-direction of a sector of the stack for a tentative INSTABAT Prototype Cell. Left - Hypothetically integrated cylindrical sensor / Right - Hypothetically integrated reference electrode.

To highlight one further example: In D1.2 concrete mechanical tests for “vibration” and “shock” of the battery cells are defined.

	Industrial-Pouch-Cell*	INSTABAT Prototype-Cell**		INSTABAT Multi-Sensor Platform/Prototype-Cell***	
	C/NMC622	C/NMC622	C/Si ₅₅₀ ⁺⁺ /NMC622	C/NMC622	C/Si ₅₅₀ ⁺⁺ /NMC622
Vibration	a. no explosion/ fire b. no leakage c. cell failure (≤0.1%)	a. no explosion/ fire b. leakage (≤1.0%) c. cell failure (≤1.0%)	a. no explosion/ fire b. leakage (≤1.0%) c. cell failure (≤1.0%)	a. no explosion/ fire b. leakage (≤10.0%) c. cell/sensor failure (≤10.0%)	a. no explosion/ fire b. leakage (≤10.0%) c. cell/sensor failure (≤10.0%)
Shock	a. no explosion/ fire b. no leakage c. cell failure (≤0.1%)	a. no explosion/ fire b. no leakage c. cell failure (≤1.0%)	a. no explosion/ fire b. no leakage c. cell failure (≤1.0%)	a. no explosion/ fire b. leakage (≤10.0%) c. cell/sensor failure (≤20.0%)	a. no explosion/ fire b. leakage (≤10.0%) c. cell/sensor failure (≤20.0%)

shows the corresponding passing criteria, differentiating for comparability between three types of cells:

- Hypothetical “state-of-the-art” (SoA) cell (TRL9)
- INSTABAT prototype base cell (TRL5)
- INSTABAT prototype cell with the integrated sensor platform (TRL4)

In addition, for the two levels of prototype cells, two different active materials are being distinguished. Here also, hard exclusion criteria for the test results are defined in D1.2:

- The integration of the Multi-Sensor platform increases the safety hazard level to > 4.
- Total failure of the sensor and/or uncontrollable shift in the sensor capabilities.

For additional information and more details, please refer to the deliverable report D1.2.

Table 1. Expected/estimated effect of vibration-test, and shock-test on industrial pouch-cell, INSTABAT prototype cell, multi-sensor platform integrated into INSTABAT prototype cell

	Industrial-Pouch-Cell*	INSTABAT Prototype-Cell**		INSTABAT Multi-Sensor Platform/Prototype-Cell***	
	C/NMC622	C/NMC622	C/Si ₅₅₀ ⁺⁺ /NMC622	C/NMC622	C/Si ₅₅₀ ⁺⁺ /NMC622
Vibration	a. no explosion/ fire b. no leakage c. cell failure (≤0.1%)	a. no explosion/ fire b. leakage (≤1.0%) c. cell failure (≤1.0%)	a. no explosion/ fire b. leakage (≤1.0%) c. cell failure (≤1.0%)	a. no explosion/ fire b. leakage (≤10.0%) c. cell/sensor failure (≤10.0%)	a. no explosion/ fire b. leakage (≤10.0%) c. cell/sensor failure (≤10.0%)
Shock	a. no explosion/ fire b. no leakage c. cell failure (≤0.1%)	a. no explosion/ fire b. no leakage c. cell failure (≤1.0%)	a. no explosion/ fire b. no leakage c. cell failure (≤1.0%)	a. no explosion/ fire b. leakage (≤10.0%) c. cell/sensor failure (≤20.0%)	a. no explosion/ fire b. leakage (≤10.0%) c. cell/sensor failure (≤20.0%)

*TRL9, ** TRL5, *** TRL4, ++ advanced (next generation) active material

Table 2. List of deliverables WP1

Deliverable Number	Deliverable Title	Lead beneficiary	Type	Dissemination level	Due date (in month)	Status
D1.1	List of requirements for smart batteries	2 - BMW GROUP	Report	Public	5	Submitted
D1.2	List of requirements for the integration of the multi-sensor platform in cells	8 - VMI	Report	Public	6	Submitted

WP2 - Development of physical sensors

Work package number	2	Leader	UAVR	
Work package title	Development of physical sensors			
Short name of participant	CNRS	IFAG	CEA	UAVR
Person months per participant	30	43	30	30
Start month	M1		End month M24	

Objectives

The main objectives of WP2 are the following:

- Develop and characterise the following physical sensors (working on aspects such as sensor hardware development, adaptation to cell environment, sensor hardware integration and test):
- Optical fiber / Fiber Bragg Grating (OF/FBG): optical fiber sensors based on Bragg gratings will be produced, characterised and tested in the cell environment to detect accurately and in real-time internal and external temperature, heat flow and strain and pressure shifts in the cells.
- Reference electrode (RE): a reference electrode will be implemented within the cell to provide “absolute” potential, impedance and polarization.
- Optical fiber / Luminescence for Thermal and Li⁺ Concentration (OF/LumT and OF/LumL): luminescent probes onto optical fibres will be developed to measure internal temperature and Li⁺ concentration inside the cells.
- Photo-Acoustic sensor (PA): a photo-acoustic CO₂ gas detector will be adapted to the cell environment and provide
- CO₂ concentration measurements.
- Adapt sensors to the cell environment, considering aspects such as electro-chemical reactivity and thermal design, and carry out in situ lab-scale tests.
- Manufacture pouch cells to be used for sensor implementation and carry out in situ lab-scale tests.
- Validate the sensor technologies and deliver sensor prototypes for integration in the INSTABAT platform.

Highlights of most significant results

WP2 intends to develop and to characterize four different physical sensors that will be used for specific cell parameters monitoring. Aspects such as the adaptation to the battery/cell environment will be considered in this WP. To successfully achieve the proposed WP2 objectives, different physical sensors have been developed, adapted and characterized to the specific sensing parameters. In this way, at UAVR, optical fiber sensors based on Bragg gratings inscribed in standard and special fibres (Polarization-Maintenance fibres) have been produced, and calibrated, specifically to real time temperature and strain detection. FBGs with higher reflectivities were produced and a linear dependence to both parameters were attained. Addressed to this, also optical interferometers (Fabry-Perot cavities), by using capillary tubes and UV glue cascaded with FBGs, are being developed to in situ and operando temperature and pressure sensing, in which a sensitivity of near 20 nm/bar was already obtained for the interferometers. The optical fiber sensors created until now presents lower dimensions (from 0.5 to 8.0 mm length) and very good chemical stability and resistance, after 9 months submerged in the electrolyte solution, do not detecting any signal damage/deterioration. From the SEM and EDS analysis, the optical fiber surfaces were not etched, where just a small quantity of precipitation of crystals (Phosphorous and Fluorine electrolyte compounds) was observed. The FBGs developed with higher reflectivity were shipped to CNRS and CEA for cell battery integration during their manufacturing (WP3). Regarding the Reference Electrode (RE) sensor, several samples were developed by IFAG, targeting the “absolute” potential, impedance and polarization cell measurements. Gold and Aluminium with different thickness (100 nm, 50 nm, and 300 nm) and geometries (Square, fork, and antenna) samples were tested and performed. Until now, two batch of RE sensors were delivered to CEA and CNRS to cells integration and test. From the experimental cell integration tests, the samples with gold films with antenna geometry and 100 and 300 nm thickness shows to be the better option as a RE sensor, due their present a stable potential after several hours of usage and higher conductivity. However, an LFP coating was necessary to be performed on the gold film.

Optical fiber Luminescence thermal probes were successfully performed to temperature monitoring in the cells. Electrochemistry test of instrumented cell was used to demonstrate the no impact of the optical fiber on the cell up from C/10 to 4C cycling. During these tests didn't was observed any degradation on the cell and on the response of the

thermoluminescence sensor. We can conclude the good operation of the thermoluminescence. The OF/LumT was inserted in 1.1Ah cell and we demonstrated the linear dependence between optical signal to the cell temperature. The accuracy of the sensor is currently of 2°C and must be improved in the future.

Luminescent probe for OF/LumLi to detect the Li⁺ concentration has been developed. It was demonstrated the efficiency of this luminescent probe to detect Lithium ion in aqueous and carbonate medium (electrolyte) with a concentration around 1M. This optical probe was successfully deposit on glass substrate by covalent bounding without degradation of sensitivity for Li⁺ detection. The next step is to deposit this probe on optical fiber and test the OF/lumLi sensor in the cell.

IFAG has adapted and provided first versions of a CO₂ sensor based on the photoacoustic (PA) principle for cell integration and real time CO₂ monitoring. In the course of the integration tests, some further adaptations were already performed, e.g., the installation of a completely new emitter and filter package. From the calibration tests in a pre-fabricated CO₂ chamber, the sensor shows a good accuracy above 5 ppm and a detection limit up to 2 ppm. The main improvements targeted in a future version of the sensor consist in a separation of the sensing chamber from the other electronics and the implementation of a connection between sensing chamber and electronics via a Flex PCB.

Summary of progress towards objectives and details for each task

Task 2.1: PHYSICAL SENSOR HARDWARE DEVELOPMENT AND ADAPTATION TO BATTERY CELL ENVIRONMENT

(Leader: UAVR; Participants: CNRS, CEA, IFAG) (M1- M24)

Subtask 2.1.1. Optical fiber / Fiber Bragg Grating (OF/FBG) sensor development and characterisation

An inherent drawback of using FBGs as sensing technology is that it suffers from a large cross sensitivity to temperature, pressure and/or strain. Simultaneous discrimination of these parameters can be achieved by recording FBGs in polarization-maintenance (PM) high-birefringent (Hi-Bi) fibres: FBGs written in Hi-Bi optical fibres are able to simultaneously discriminate temperature and strain (longitudinal and transverse components). The basis for measuring two parameters with an FBG is to have a different sensitivity of the Bragg wavelength. This is achieved in Hi-Bi gratings because the shift of the reflection bands, for each polarization, is different and depends on the angle of the application of the external load. The displacement of both Bragg wavelengths can be used in a matrix equation to determine the two physical parameters: temperature and strain. As a consequence of the internal stress profile, the optical reflection spectrum of an FBG written in Hi-Bi fibres, with non-polarized light focused on the fiber, has a two-peak structure corresponding to the two orthogonal polarization modes of the fiber (see Figure 3); the X and Y polarizations of the LP₀₁ modes are split and each one has a different effective index. These linear polarizations are the slow (X-axis) and fast (Y-axis) modes associated with the principal directions of the refractive index profile of the fiber. To use an optical fiber sensor composed of FBG in Hi-Bi fiber it is necessary to characterize the grating properties in the presence of the parameters to be measured, as the specific dependence of these properties can induce.

Different type of PM fibres was started to be used in the FBG recording process, such as Bow-Tie, PANDA, and Elliptical Cladding Hi-Bi fibres, the PANDA fibres were selected as to be better option to perform all the process, since the FBG sensors recording up to the cell battery integration, due to their easier fiber handling, simplicity of the recording process and very good FBG peaks reflectivity's and reproducibility. Also, FBG sensors recorded on standard Photosensitive (PS) fibres are being used, because they can be used externally of the pouch cells as a temperature sensor, or internally for calibrations proposes. All the sensors produced, after a pre-calibration step, are shipped to CNRS and CEA partners to pouch cell integration during the battery manufacturing process.

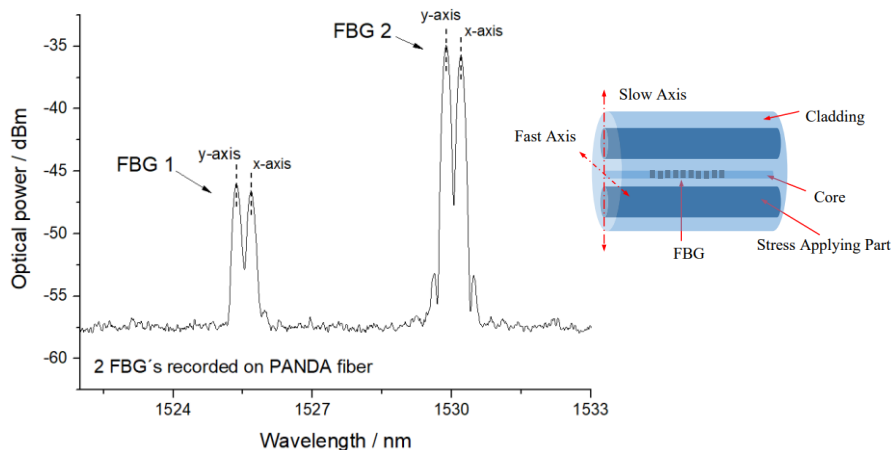


Figure 3. Optical reflection spectrum from the structure with two superimposed Bragg gratings in Photosensitive PM PANDA Hi-Bi fiber. FBGs were inscribed using different phase masks by pulsed Q-switched Nd:YAG UV laser installed in the UAVR lab.

FBGs fabrication in PM PANDA Hi-Bi fibres:

- Many FBG sensors recorded on PM PANDA Hi-Bi fibres with higher reflectivity were performed after a pre-hydrogenation step for 1 week. This step of fiber hydrogenation was applied because the PM PANDA fiber is not photosensitive, and to get a very good reflectivity value of the FBG peaks. From Figure 4, can be observed that all FBGs presents peaks values near of -20 dBm, which is a very good result, with a birefringence value around 4.2×10^{-4} .

FBGs fabrication in standard PS fibres:

- Several FBG sensors are being also recorded in standard PS fibres and a very good reflectivity and reproducibility has been achieved. To multipoint monitorization, different wavelength peaks are used.

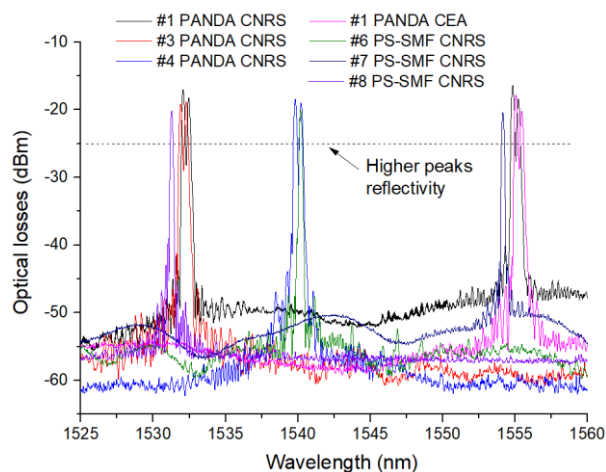


Figure 4. Spectral response of some FBG sensors recorded in PM Hi-Bi PANDA and PS fibres at UAVR lab, by using the UV laser, after the fiber hydrogenation, and shipped to CNRS and CEA. Double FBG peaks reflectivity higher than -25 dBm.

- Temperature and strain calibrations:

All the FBG sensors performed until now were calibrated to temperature and strain, by using a climatic chamber (between 5 °C and 60 °C) and a micrometre translation stage (between 0 and 2000 $\mu\epsilon$), respectively. As expected, different sensitivities were obtained for the two peaks (x and y). Regarding the temperature sensitivities, values around 9.0 $\text{pm}/^\circ\text{C}$ were obtained, in which higher values were register on the y-axis (fast) peak, with a difference near of 0.5 $\text{pm}/^\circ\text{C}$ for the x-axis (slow) peak. From the strain calibration, sensitivities around 1.20 $\text{pm}/\mu\epsilon$ were determined, however with higher values on the x-axis (slow) ($\sim 0.01 \text{ pm}/\mu\epsilon$). All these sensitivities will be used on the simultaneous discrimination of both parameters through the matrixial method, as following described (Eq. 1):

$$\begin{bmatrix} \Delta\lambda_{FBGf} \\ \Delta\lambda_{FBGs} \end{bmatrix} = \begin{bmatrix} k_{FBGf\varepsilon} & k_{FBGfT} \\ k_{FBGs\varepsilon} & k_{FBGsT} \end{bmatrix} \begin{bmatrix} \Delta\varepsilon \\ \Delta T \end{bmatrix} \quad (Eq. 1),$$

where $k_{FBGf\varepsilon}$, and k_{FBGfT} are the strain and temperature sensitivities of the FBG fast peak, respectively, and $k_{FBGs\varepsilon}$ and k_{FBGsT} are the strain and temperature sensitivities of the FBG slow peak, respectively. A sensitivity matrix for simultaneous measurement of strain and temperature can be derived as (Eq. 2):

$$\begin{bmatrix} \Delta\varepsilon \\ \Delta T \end{bmatrix} = \frac{1}{M} \begin{bmatrix} -k_{FBGsT} & k_{FBGfT} \\ k_{FBGs\varepsilon} & -k_{FBGf\varepsilon} \end{bmatrix} \begin{bmatrix} \Delta\lambda_{FBG} \\ \Delta\lambda_{FP} \end{bmatrix} \quad (Eq. 2),$$

where $M = k_{FBGs\varepsilon} \times k_{FBGfT} - k_{FBGsT} \times k_{FBGf\varepsilon}$ is the determinant of the coefficient matrix, which must be non-zero for possible simultaneous measurement.

Hybrid sensing configuration to pressure and temperature discrimination:

To simultaneously discriminate and sense pressure and temperature variations during cell operation, UAVR are developing new optical fiber sensors configurations based on an in line FBG recorded near a Fabry-Perot interferometer cavity, forming a hybrid configuration, which is performed by splicing a single mode fiber (SMF) to one hollow core silica tube (~ 200 μm), with a very small section of a UV curable glue in the fiber tip. This small portion created by the silica tube and the UV glue will perform a double light interference. The first one between the SMF and the 1st UV glue surface, and the second one between the two surfaces of the UV glue. This constructive interference will promote a sensitivity increase in the resultant spectral response, which can be followed by performing an envelope filter on the spectrum. By tracking the minimum of this filter, it will be possible to attain the pressure and temperature shifts. In this case, the simultaneous discrimination of both parameters, will be obtained by recording FBG sensors near of this region. As the FBG sensors will present different pressure and temperature sensitivities, by using the same matrixial method (Eq. 1 and Eq. 2), a temperature and pressure variation can be tracked.

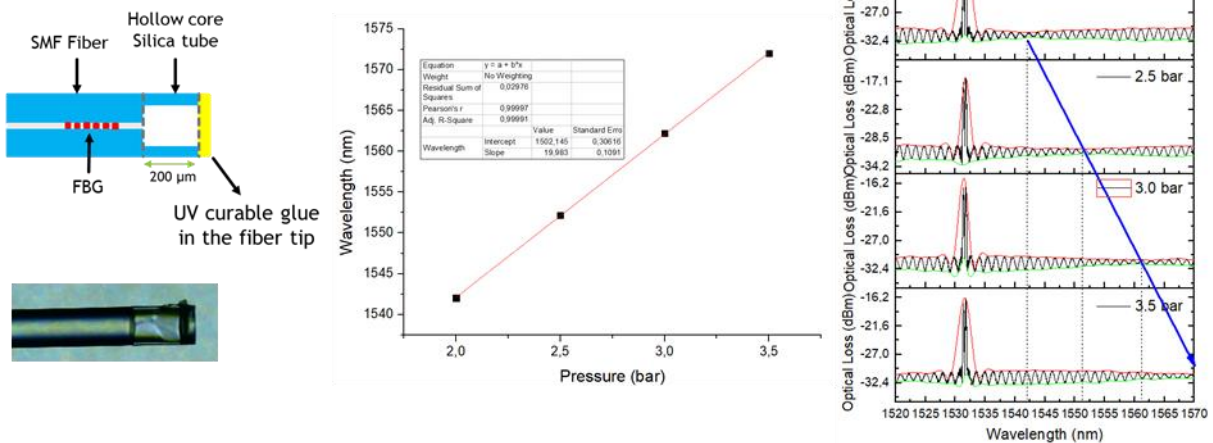


Figure 5. Hybrid sensor configuration and pressure calibration between 2.0 and 3.5 bar with the respective spectral response.

- Hybrid sensor pressure calibrations:

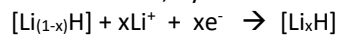
After the initial hybrid sensing configuration approach, an experimental pressure characterization was performed on the illustrated sensor. From the data analysis, a linear and impressive sensitivity of near 20 nm/bar was obtained from the envelope and an almost insensitivity value (0.1 pm/bar) has result for the FBG sensor (Figure 5). The next steps will be to improve the hybrid sensor reproducibility and their spectral response, by using different dimensions for the hollow core silica tube by improving the number of minimums that will appear in the envelope filter, and/or by varying the UV glue dimensions on the fiber tip to increase the optical losses. A temperature characterization of the hybrid sensor will be also performed to attain their sensitivities. It is expected to obtain higher sensitivity values for the envelope due the higher thermal expansion of the UV glue.

Subtask 2.1.2 Reference Electrode (RE) sensor development

The reference electrode (RE) will provide measurements of “absolute” potential, impedance and polarization. Currently, there is no reference electrode is present on the market for lithium-ion systems. This explains why the literature reports the use of “homemade” reference electrodes based on different materials supported on tabs or metal grids ^{1,2}. Three main families of materials can be used: insertion materials such as $\text{Li}_{(1-x)}\text{FePO}_4/\text{LiFePO}_4$ (LFP) ³ or $\text{Li}_4\text{Ti}_5\text{O}_{12}/\text{Li}_{(4+x)}\text{Ti}_5\text{O}_{12}$ (LTO) ⁴, lithium alloy metals (e.g. $\text{Li}_x\text{Al}/\text{Al}$ ⁵ or $\text{Li}_x\text{Au}/\text{Au}$ ⁶. They are identified as a possible reference material because:

1 - Their thermodynamic potential is independent of the lithium ion concentration in the electrolyte. It is fixed:

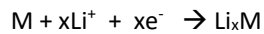
- For biphasic insertion materials, by the ratio between delithiated active sites and lithiated active site:



$$\text{Nernst Law: } E = E^0 + \frac{RT}{nF} \ln\left(\frac{1-x}{x}\right)$$

with H = insertion structure, x = insertion rate

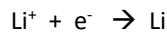
- For alloys, by the lithium concentration in the solid phase



$$\text{Nernst Law: } E = E^0 + \frac{RT}{nF} \ln\left(\frac{1}{x}\right)$$

with x = lithium concentration in the solid phase

This is not the case for the Li^+/Li couple, which is nevertheless widely used as a reference electrode⁷, its redox potential being dependent on the lithium ion concentration in the electrolyte:



$$\text{Nernst Law: } E = E^0 + \frac{RT}{nF} \ln\left(\frac{[\text{Li}^+]}{1}\right)$$

The appearance of a lithium concentration gradient in the inter-electrode space can then modify the potential of the electrode.

2 - Their lithium insertion/desinsertion curves show a potential plateau over a wide range of lithiation (Figure 6). This implies, before their use, a prior electrochemical step of delithiation (LFP) or lithiation (LTO, metal alloy) to place the insertion potential of the material on the plateau.

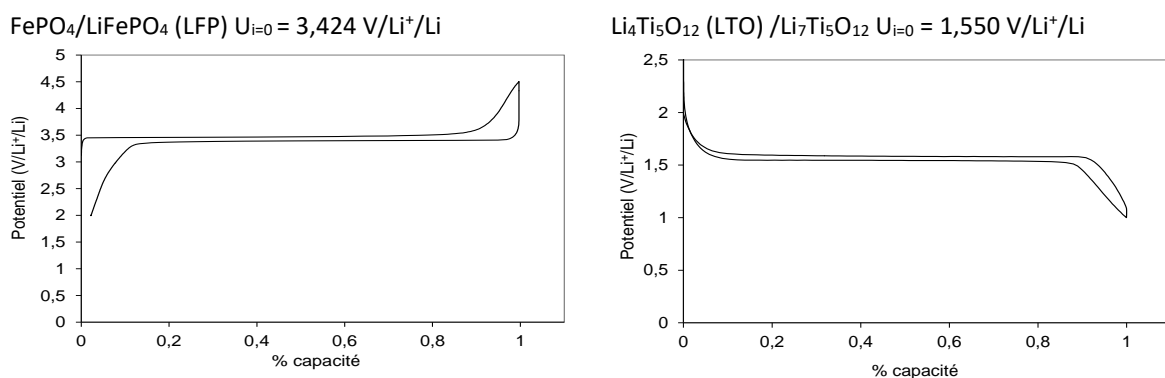


Figure 6. Galvanostatic curves in lithiation/delithiation of LFP and LTO (at C/10).

During cell operation, the electrochemical profiles provided by the reference electrode could be used to control the end of charge, no longer by the cell voltage, but by the potential of the negative electrode. The appearance of metallic lithium could thus be avoided leading, consequently, to gains in lifetime. But this therefore implies that the reference electrode can then be easily integrated into commercial cells and be able to provide a reliable and stable response over time. In the INSTABAT project, three electrochemical couples have been chosen:

³ F. La Mantia, C.D. Wessells, H.D. Deshazer, Yi Cui, *Electrochemistry Communications*, Vol. 31,2013, 141-144

⁴ I. Jiménez Gordon, S. Grugeon, A. Débart, G. Pascaley, S. Laruelle, *Solid State Ionics* 237 (2013) 50–55

⁵ I.G. Kiseleva, L.A. Alekseeva, A.V. Chekavtsev, P.I. Petukhova, *Soviet Electrochemistry*, 18 (1982) 114-117.

⁶ J. Zhou, P. H. L. Notten, *J. Electrochem. Soc.*, 151 (12) A2173-A2179 (2004)

⁷ J. Hou, R. Girod, N. Nianias, T.-H. Shen, J. Fan, V. Tileliz, *J. Electrochem. Soc.* 167 (2020) 110515

- Au alloy (LixAu/Au)
- Aluminum alloy (LixAl/Al)
- LiFePO4 (LFP)

In discussions between the partners CEA, CNRS and IFAG, it was agreed, based on experience and the fundamental physical properties, that the most promising metallic materials for RE sensors were Gold (Au) and Aluminium (Al). Furthermore, the partners decided that three different design variants for the end of the RE sensor reaching into the cell would be considered: “Square”, “fork” and “antenna” (see Figure 7 - Left). Also, a general thickness of 100nm for the structures was targeted, with additional variants of 50nm and 300nm thickness for the RE sensor made from Au.

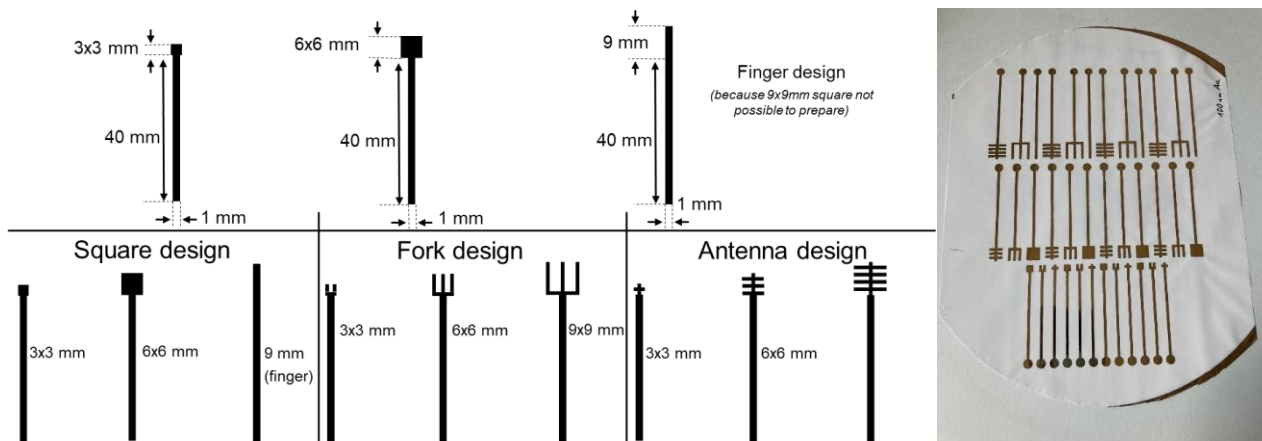


Figure 7. Left - Final design variants for the RE sensor made from metallic materials. Width (1mm) and length (40mm) of the finger were fixed. For Au samples, different thicknesses were used. For the end of the RE sensor inserted into the cell, a square, fork, and antenna design were chosen. Right – Samples manufactured with an 8 inch wafer backend sputtering process directly onto the separator sheet.

In order to sputter the metals via hard mask directly onto the separator sheets from Celgard[®] provided by VMI, IFAG established a backend process for 8 inch wafers adapted to these geometries. After an optimization of the design, avoiding large open areas in the hard mask which lead to excessive heat generation destroying the separator sheets, IFAG was eventually able to manufacture the desired RE sensor variants (see an example in Figure 7- Right). Achievement of the target thickness was controlled using a profilometer, indicating a variation of merely 4-6% between the centre and the edge of the wafer. In addition, resistivity measurements of the samples were performed via 4-point probe, confirming a low standard deviation of 10%. IFAG delivered a first batch with 4 pieces of each variant (i.e., a total of 144 RE sensors) to both, CEA and CNRS, in July 2021 for integration into the battery cell and testing at cell level. A second batch consisting of 12 pieces of each design variant only for the 100nm and 300nm RE sensors made from Au (i.e., another 216 RE sensors) was delivered to CEA in February 2022.

According to the primary tests, we have seen that:

- the potential of LixAu (with various tested thicknesses) are not stable after lithiation.
- the conductivity of aluminum was not sufficient to have an usable LixAl

Gold sample with LFP coating has been finally retained as reference electrode. A stability study of the potential of the FePO₄/LiFePO₄ couple was carried out to determine the validity of its response over time. This study was carried out by following the open circuit potential (OCV) of Li_{0.5}FePO₄ against lithium over time and at three temperatures 25°C, 45°C and 55°C. Before launching the temperature test, the delithiation of LiFePO₄ is carried out electrochemically to place the potential of the material at mid-plateau (“activation” step) (Figure 8).

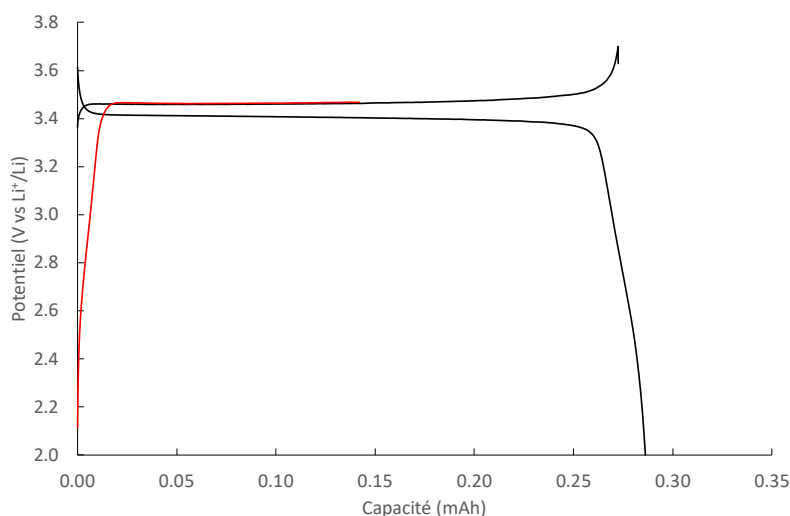


Figure 8. Lithiation and delithiation curves of LFP reference electrode (black line) and delithiation at 50% of the lithiation capacity to place the potential in the middle of the plateau (red line) (activation step)

Subtask 2.1.3 Optical fiber / Luminescence (OF/LumT and OF/LumL) sensors development

From the literature review, different type of optical probes for temperature measurement and Lithium concentration measurement were identified. We detail the work for each probe below.

Thermoluminescent probe (OF/LumT)

There is a large amount of literature on thermoluminescent phosphors. To find the more appropriate candidate for INSTABAT, some requirements were fixed (see D1.1 and D1.2):

- The optical probe must be stable and compatible with the electrolyte and the electrochemistry environment of the cell.
- The sensitivity and the temperature range must be compatible with the application.
- The excitation wavelength used to measure doesn't induce photo degradation of polymeric material inside the cell.
- The luminescence of probe must be easily detectable.

We identified a first promising candidate for the thermoluminescent probe based on Gd_2O_2S particles doped with Er^{3+} and Yb^{3+} . Thereafter, we started to work on a second candidate based on GdV_2O_4 particles doped with Er^{3+} and Yb^{3+} . Calibration tests have been carried out on Gd_2O_2S and GdV_2O_4 powder to determine its sensitivity to temperature. Then we are developing coating protocols to perform a deposition of these particles onto the optical fiber tip. Different formulations (sol-gel and polymer) were studied to optimize the powder deposition and the luminescence intensity of the probe on fiber. Tailored sol-gel formulations have been synthesized for both phosphors. The goal is to deposit phosphor particles as close to the optical fiber tips as possible to optimize the optical and the mechanical performances (the modified fibres must be robust enough to be put and sealed inside the pouch cell battery).

Sol-gel formulation has been modified to enhance the gelification time by acting on the catalyst choice. All the experiments have been carried out at room temperature. Finally, a PMMA varnish has been locally applied to wrap and protect the active sensing zone. PMMA has been chosen because it can work in carbonate based electrolyte (the thickness of this protective layer does not impact the thermal measurement). At this time, the sol-gel formulation performed very well for Gd_2O_2S phosphor. Several samples have been tested (all of them showing equivalent thermal sensing performances).

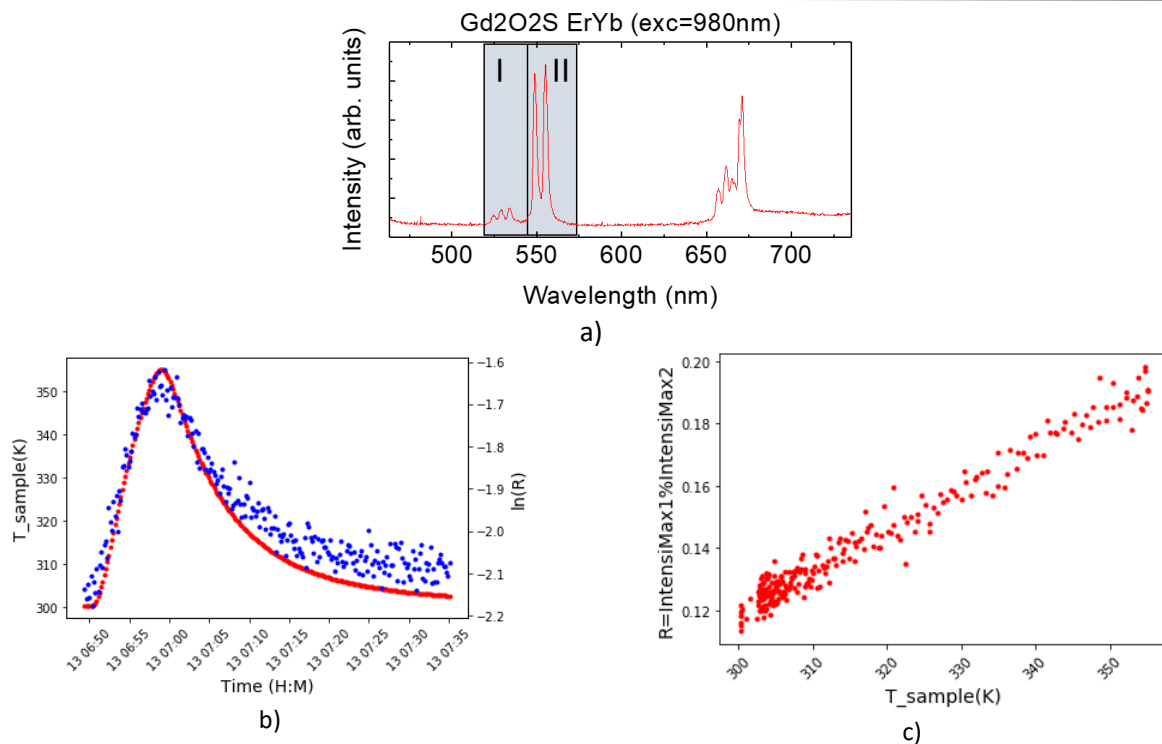


Figure 9: Gd₂O₂S:ErYb – a) Luminescence spectra with the two pics used for thermoluminescence ratiometry (I_I/I_{II}), b) Variation of luminescence intensity ratio in temperature, c) Calibration curve

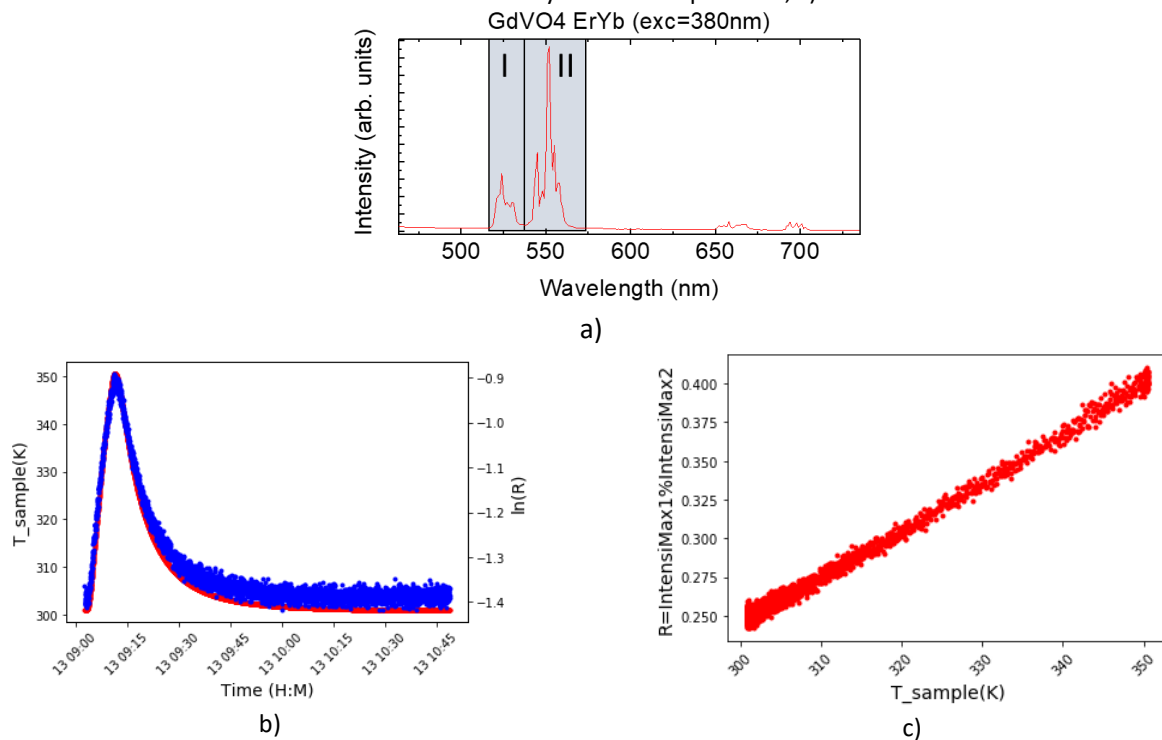


Figure 10. GdVO₄:ErYb – a) Luminescence spectra with the two pics used for thermoluminescence ratiometry (I_I/I_{II}), b) Variation of luminescence intensity ratio in temperature. c) Calibration curve

An innovative deposition technique was developed during this work and patented. The fibres are calibrated in temperature prior to using as thermal sensors for cell monitoring (see subtask 2.3).

The thermal sensitivity of Gd₂O₂S phosphor is not high enough for cell monitoring. Then, we are testing the second promising probe material with a higher thermal sensitivity from literature: GdVO₄:Er,Yb. This material was synthesized

by CEA and tested in powder. The results confirm the higher thermal sensitivity for this phosphor. However the deposition of the powder on optical fiber require to adjust the protocol. This work still under progress.

Lithium luminescent probe (OF/LumLi)

An extended state of the art of lithium luminescent probe was done at the beginning of the project and published in a review. From this work, we didn't identify a concept of luminescent probe working in carbonate environment (electrolyte solvent). We are developing a new concept of molecular luminescent probe (patent pending) to detect the Lithium in carbonate. This probe was tested first in aqueous medium and secondly in carbonate medium (EC:DEC, 1:1) with various concentrations of LiPF₆ (Figure 11). The results shown in Figure 11, the optical signature changes with the concentration of Lithium. This optical probe works with two fluorescence peaks. The peak at 440 nm (red curve) is independent of the LiPF₆ concentration and is used as reference. The intensity of the peak at 370nm increases with the Lithium concentration. This optical probe was covalently bonded on glass substrate and tested with the same conditions to validate the possibility of the deposition on optical fiber. The next step is to deposit this probe on the optical fiber and test it first in electrolyte environment and then inside the cell.

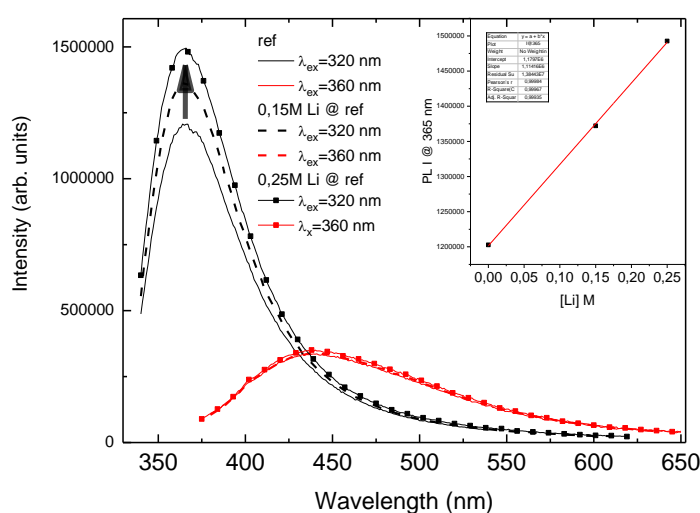


Figure 11. Luminescence spectra of optical Li⁺ probe in electrolyte (EC:DEC,1:1) for 3 different concentration of LiPF₆ : 0, 0.25, 0.15M.

Subtask 2.1.4 Evaluation and adaptation of a CO₂ sensor based on the photo-acoustic principle (PA)

After a careful joint analysis of the requirements, IFAG provided several samples of what was considered the most suitable existing engineering prototype of a PA-based CO₂ sensor (denoted as “PAS Gen 1.0” in Figure 12) to CEA and CNRS in December 2020, for a basic evaluation of the usability in the context of a LIB cell. The open architecture implementation of this PAS prototype consists of a gas measuring cell with an infrared (IR) emitter, a microphone with a high “signal-to-noise-ratio” (SNR) as the acoustic detector, and an XMC™ microcontroller for data processing (see Figure 13). The diffuser port on the top side of the measuring cell allows for efficient gas exchange while maintaining dust protection. The sensor module allows for integration via surface mount soldering via the pads on the bottom side of its PCB. All the key components were developed in-house at IFAG. To ensure efficient and quick evaluation, the sensor was provided to CEA and CNRS together with an evaluation kit (ensuring communication to a PC GUI via micro USB and a 12V power supply for the IR emitter) and an easy-to-use PC graphical user interface. A series of tests was performed on these early samples by CEA and CNRS, using different approaches to emulate the incorporation of these PA-based CO₂ sensor into an operating cell. These tests confirm the basic gas sensing functionality during battery operation, successfully concluding Phase 1 of subtask 2.1.4. However, the tests also revealed certain deficiencies of PAS Gen 1.0.

Based on these test results, IFAG implemented several improvements of the PA-based CO₂ sensor. The main change in the hardware consisted in the installation of a completely new emitter and filter package. More concretely, the emitter package was changed from a “liquid crystal polymer” (LCP) to a ceramic package, including an upgraded filter and sealant glue. This change is fundamental to enable the required measurement of extremely low CO₂ values (at about 2ppm) with relatively low noise and generally increases the reliability of the sensor. IFAG also introduced a temperature feedback loop to the sensor system, to improve the stability of the output values. In order to fully support these hardware changes and the related added functionality, an upgrade of the firmware was required, both on the level of the microcontroller and on the level of communication. Finally, the software was upgraded to allow a calibration of the PA-based CO₂ sensor in the actual battery environment. The resulting version is included as “PAS Gen INSTABAT Special 1.0” in the overview in Figure 13. Two samples of this version were provided to CEA in September 2021 and six more in February 2022.



Generation	PAS Gen 1.0	PAS Gen INSTABAT special 1.0	PAS Gen INSTABAT special 2.0
Status	Engineering Prototype 13.8 x 14 x 7.5 mm ³	INSTABAT special release 1.0 13.8 x 14 x 7.5 mm ³	INSTABAT special release 2.0 13.8 x 7 x 7.5 mm ³
Facts and purpose	<ul style="list-style-type: none"> • CO₂ sensing only • Smallest CO₂ sensor available in the market • Learnings in the field • Dual power supply (3.3V + 12V) 	<ul style="list-style-type: none"> • CO₂ sensing only • High performance then PAS Gen1.0 • With new and powerfull emitter/filter package • Capability of temperature feedback loop • Updated firware/software capabilities • Dual power supply (3.3V + 12V) 	<ul style="list-style-type: none"> • CO₂ sensing only • Same performance as INSTABAT special release 1.0 • Cost / size down are the main focus • Dual power supply (3.3V + 12V)

Figure 12. Different generations of the PAS CO₂ sensor by IFAG, as detailed in the text.

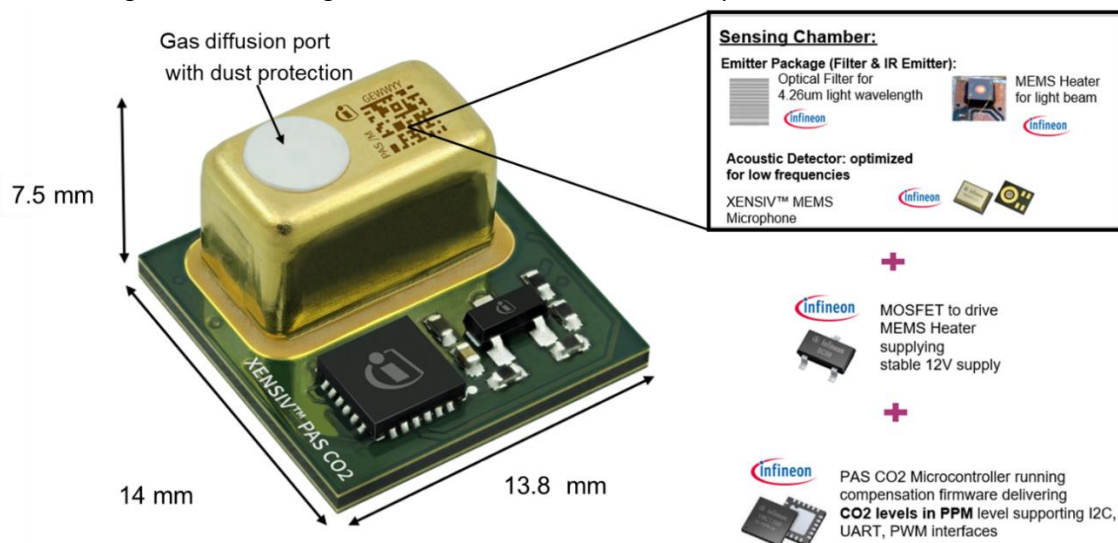


Figure 13. Basic components of the PAS CO₂ sensor Gen 1.0 by IFAG

Subtask 2.1.5. Sensors stability and adaptation related to the battery cell environment

Optical fiber (OF/FBG)

The optical fiber sensors that will be used to monitor temperature, strain, and pressure variations inside the cells, will be manufactured in different types of optical fibres (as described on deliverable 2.2 of *INSTABAT* projects). These optical fibres are typically composed by silica, and as they will be integrated into the pouch cells, together with the electrolytic solution (EC/EMC (3:7 vol.) 1M LiPF₆ + 2%w VC, Sol-Rite™), stability and adaptation tests are being carried out. In this way, stability tests were started to be designed with a row number of samples. Different types of optical fibres were prepared and inserted in aluminium bottles (50 mL capacity), submerged in the electrolytic solution (~25 mL). In total, 15 samples were prepared, 6 with SMF fibres, 6 with PANDA fibres, 2 with FBG sensors inscribed on PANDA and BOW-TIE fibres and 1 with a photonic crystal fiber. All the bottles were inserted in a chamber with controlled pressure and permanent nitrogen environment, at room temperature. The optical spectra of the fibres with the FBG sensors have been registered every week. One bottle with the SMF and PANDA fibres without FBG sensors, will be removed from the bottles on the months 3, 6, 9, 12, 18, and 24, to perform a characterization by Scanning electron microscopy (SEM) and Energy-dispersive X-ray spectroscopy (EDS) analysis over time.

- SEM and EDS analysis:

As of the date of this report, just three SEM and EDS analysis were performed, corresponding to the optical fibres immersed at 3, 6, and 9 months in the electrolyte. In the standard optical fibres, it was totally removed the coating layer and cleaned with wipes (Kimtech) and ethanol. To observe whether there were some particulate depositions, it was conducted the recovery in the air rather than a protective atmosphere. The SEM images were acquired using a Vega 3 SBH system (TESCAN) with a secondary electron detector, high voltage of 5.0 kV and working distance of 14.93 mm. The optical fiber samples were spirally affixed in the aluminum sample holder using double sided carbon tape. EDS was performed using a system incorporated into the Vega 3 SBH SEM. The specific parameters of the EDS measurements varied depending on the sample observed. SEM coating Unit E5000 from Polaron Equipment Limited was used to deposit the carbon film. In Figure 14 and Figure 15, are presented the SEM and EDS images taken from the PANDA optical fibres during the three different times.

Figures 6. A) and B) represent a standard and PANDA fiber 3 months in the electrolyte, respectively, where it is possible to see a cleaned fiber without material deposition and a small presence of precipitates in the fiber surface. Figures 6. C) and D) are shown the PANDA fibres, after 6 and 9 months immersed in the electrolytic solution, respectively, and it can be observed the presence of more quantity of precipitates on both fiber surfaces, and an increase of the crystal's dimensions can also be observed.

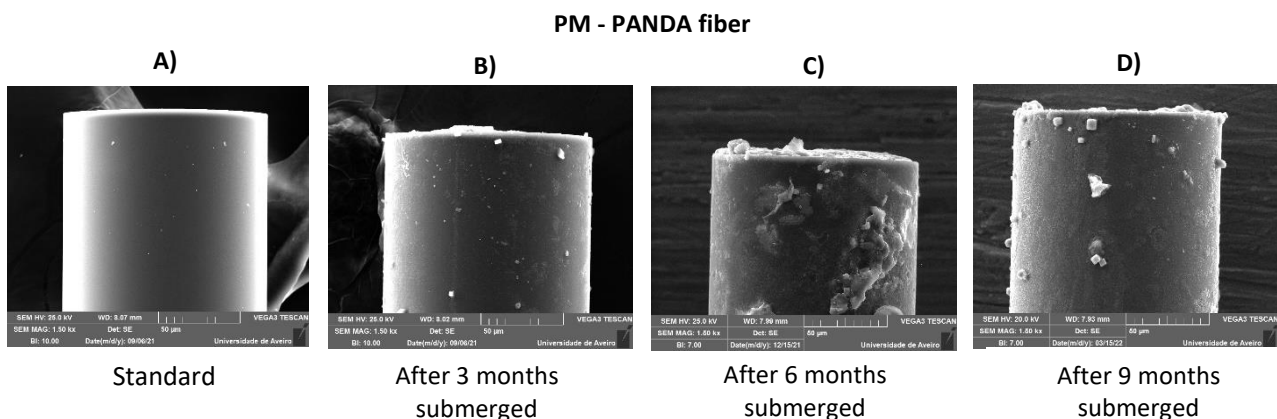


Figure 14. SEM characterization of a standard and after 3, 6 and 9 months of a PM-PANDA fiber immersed on the electrolytic solution, LiPF₆.

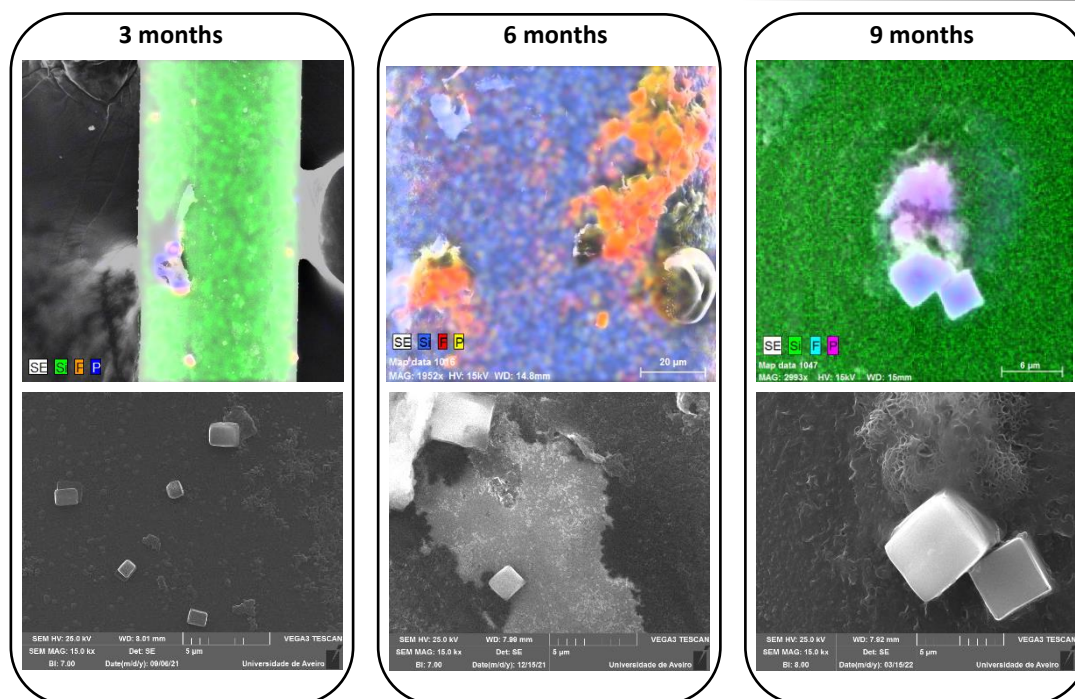


Figure 15. EDS analysis after 3, 6 and 9 months of a PM-PANDA fiber immersed on the electrolytic solution.

By an EDS analysis, it was possible to conclude that these precipitates are composed by phosphorus (P) and fluorine (F) elements, as shown on Figure 7. However, no degradation/etching phenomena were observed on the fiber surfaces. After 9 months, crystal dimensions of $\sim 5.0 \mu\text{m}$ can be observed.

In Figures 7 and 8, it is presented the EDS analysis for the PANDA fibres, after 3, 6, and 9 months immersed in the electrolytic solution. In all cases, it was identified the presence of a characteristic peak of phosphorus (P), silicon (Si), and fluorine (F) elements. As the Si element is one of the materials that compose the optical fiber, it was well identified on the EDS analysis. However, the presence of peaks for the P and F elements, reveal the existence of some precipitates, composed by these elements, on the fiber surfaces. In both EDS analysis, the F element represents a little higher peak quantity.

It is important to mention that, if during the following tests (SEM and EDS analyses for the next months), any structural change will be observed and any corrosion can occur in the optical fibres surface, due to a strong interaction with the electrolyte, which promotes an optical spectral change, an adaptative procedure should be considered and implemented. In this way, an alternative solution could be the integration of the optical fibres in a superficial layer of the pouch cells, or by using a protective material around the fibres, reducing their contact with the electrolytic solution.

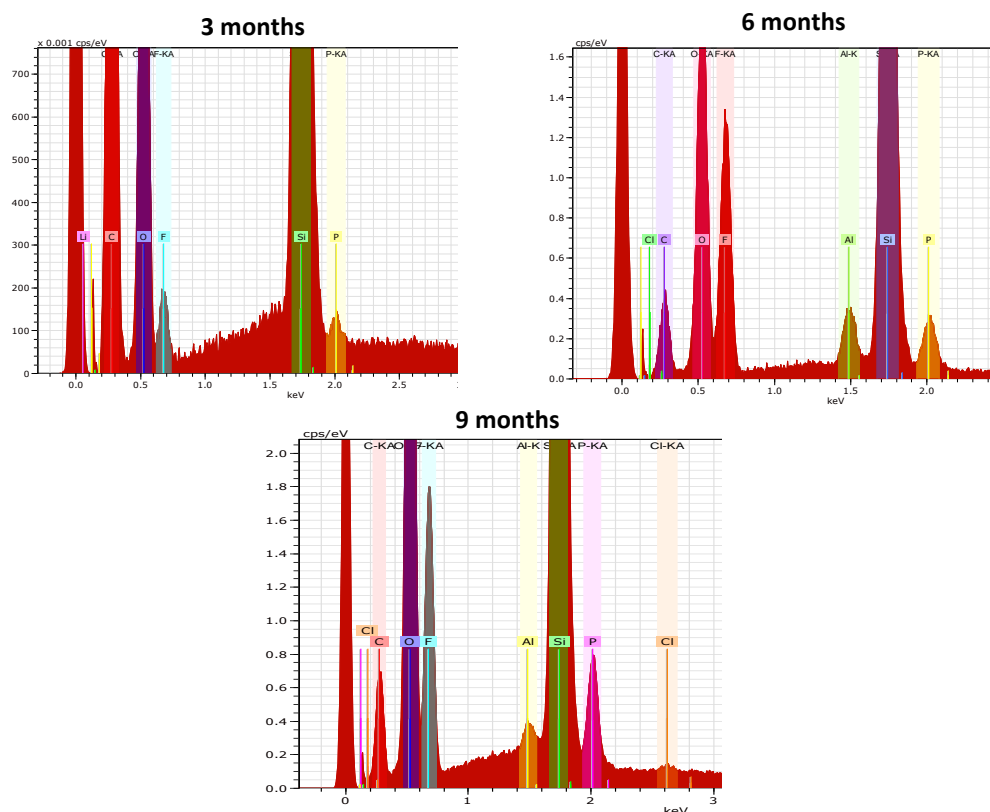


Figure 16. EDS analysis for the PANDA fiber after 3,6, and 9 months immersed in the electrolytic solution.

Optical fiber (OF/Lum)

The optical fiber used (FT200EMT) presents an external coating of Tefzel (a fluoropolymer with a high chemical and mechanical resistance), which protects the fragile cladding and the core of the wave guide. The integration of this specific optical fiber in pouch cells has been carried out by a thermo-sealing step. The preliminary tests have demonstrated the good operation of the optical fiber after this integration step. Furthermore, the mono-stacked pouch cells instrumented with a temperature sensor have presented the same thermoluminophore emission spectrum than the temperature sensor alone before insertion, indirect proof of a correct integration of this sensor inside the pouch cell.

The presence of the electrolyte did not degrade the optical fiber during a short time (< 2 months). The stability tests are currently performed for a longer time at two temperatures ($T = 25^{\circ}\text{C}$ and $T = 55^{\circ}\text{C}$). The integrity of the thermoluminophore deposit on the end of the optical fiber has been indirectly proved by the conservation of the emission intensity of the thermoluminophore on the temperature sensor inserted inside the mono-stacked pouch cell. We performed this test after formation and after 4 months (note that this sample was conserved at the fridge at 5°C between the two experiments).

Reference electrode

We have followed the OCV potential of $\text{Li}_{0.5}\text{FePO}_4$ over time and then proceeded to relithiation to evaluate the capacity consumed during the elapsed period. The percentage of capacity lost per hour of storage at 25°C , 45°C and 55°C is shown in Figure 17. Capacity loss is very small at 25°C and is doubled at 45°C . At 55°C , the loss of capacity is very rapid, implying a potential drift in the shorter term, which reduces its useful life.

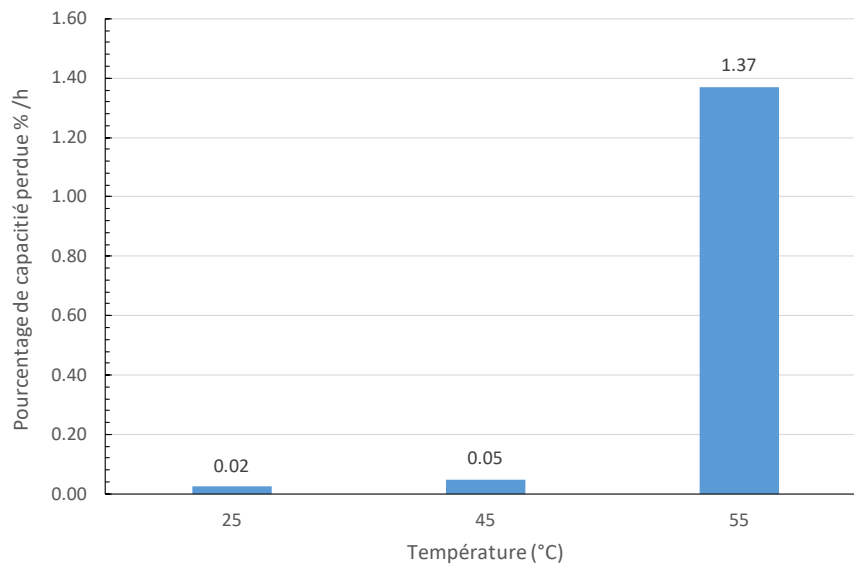


Figure 17. Percentage of capacity loss per hour at different temperatures

This loss of capacity is not irreversible as we have shown by reactivating the LFP stored at 55°C after its potential has drifted. Figure 18 shows that the effective capacity of the LFP reference electrode before and after storage at 55°C is not impacted and the potential profile still shows a very stable plateau. Thus, after reactivation, the LFP reference electrode is functional again.

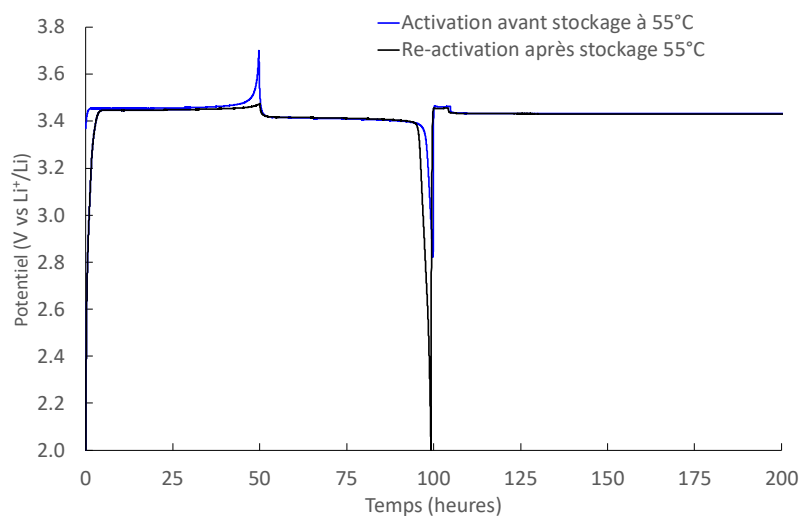


Figure 18. Re-activation of the reference electrode after drifting of the potential by storage at 55°C: delithiation/lithiation curves of LFP and delithiation at 50% of the lithiation capacity to place the potential in the middle of the plateau before (blue line) and after storage (black line)

To conclude, the stability of the LFP potential over time could be achieved at cell scale by reactivating the reference electrode before the appearance of a drift of its potential.

TASK 2.2: SENSOR HARDWARE INTEGRATION AND TEST

(Leader: CNRS; Participants: UAVR, CEA, IFAG) (M6-M24)

The sensor integration in the battery cell environment is being performed, by execution of long-term chemical resistance tests to certify that all physical sensors are adapted. Ageing tests will be performed: OF/FBGs by UAVR and CNRS, RE and PA by CNRS; OF/LumT, RE, OF/LumL and by CEA. Three main features will be covered:

- 1) Impact on the cell performance and safety of batteries containing the different sensors;

- 2) Impact on the performance of the different sensors when implanted in the battery cells;
- 3) Sensor positioning in the cell.

Subtask 2.2.1. Optical fiber / Fiber Bragg Grating (OF/FBG) sensor integration and test

The FBG sensors were being tested and integrated in different battery configurations to evaluate their performance during cells operation.

At UAVR, these sensors started to be integrated in a rechargeable cylindrical 18650 lithium battery by performing a central hole of the negative electrode (as shown Figure 19). Only to internal temperature monitorization, two FBGs were used in different locations (one in the centre and the other near the positive electrode) in a single and “free” optical fiber. To perform the optical fiber integration in safety conditions, the battery was firstly discharged up to 3.35V, to decrease their energy and the drilling process was performed in a glovebox with controlled nitrogen atmosphere. After that, an epoxy resin was used to seal the battery hole. After and before the battery drilling and optical fiber integration, the voltage value was not affected, registering also 3.35V. During the first tests, a slow charge (0.5 to 0.1 C) and 1.2 C discharge steps were applied and the FBGs signals were tracked during their operation. From the results, a successful temperature tracking was performed and higher ΔT values were recorded for higher C-rates and when the battery reaches the 3.0 V during the discharge step ($\sim 14.0\text{ }^{\circ}\text{C}$). A very slow difference of ΔT values was also detected between the two locations, during the charge step, which can be correlated with a thermal flow from the centre to the positive electrode. This preliminary test shows that the FBG sensors are able to be integrated and to detect temperature variations inside the cells. The next steps will be integrating the hybrid sensor configuration in these batteries as a proof of concept of real time temperature and pressure monitorization.

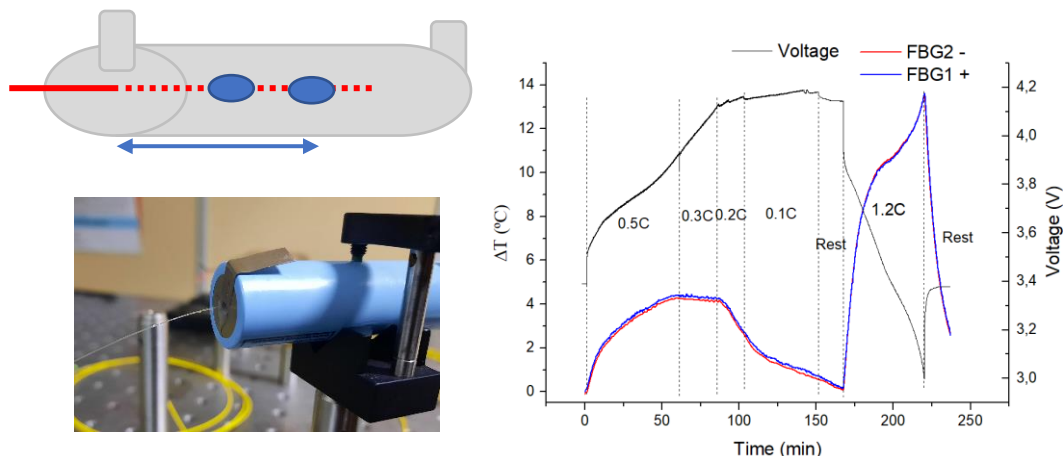


Figure 19. Preliminary FBG sensors integration and cycling test performed in an 18650-lithium battery

The OF/FBG sensors are also be integrated in pouch cells configurations at CNRS (Figure 20). For that, two prepositions will be tested. On the first one, the optical fibres will be attached to the pouch bag and placed inside the cathode material. This will enable the real time temperature and strain monitorization during cell operation. For the second preposition, the optical fiber is placed between the negative electrode and the separator, being attached to the electrode material with epoxy. This preposition allows also the monitorization of temperature and strain promoted between the negative and separator materials. For that, the shipped FBGs on PANDA fibres will be tested.

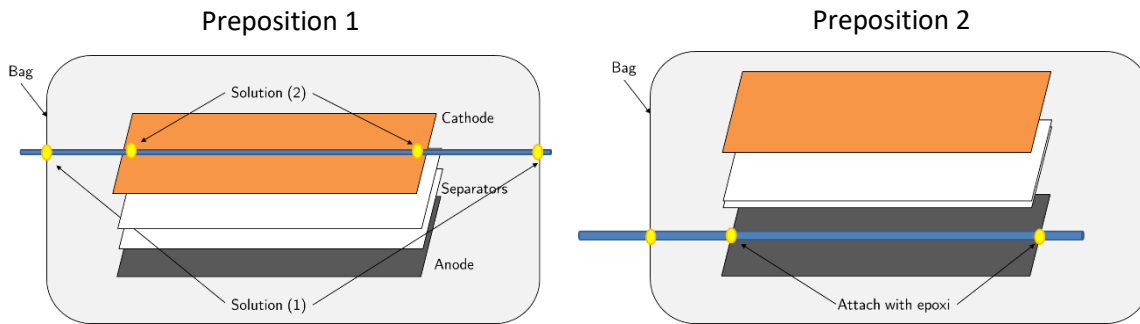


Figure 20. Different preposition tested to optical fiber integration in the lithium pouch cells.

Subtask 2.2.2 Reference electrode (RE) integration and test

After a preliminary test on the RE samples with different shapes and coatings, it was selected the antenna shape with gold coating and an additional LFP layer. The RE sensor was located in a central position on the active area of the cell. To analyze if the lithiation/delithiation of gold was reversible, it has been performed 10 galvanostatic cycles (Figure 21 A). That is an important aspect to consider in the perspective of taking to reinitialize the RE periodically in the event of a drift of its plateau potential. A capacity fading was observed cycles (Figure 21 B), however without a strong degradation of the plateaus, making it possible to provide for reactivation of the RE in the event of a shift of its potential.

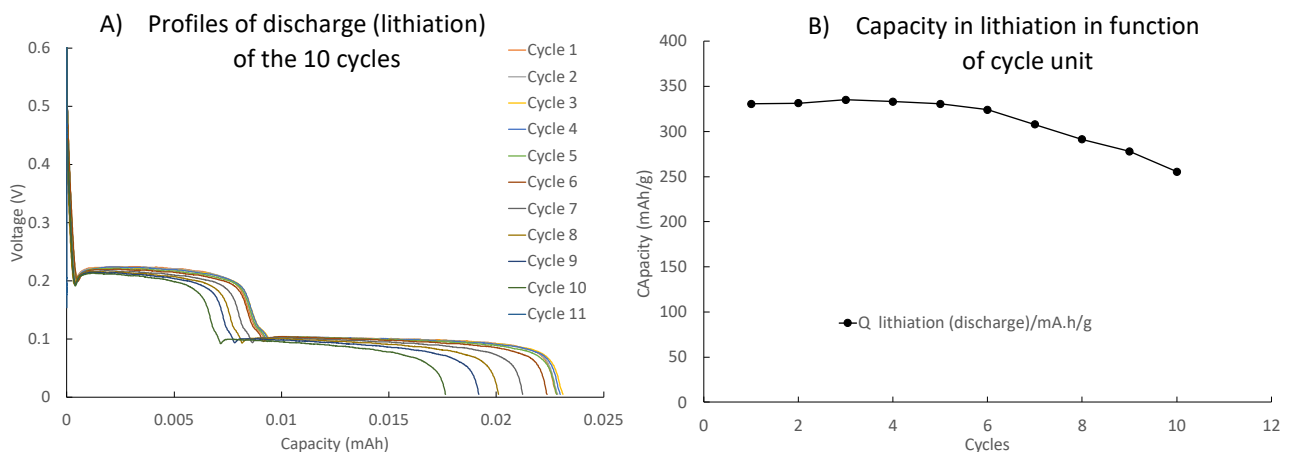


Figure 21. Lithiation/delithiation cycles of Gold ($I = 6 \mu\text{A}$, [1V – 10 mV]). A) Profiles of discharge during the 10 cycles. B) Capacity in lithiation in function of cycle number.

The electrochemical protocol applied consisted to a first delithiation/lithiation cycle at $42 \mu\text{A/day}$ and $67 \mu\text{A/day}$ to evaluate the LFP capacity. A partial delithiation step was then performed to fix the state of lithiation of LFP at 50%. The potential of LFP was recorded to evaluate its stability over time (Figure 22). It can be seen that the potential was stable over time. Therefore, for the integration in pouch cells, electrodes with a gold deposit coated with LFP will be used.

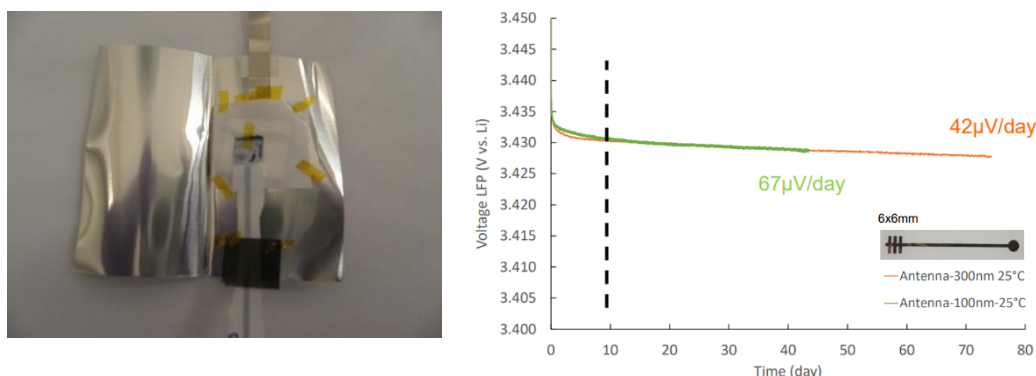


Figure 22. Left - Pouch-cell with LFP/Au film electrode before sealing. Right – Stability test of LFP/Au during 75 days for two different Au thickness (100 and 300 nm) (state of lithiation = 50%).

Subtask 2.2.3. Optical fiber / Luminescence (OF/LumT and OF/LumL) integration and test

This work has been performed initially with mono-stacked pouch cells (CEA lab standard cell with Varta electrodes) (Figure 23). We demonstrated in the Deliverable D3.1 (Figure 11, page 14) that the instrumentation of pouch cells with optical fibres does not modify the percentage of irreversibility (1st cycle of formation protocol) : $15.1 \pm 1.3\%$ for non-instrumented pouch cells and $15.1 \pm 1.1\%$ for instrumented pouch cells. The electrochemical protocols used on these non-instrumented and instrumented cells were similar. A small decrease on the discharge capacity per gram of NMC and the discharge capacity per surface of NMC (positive electrode) was observed in comparison with non-instrumented pouch cells (see Figure 9, page 13 in Deliverable D3.1): 155.7 ± 1.1 mA.h/g for non-instrumented pouch cells and 149.2 mAh/g for instrumented pouch cells. However, this small variation can be explained by the experimental variability between the samples. It is mainly due to the manual assembling protocol of mono-stacked pouch cells. We give on Figure 24 an example of the formation curves for a pouch cell instrumented with an optical fiber and for a non-instrumented mono-stacked pouch cell.

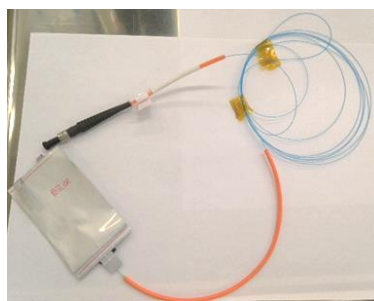


Figure 23. Integration of an OF-LumT sensor in a pouch cell (monolayer).

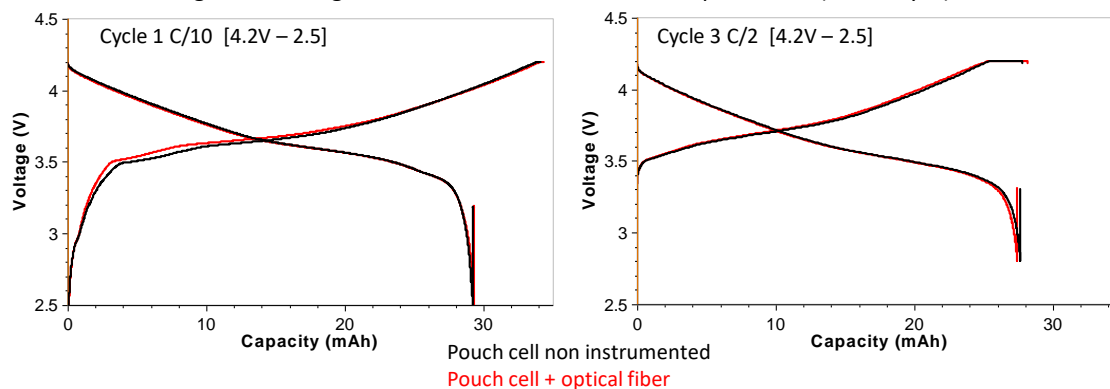


Figure 24. Example of the formation curves for the first cycle at C/20 and the third cycle at C/2 for a pouch cell instrumented with an optical fiber and for a non-instrumented pouch cell.

Regarding the capacity and internal resistance measurement, a variability in C/5 capacity and internal resistance at 25°C were observed for instrumented and non-instrumented pouch cells, which is explainable by the experimental reproducibility of assembly (Figure 16). Comparatively, the charge and discharge capacities and internal resistance remained in the same range. The integration of the optical fiber on pouch cells does not really modify the electrochemical properties of the pouch cells.

	Non instrumented pouch cell	Instrumented pouch cell
Internal resistance (Ω)	1.39 ± 0.03	1.28 ± 0.19
Capacity C/5 (mAh)	28.76 ± 0.67	27.96 ± 0.21

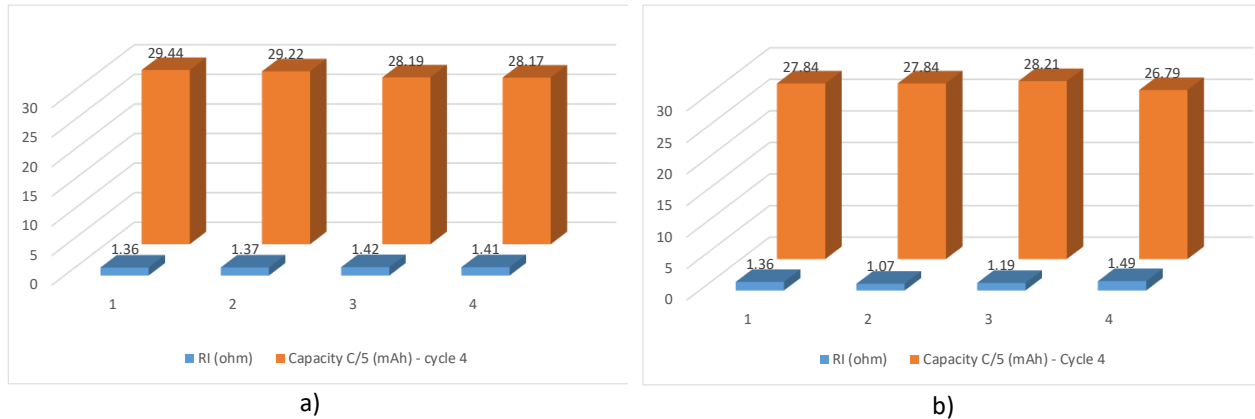


Figure 25. Comparison of the charge and discharge capacities of charge and discharges for non-instrumented pouch cells (a) and pouch cells instrumented with thermoluminescent optical fibres (b)

The instrumented cell with OFLumT sensor has been tested in cycling condition with a C/2 charge and C/2, C and 2C discharges. External cell temperature was measured with a K-type thermocouple is used as reference temperature. Figure 26 shows the results. We can clearly show the variation of luminescence spectra during the high discharge rate is correlated to the cell temperature increase. Unfortunately, the increase of cell temperature is low (less than 2°C). In this case, the sensor accuracy is too low. To improve the sensor, we need to work on the optical probe to improve the accuracy.

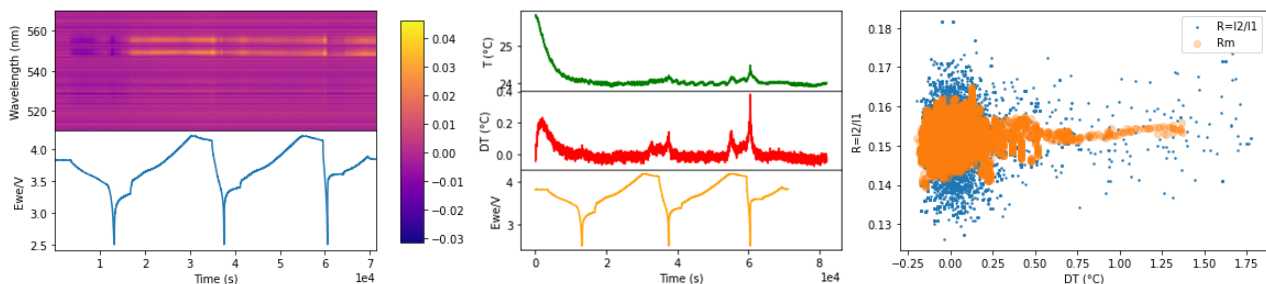


Figure 26. Test of OFLumT sensor inside a pouch cell (monocell) under cycling condition: Optical spectra variation and cell potential over the time (left). Absolute and relative surface temperature as function of time compared to cell potential (center). Calibration curve of luminescent signal (peak ratio) versus relative temperature with and without noise reduction (right).

To qualify the sensor and have a reliable proof of concept, we have decided to test cells with higher capacities. Therefore, we also used commercial cells (Lifun 1.1 A.h NMC622/graphite) provided by CNRS. A first experiment with external measurements (OFLumT sensor placed in the center of the cell surface) with a charge rate of C/2 and discharge rates of 1D, 2D, 2D and 4D has shown a temperature increase from 3°C to 17°C in discharge (depending on the regime). We observe a good detection of the temperature increase by the OFLumT sensor (see yellow curve) with a linear dependence on the temperature. The sensor shows a good resolution for a temperature variation of 2°C.

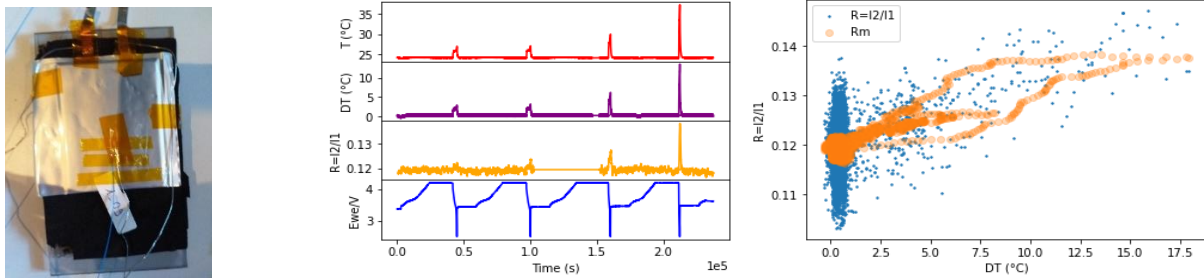


Figure 27. Test of OFLumT sensor outside a pouchcell (1.1 Ah) (left) under cycling condition (C/2; 1D, 1D, 2D and 4D): Absolute and relative surface temperature variation, response of OFLumT sensor placed on the cell surface and cell potential over the time (center). Calibration curve of luminescent signal (peak ratio) versus relative temperature with and without noise reduction (right).

A Lishen cell of 1.1Ah was instrumented with OFLumT in the center of the electrode stacks and tested in cycling conditions:

Four cycles at rates of 4D + D/5 and C, then at rates of C/2, D/5, C, D/5, 2C). The Figure 28 shows the comparison between the luminescent signal and the surface temperature variation over the cycling protocol. We observe then a good correlation between these two signals. The signal from the sensor is linearly dependent on the temperature with a reduced noise after data treatment. This data treatment improves the accuracy of the sensor around 1°C.

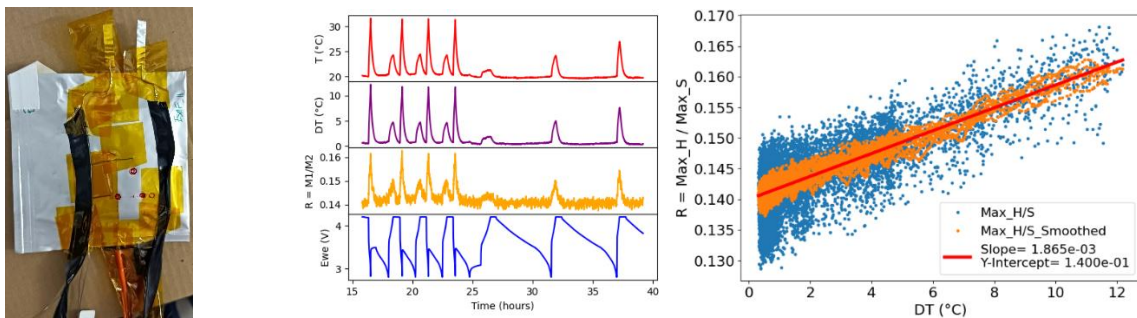


Figure 28. Test of OFLumT inside a pouchcell (1.1A.h) (left) under cycling condition (C, 4D + D/5, C/2+D/5, C+D/5 and 2C/D/5): (left) Absolute and relative surface temperature variation, response of OFLumT sensor inside the cell and cell potential variation (left). Calibration curve of luminescent signal (peak ratio) versus relative temperature with and without noise reduction (right).

To conclude this part, the integration of the OFLumT sensor inside the cell has no impact on the cell performances. These results show the operability of the sensor inside the cell. The optical response inside and outside the cell have the same temperature dependency. Accuracy of the OFLumT is around 1°C with appropriate data treatment and will be improved to fit with the requirements of the project. Finally, these results validate the sensor integration inside the cell and this sensor will be used for the ageing tests on multilayer cells (WP3).

Subtask 2.2.4. Gas sensor (PA) integration and test

Two versions of Infineon PAS CO₂ sensors have been tested at CEA institute (see Figure 12 and Figure 29). For both versions, a dedicated software developed by Infineon is necessary to collect the data measured by each sensor. These sensors are designed to perform CO₂ measurements in air atmosphere. Furthermore, they must operate in conditions close to the atmospheric pressure. Then, these sensors must be calibrated in neutral atmosphere and in harsh atmosphere with electrolyte vapour. Their sensibility and detection limits in these atmospheres must also be determined. We first performed calibration and sensitivity tests in Ar.

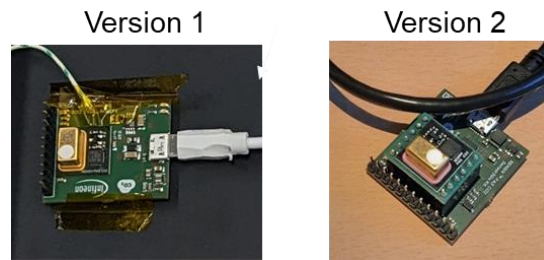


Figure 29. Two versions of Infineon PAS CO₂ sensor tested (version 1=PAS GEN 1.0, version 2= PAS Gen INSTABAT special 1.0 cf Figure 12)

A hermetic chamber was specially designed by CEA and manufactured to perform gas concentration measurements on opened cells under cycling condition (see Figure 30). This chamber has been also used to perform sensors calibrations. Two different approaches have been used to perform sensors calibration: 1- with gas cylinder at different concentration; 2- with an Alytech Gasmix™ Nomad dilution bench (see Figure 30).

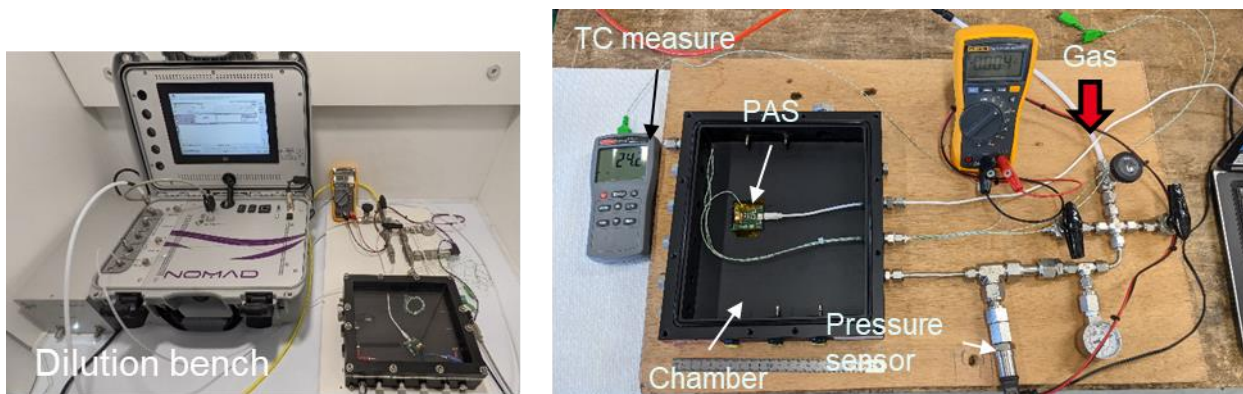


Figure 30. Setup for CO₂ sensors calibration: dilution bench (on the left) and hermetic chamber with inlet pipe circuit.

The gas cylinders had calibrated CO₂ concentrations from 100 ppm to 5000 ppm. The dilution bench is used to calibrate sensor at decreasing concentrations from 50 ppm to 2 ppm. Results are shown in Figure 31. The post processing of these data gives us the calibration in Ar for the first version of PAS CO₂ sensors as shown in Figure 32. PAS CO₂ sensors measure CO₂ in Ar with a good correlation to CO₂ in air with a monotonic variation. The detection limit is detected up to 2 ppm with relatively low error. However, we did not test the sensors below 2 ppm during this campaign. Calibration tests are currently performed on sensors from a PAS Gen INSTABAT special 1.0 version.

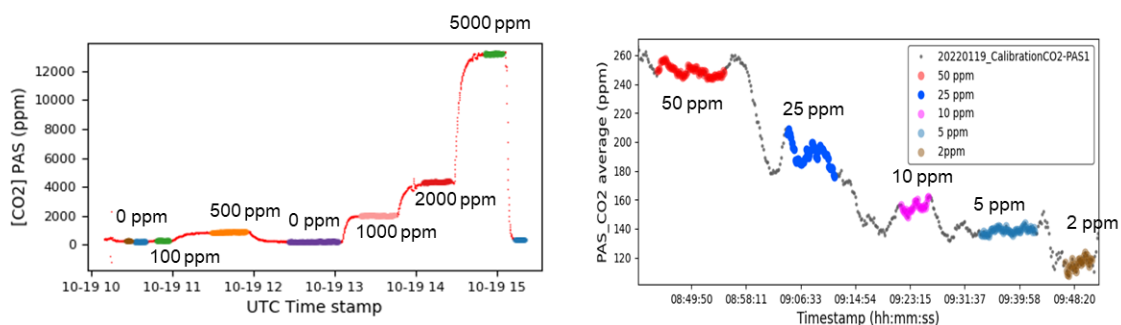


Figure 31. Calibration data from the first version of PAS CO₂ (PAS Gen 1.0) sensor using gas cylinders (left) and gas dilutor (right)

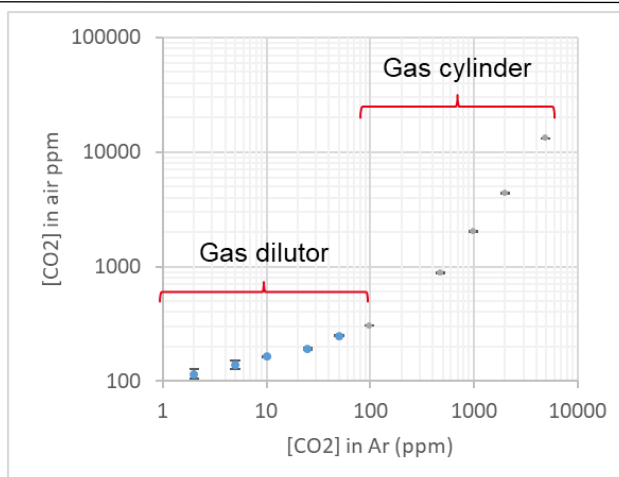


Figure 32. Calibration curve between CO₂ concentration in Ar (from the gas dilutor and gas cylinders) and CO₂ concentration in air (measured by the sensor) for the first version of PAS CO₂ sensor (PAS Gen 1.0).

The PAS Gen 1.0 sensor provided by Infineon has been implemented in battery by CNRS using a different strategies. The first one, shown in Figure 33 a, consists of placing the bag containing the electrolyte and the jelly roll and the PAS sensor in a larger pouch bag. In this case, the sensor is not directly in contact with electrolyte and can sense the gas passing through the hole drilled in the pouch cell in glovebox. A hole is drilled in the big pouch bag to allow the large USB cable to power the PAS sensor. It is then covered with epoxy resin cured for 24 hours to avoid leaks. In this configuration, the cell cannot be vacuum sealed or degassed after the formation cycles, which is likely to affect cell performances. However, as observed in Figure 33b and 33c, the performances of the cell instrumented with PAS CO₂ sensor are only slightly lower than the pristine cell performances. Then this configuration can be used for the implementation of the PAS sensor inside cells since the different parameters influencing its values can be decoupled.

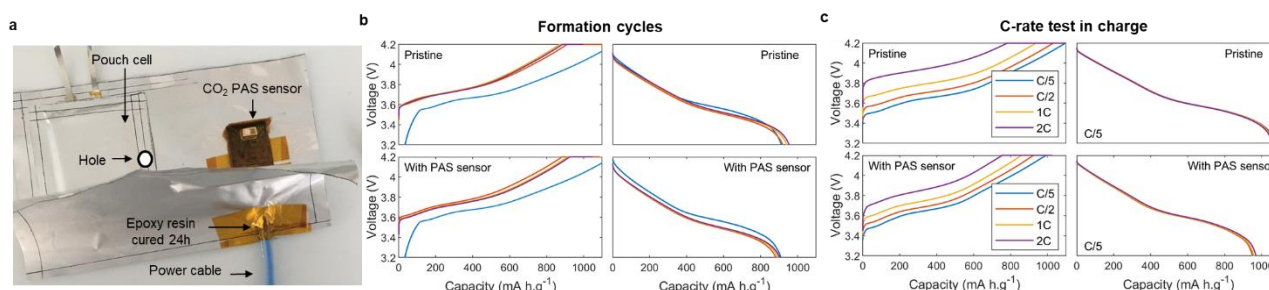


Figure 33. (a) Picture of the instrumented bag with a pouch cell and the PAS CO₂ sensor. To allow contact between the gas and the sensor, a hole is drilled in the pouch cell in glovebox. The power cable passes in the bag through a hole covered with epoxy resin cured for 24 hours to avoid leaks. Formation cycles (b) and C-rate test in charge (c) at 25°C for pristine LiFUN cell (top) and LiFUN cell instrumented with CO₂ PAS sensor.

Indeed, different parameters seem to influence the value of the sensor. As demonstrated in Figure 34a, when the cell is cycled, the sensor responds with an increase of the CO₂ concentration during charge and a decrease during discharge. However, the value of 6000 ppm is not realistic. By reproducing the measurements, the same variation is observed but the value of -25000 ppm was obtained. Regarding the variation, the influence of other parameters has been confirmed. Indeed, by changing the temperature of the oven containing the cell, we observe an important variation of the CO₂ concentration given by the sensor (see Figure 34b). The sensor is then also sensitive pressure. As described in WP2, Infineon is now working on a new version of its sensor. More investigation are required in the future to understand the impact of the protocol of sample preparation to the sensor response. The impact of the pressure during the sample preparation and cycling must be study in deeper way to manage the response of the sensor.

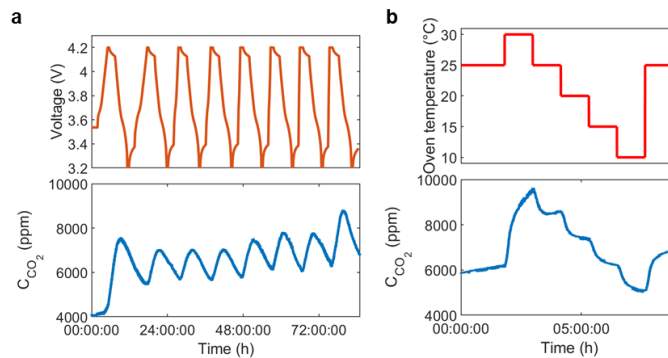


Figure 34. (a) C-rates in charge test and CO₂ concentration given by PAS sensor. (b) Variation of the CO₂ concentration given by the sensor in function of the temperature of the cell

Beyond highlighting the basic functionality, the tests performed at CEA and CNRS on the PAS Gen 1.0/ PAS Gen INSTABAT Special 1.0 samples also clearly demonstrate that the implementation of the PAS CO₂ sensor still imposes severe physical limitations for future integration into the cell. The size of the sensor system (refer to Figure 12 for the dimensions) and the connection via a USB cable were identified as the main hurdles in this regard. To overcome these obstacles, IFAG has started to work on another design, denoted as “PAS Gen INSTABAT Special 2.0” in the overview in Figure 12. As indicated there, the main improvements targeted in this version consist in a separation of the sensing chamber from the other electronics (thereby instantly halving the size of the part of the sensor to be integrated into the battery cell) and the implementation of a connection between sensing chamber and electronics via a Flex PCB. The work on this new generation is still in progress at IFAG.

Table 3. *List of deliverables WP2*

Deliverable Number	Deliverable Title	Lead beneficiary	Type	Dissemination level	Due date (in month)	Status
D2.1	Report on present state-of-art for sensors in Liion batteries	7 – UAVR	Report	Public	3	Submitted
D2.2	Protocol for sensors fabrication	7 – UAVR	Report	Confidential	12	Submitted
D2.3	Protocol for sensors adaptation to cell environment	7 – UAVR	Report	Confidential	15	Submitted
D2.4	Report on sensor integration feasibility and impact on cell and sensors performance	3 – CNRS	Report	Confidential	24	N/A
D2.5	Prototypes of each finalised sensor	7 – UAVR	Demonstrator	Public	24	N/A

Table 4. relevant Milestones associate to WP2

Milestone Number	Milestone Title	Lead beneficiary	Due date (in month)	Status
MS3	Sensors prototype available and validated in battery cell environment	7 – UAVR	24	N/A

WP3 - Correlation between measured/estimated parameters and physico-chemical degradation phenomena occurring in the battery cell

CNRS, CEA, UAVR

Work package number	3	Leader	CNRS						
Work package title	Correlation between measured/estimated parameters and physico-chemical degradation phenomena occurring in the battery cell								
Participant number									
Short name of participant	UAVR	CEA	CNRS						
Person months per participant	7	11	35						
Start month	M6		End month				M32		

Objectives

The objective of WP3 is to correlate the physical sensor measurements (sensor signals output) and the virtual sensors estimations with the physico-chemical phenomena occurring in Li-ion battery cells. The main objectives of this WP are the following:

- Characterise the electro-chemical performance of pristine and instrumented cells;
- Identify the significant physical sensor outputs during cycling conditions;
- Characterise significant physico-chemical phenomena of the battery cells, in particularly signals correlated to degradation;
- Validate virtual sensors values with respect to the reference Newman model and outputs from sensors in instrumented cells;
- Correlate physical/virtual sensor output signals to physico-chemical phenomena of the battery cells.

Highlights of most significant results

Batteries are evolving systems, throughout their life the electrolyte and material will degrade to form interfaces, soluble products and gaz. By using sensors developed in WP2, these phenomena can be detected and understood providing unique information about degradation mechanism.

The first challenge of WP3 is to implement the different sensors to battery without affecting the electrochemical performances. In this context, pouch cell have been tested with or without sensors. In order to compare results between the different partners of the project, we agreed on material, electrolyte and electrochemical protocol (detailed in task 3.1). In doing so, electrochemical tests on pristine cells at different temperatures have been performed. Moreover, experimental conditions have defined to reproduce the extreme conditions that batteries can undergo during their life (temperature, current). These tests will later be used as a reference for comparison with instrumented pouch cells and highlight the good performance of the material/electrolyte combination, giving confidence in their potential use in real applications.

Knowing this, different tests of sensor integration have been carried out. Regarding the optical fibres, their small diameter, their good chemical stability in organic electrolytes (see WP2) and their robustness allow their integration directly during the sealing of the pouch bag. Indeed, it is possible to place the fiber between the upper and lower part of the bag, during the welding at high temperature, the polymer covering the bag will melt slightly ensuring a good sealing. Thanks to this easy integration, optical fiber sensors have been integrated into pouch cells without affecting the electrochemical performances. Using the same strategy, reference electrode sensor can be implemented at different position inside the cell without any problems. The greatest difficulties concern the integration of the CO₂ PAS sensor. Indeed, either because its diameter and its sensitivity to atmospheric conditions, these sensors cannot be implemented easily. However, while IFAG is already working on a reduction of the dimensions, CEA and CNRS explore two different ways for their integration. From CEA, a special box containing the sensor is under development. Thanks to a capillary, the gas will be able to pass from the pouch cell to the box. CNRS chose to implement the sensor using a second bag that can contain the pouch cell (jelly roll in a first bag) and the sensor. The bag of the pocket cell is pierced to allow gas to pass from the first bag to the second containing the sensor. The sensor power cable is attached to the bag with epoxy. In this configuration, the sensor is located close to the pouch cell but is isolated from direct contact with the electrolyte. However, during the cycle, the evaluation of the sensitivity of the first version of the PAS sensor to temperature,

pressure and humidity require more data to have proper exploitation of the results. Discussion within the WP2 is still necessary for this sensor.

Currently, only the FBG sensor, the Tlum sensor and the reference electrode are at a sufficient stage of development to adapt to the battery environment and be integrated without affecting electrochemical performance. However, the optical sensor and reference electrode already provide valuable information for the understanding of chemical degradation phenomena. Indeed, we have shown that FBG sensors are mostly temperature sensitive and by using a thermal capillary to protect the sensor from deformation or change in curvature during the pouch cell cycle, we were able to measure the temperature inside the jelly-roll in operando with very good accuracy. In addition, by placing FBG sensors inside, on the surface, and within a few centimetres of the pouch cell, heat transfer can be measured. In this context, a thermal model can be solved allowing to calculate heat, enthalpy and entropy. These energies are directly related to the chemical phenomena and allow accurate identification and characterization of SEI formation and cell aging. Using the Tlum sensor similar results could be obtain in theory. This sensor has the advantage of being totally insensitive to strain, pressure or curvature. However, if the preliminary results are encouraging the accuracy of the TLum is around $\pm 1^\circ\text{C}$ which does not allow to observe low current phenomena as well as the cascade reaction occurring during electrolyte decomposition. Concerning reference electrode, their used is well known since decades. The reference allows the distinction of contribution to current and voltage of each cell component to the overall battery performance and to study the degradation mechanism of individuals electrodes. The first results show that the gold film deposited on a separator and covered with a LFP can be used as a stable reference electrode without affecting the electrochemical performance.

Summary of progress towards objectives and details for each task

TASK 3.1 ACCELERATED TESTS ON INSTRUMENTED CELLS

(Leader CEA, participants CNRS, UAVR) (M6-M30)

CNRS and CEA have defined in the beginning of the project the electrochemical test protocols used to characterize the instrumented cells. To remind, two formats of cells have been tested:

- Standard CEA lab format with VARTA positive and negative electrodes (nominal capacity 29.6 mAh at C/5, RT)
- Li-FUN cell (nominal capacity 1170 mAh at C/5, RT)

The specifications of both cells are given in Table 5. They are almost similar in terms of nature of active materials and electrode coatings but the particle sizes and electrode porosities are not known that will influence their respective performances.

Table 5. Cell specifications

	Li-FUN cell	Standard CEA lab format
Nominal capacity (mAh) at RT (C/5)	1170	29.6
Voltage range (V)	4.2 – 3.0	4.2_ - 2.7
Cathode		
Cathode material	LiNi _{0.6} Mn _{0.6} Co _{0.2} O ₂	
Coating weight (mg/cm ²)	16.7	17.5
Active material loading (wt%)	0.964	/
Mass active material (g)	7.083	/
Real capacity (mAh/cm ²)	2.8	2.9
Coating thickness (μm)		61
Anode		
Anode material	Artificial Graphite	Graphite
Coating weight (mg/cm ²)	10.0	9.3
Active material loading (wt%)	9.948	/
Mass active material (g)	/	/
Real capacity (mAh/cm ²)	/	3.2
Coating thickness (μm)		55

Formation protocol

The formation protocol is conformable to the protocol proposed by VARTA. The test conditions are given in Figure 35 and Table 6.

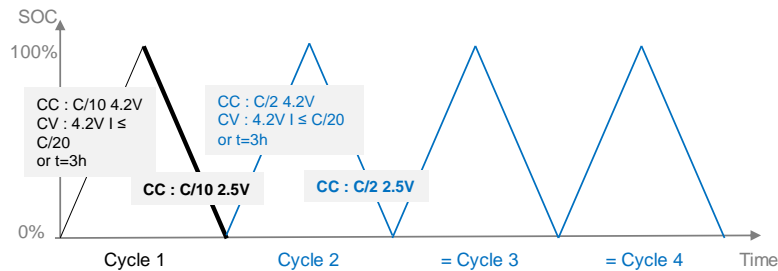


Figure 35 Schematic diagram of the formation protocol

Table 6 Formation protocol

Cycle	Value	Type	Limit
0		Rest	2h
1	C/10	CC charge	4.2 V
	4.2 V	CV charge	$I \leq C/20$ or $t=3h$
	C/10	CC discharge	2.5 V
		Rest	5h
2-4	C/2	CC charge	4.2 V
	4.2 V	CV charge	$I \leq C/20$ and $t=3h$
		Rest	5 min
	C/2	CC discharge	2.8 V
		Rest	5 min
	5 (→ if storage after)	C/2	CC charge

Note: The voltage limit in discharge will be 3.0V for Li-FUN cell.

Capacity and internal resistance measurement

The capacity and internal resistance measurement protocol is given in Figure 36 and Table 7. The internal resistance is measured at 50% of SOC.

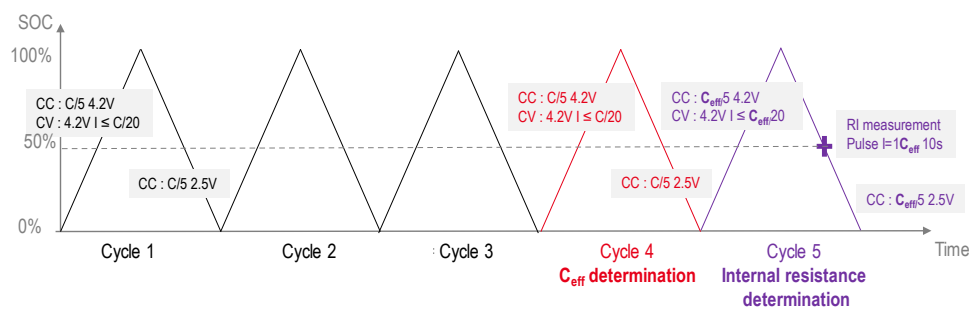


Figure 36. Schematic diagram of the capacity and internal resistance measurement protocol

Table 7. Capacity and internal resistance measurement protocol

Cycle	Value	Type	Limit
0		rest	5 min
1-3	C/5	CC charge	4.2 V
	4.2 V	CV charge	$I < C/20$
		rest	30 min
	C/5	CC discharge	2.5 V
		rest	30 min
4	C/5	CC charge	4.2 V
	4.2 V	CV charge	$I < C/20$
		rest	30 min
	C/5	CC discharge	2.5 V → Effective capacity C_{eff}
		rest	30 min
5		rest	30 min
	$C_{eff}/5$	CC charge	4.2 V
	4.2 V	CV charge	$I < C_{eff}/20$
		rest	1 h
	$C_{eff}/5$	CC discharge	2h30 → SOC 50%
		rest	30 s
	C_{eff}	CC discharge	10s → Internal resistance calculation
	$C_{eff}/5$	CC discharge	2.5V
		rest	30 min
6 (if storage after)	$C_{eff}/5$	CC charge	1h30 SOC 30%

Note: The voltage limit in discharge will be 3.0V for Li-FUN cell.

C-rate test

The C-rate tests are given in Figure 37 and Table 8 for discharge and in Figure 38 and Table 9 for charge. The test will be performed at 3 different temperatures: 25°C, 45°C and at -10°C. The value of the low temperature was chosen according to the test results performed on instrumented pouch cells with LFP reference electrode at -10°C.

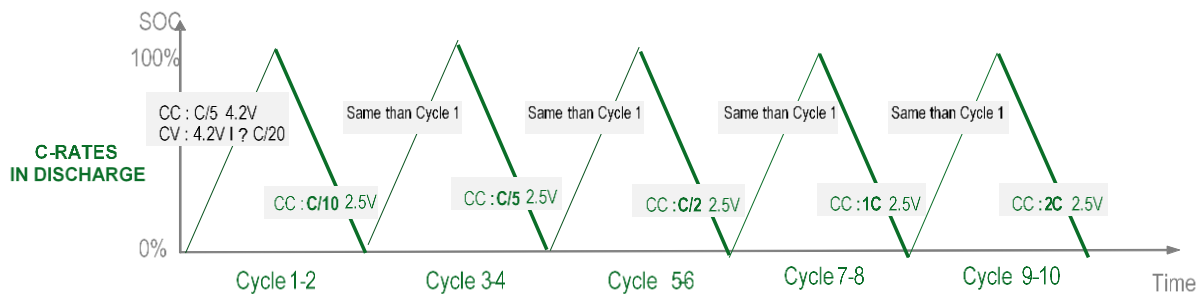


Figure 37. Schematic diagram of the C-rate test in discharge

Table 8. C-rate test in discharge

Cycle	Value	Type	Limit
0		rest	5 min
1-2	C/5	CC charge	4.2 V
	4.2 V	CV charge	$I < C/20$
		rest	240 min
	C/10	CC discharge	2.5 V
		rest	240 min
3-4	C/5	CC charge	4.2 V
	4.2 V	CV charge	$I < C/20$
		rest	240 min
	C/5	CC discharge	2.5 V
		rest	240 min
5-6	C/5	CC charge	4.2 V
	4.2 V	CV charge	$I < C/20$
		rest	240 min
	C/2	CC discharge	2.5 V
		rest	240 min
7-8	C/5	CC charge	4.2 V
	4.2 V	CV charge	$I < C/20$
		rest	240 min
	1C	CC discharge	2.5 V
		rest	240 min
9-10	C/5	CC charge	4.2 V
	4.2 V	CV charge	$I < C/20$
		rest	240 min
	2C	CC discharge	2.5 V
		rest	240 min

Note: The voltage limit in discharge will be 3.0V for Li-FUN cell.

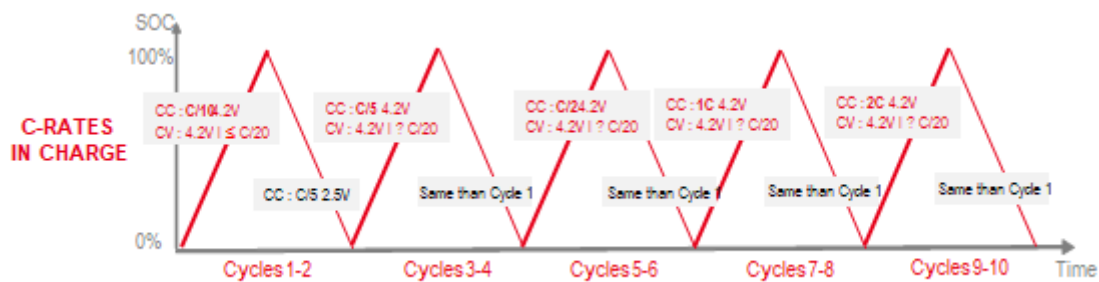


Figure 38. Schematic diagram of the C-rate test in charge

For each current rate, 2 cycles will be performed in order to verify if the thermal profile changes between the first to the second cycle. Note that the rest of 240 min between the charge and discharge step is required allowing the cell temperature to do back at the regulated temperature and thus to control the good response of the temperature sensor.

Table 9. C-rate test in charge

Cycle	Value	Type	Limit
0		rest	10 s
1-2	C/10	CC charge	4.2 V
	4.2 V	CV charge	$I < C/20$
		rest	240 min
	C/5	CC discharge	2.5 V
3-4	C/5	CC charge	4.2 V
	4.2 V	CV charge	$I < C/20$
		rest	240 min
	C/5	CC discharge	2.5 V
5-6	C/2	CC charge	4.2 V
	4.2 V	CV charge	$I < C/20$
		rest	240 min
	C/5	CC discharge	2.5 V
7-8	1C	CC charge	4.2 V
	4.2 V	CV charge	$I < C/20$
		rest	240 min
	C/5	CC discharge	2.5 V
9-10	2C	CC charge	4.2 V
	4.2 V	CV charge	$I < C/20$
		rest	240 min
	C/5	CC discharge	2.5 V
5 (if storage after)	C/5	CC charge	1h30 SOC 30%

Note: The voltage limit in discharge will be 3.0V for Li-FUN cell.

Fast ageing protocol

CNRS has proposed to qualify some sensors a specific test described in Table 10. It consists of evaluating the sensor response during overcharging at 4.4 V for 24 h and at 55°C. These conditions allow to produce heat, gas and lithium-plating, that will be identify respectively by thermal fiber, gas sensor and reference electrode.

Table 10. Fast ageing protocol

Lab	Cycle	Value	Type	Limit	
CNRS	25°C	1-5	1C	CC charge	4.2 V
			Rest	240 min	
		1C	CC discharge	3 V	
		Rest	240 min		
	25°C	+ Pulse 1C and 1.5C for FBG/OF thermal model calibration			
	55°C	6-16	1C	CC charge	4.4 V
			4.4 V	CV charge	t=24h
			rest	240 min	
		1C	CC discharge	3 V	
		rest	240 min		
25°C	17	+ GITT at 1C for OF/FBG entropy calculation			
25°C	18-22	1C	CC charge	4.2 V	
		Rest	240 min		
	1C	CC discharge	3 V		
	Rest	240 min			

Cycling protocol

CEA has proposed to develop a cycling protocol (Figure 39) in charge and according to a discharge protocol based on the World harmonized light vehicles test procedure (WLTP)⁸. This discharge profile is representative of a worldwide statistic study realized on real driving profiles. The methodology applied to calculate the WLTP cycle for the two format of cells is presented schematically in the Figure 40. It consists of converting the WLTP cycle corresponding to the ZOE electric vehicle for which the characteristics of the cell present in the battery pack are known in power per surface area of the positive electrode. The WLTP cycle can be thus calculated for the Li-FUN cell and the CEA lab standard format for which the positive electrode surfaces are also known. Note that CEA has proceeded to the dismantling of a Li-FUN cell to measure the electrode dimensions.

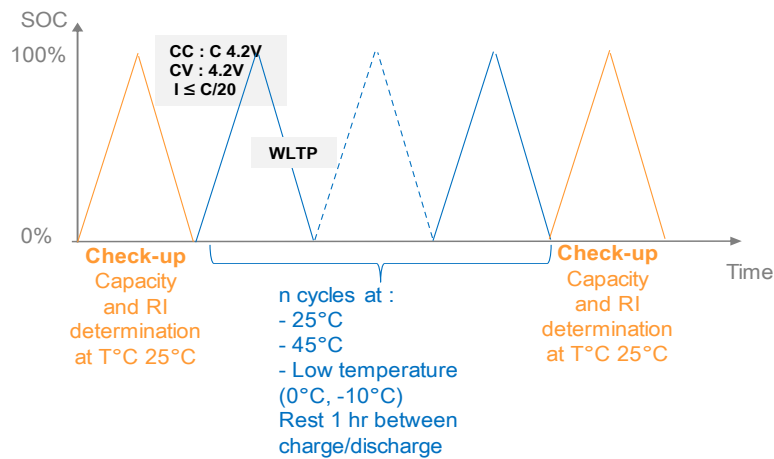


Figure 39. Schematic diagram of the cycling protocol

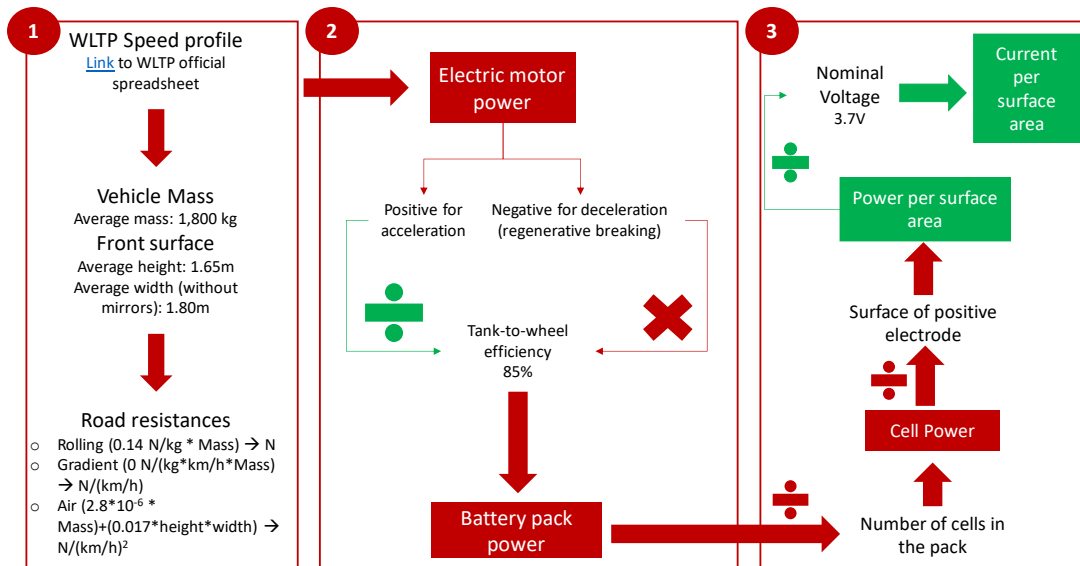


Figure 40. Illustration of the WLTP Power calculation procedure

The protocols for Li-FUN and mono cells prepared with VARTA electrodes are reported in the Figure 41 and Figure 42

⁸ Addendum 15: United Nations Global Technical Regulation No. 15. United Nations; 2019.
<https://unece.org/transport/documents/2021/01/standards/addendum-15-united-nations-global-technical-regulation-no-15-Spreadsheet>
<http://www.unece.org/fileadmin/DAM/trans/doc/2012/wp29grpe/WLTP-DHC-12-07e.xls>

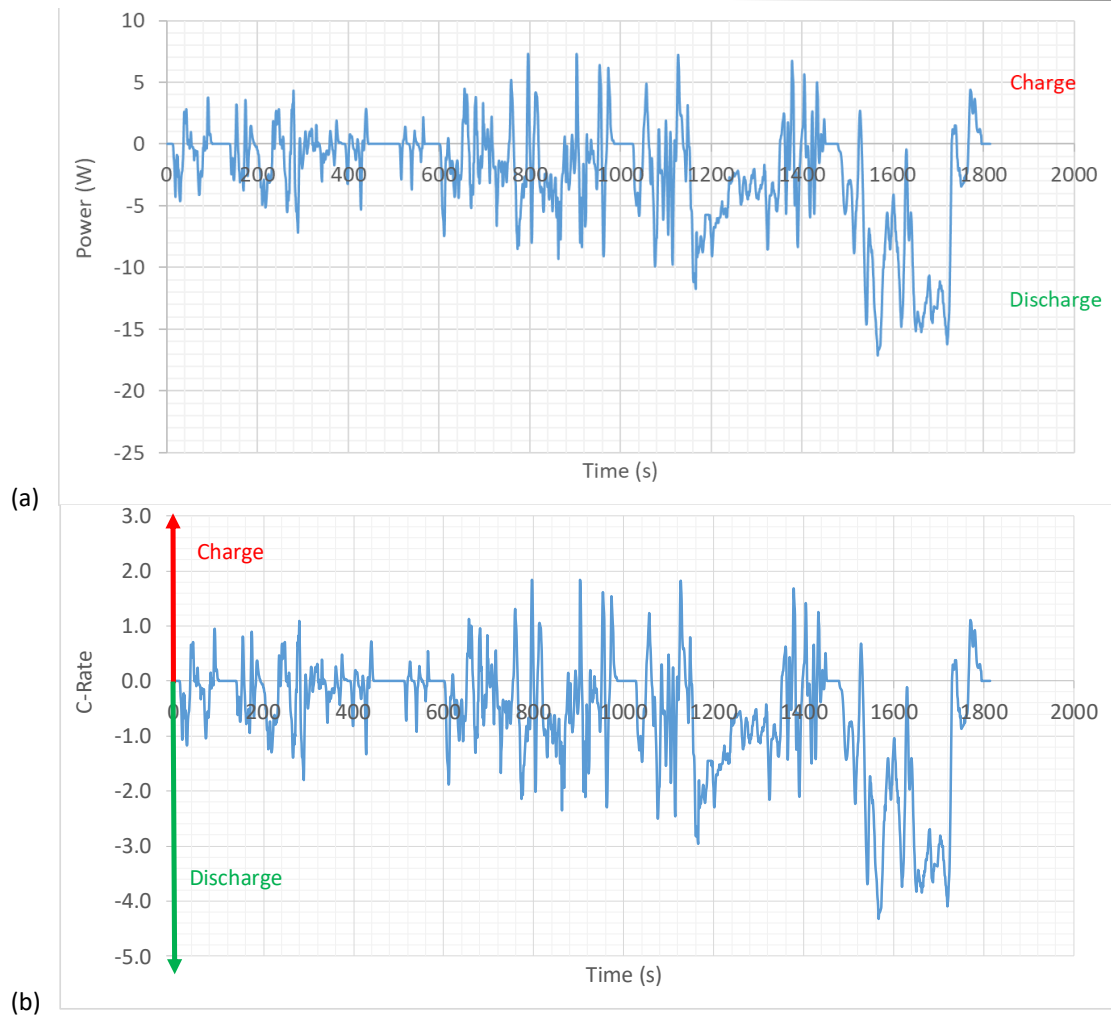


Figure 41. (a) WLTP protocol for Li-FUN cell in power. The corresponding current rates are given in (b).

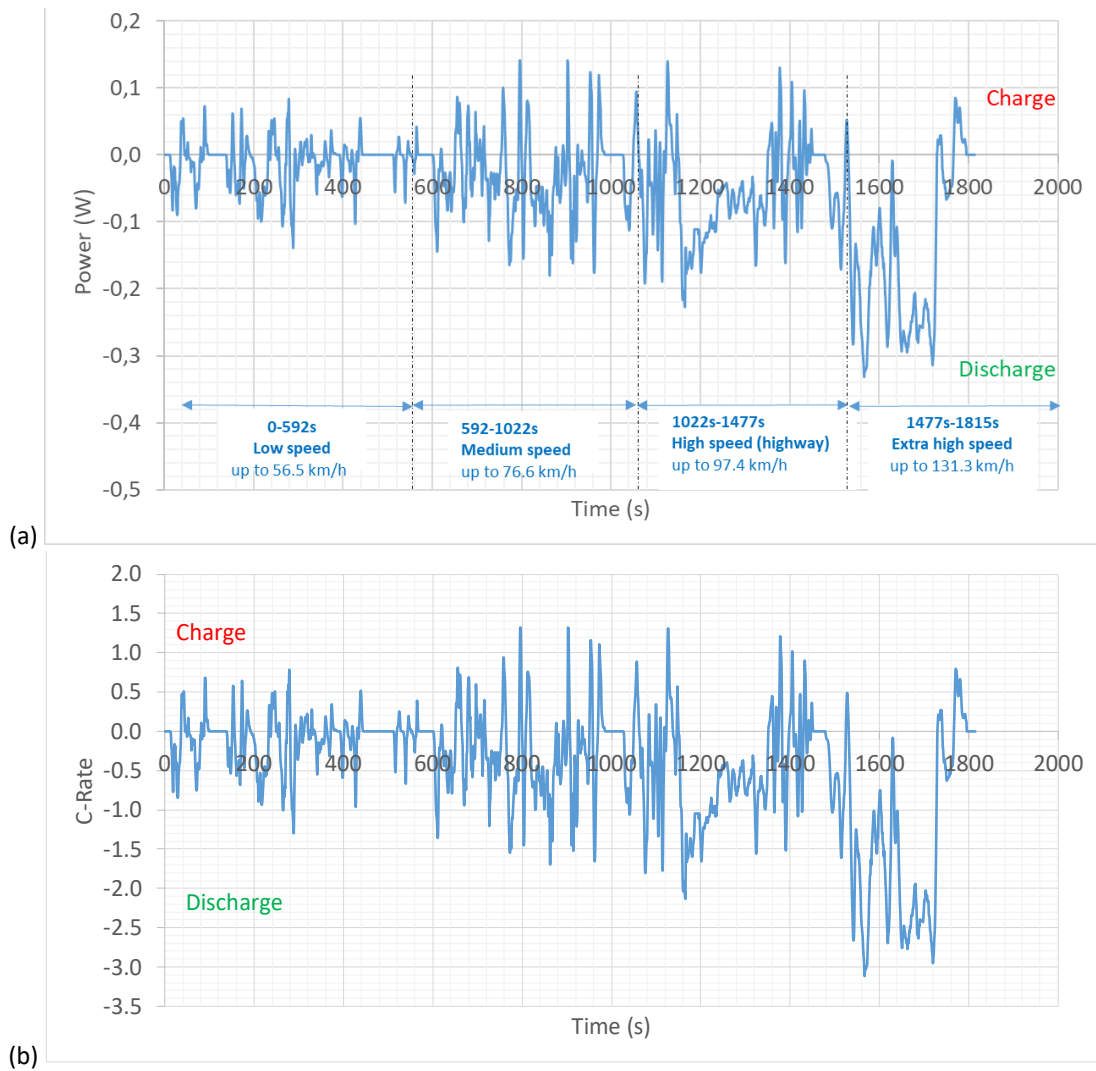
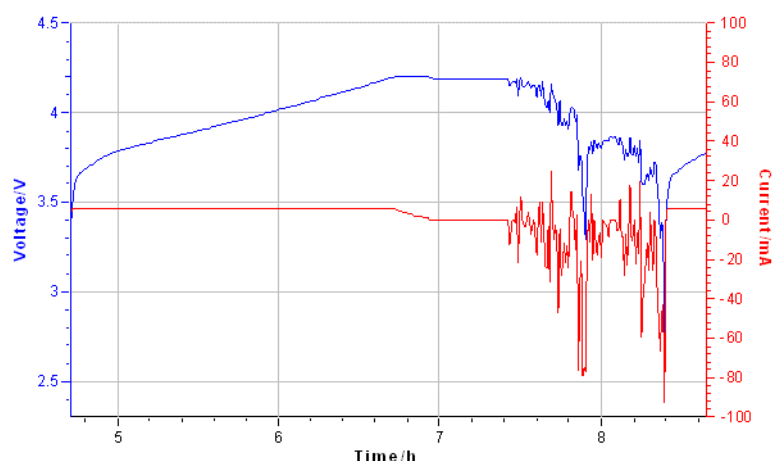
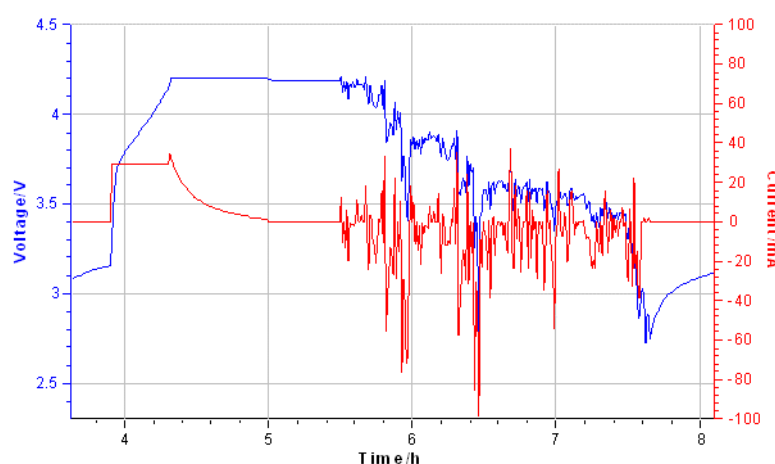


Figure 42. (a) WLTP protocol for mono cells prepared with VARTA electrodes in power. The corresponding current rates are given in (b).

We proposed to apply successive WLTP cycles in the aim to cycle the cell on a deep range of state of charge. Indeed, we have observed that if we launch two WLTP cycles (profile 1), the limit in low voltage (2.5V) is reach during the second cycle when the cell is submitted to the highest power peaks in discharge. The state of charge of the cell is only of 58.7%. By looping x full WLTP cycle up to 2.6V, x Medium speed WLTP cycle up to 2.5V and x Low speed WLTP up to 2.5V (Profile 2), it is possible to decrease greater the state of charge up to 35.2% allowing to accelerate the cell aging.



(a) Profile 1



(b) Profile 2

Figure 43. WLTP protocols : Profile 1 (2 full WLTP), Profile 2 (loop : x full WLTP cycle up to 2.6V, x Medium speed WLTP cycle up to 2.5V and x Low speed WLTP up to 2.5V (Profile 2)).

Table 11. State of charge reached after profile 1 and profile 2

Nominal capacity at C/5 (mAh)	28.8				
Capacity at C/0.8 (= mean current = 37mA during WLTP cycle)	16.179				
Profile 1					
Charge capacity 1C (mAh)	11.907				
WLTP cycle - Profile 1 (mAh)	<table border="0" style="width: 100%;"> <tr> <td style="width: 50%; text-align: right;">Charge capacity (mAh)</td> <td>2.348</td> </tr> <tr> <td style="width: 50%; text-align: right;">Discharge capacity (mAh)</td> <td>14.234</td> </tr> </table>	Charge capacity (mAh)	2.348	Discharge capacity (mAh)	14.234
Charge capacity (mAh)	2.348				
Discharge capacity (mAh)	14.234				
Discharge capacity WLTP (mAh)	11.886				
SOC reached considering the capacity at C/0.8	26.5%				
SOC reached considering the capacity at C/5	58.7%				
Profile 2					
Charge capacity 1C (mAh)	18.569				
WLTP cycle - Profile 2 (mAh)	<table border="0" style="width: 100%;"> <tr> <td style="width: 50%; text-align: right;">Charge capacity (mAh)</td> <td>4.319</td> </tr> <tr> <td style="width: 50%; text-align: right;">Discharge capacity (mAh)</td> <td>22.977</td> </tr> </table>	Charge capacity (mAh)	4.319	Discharge capacity (mAh)	22.977
Charge capacity (mAh)	4.319				
Discharge capacity (mAh)	22.977				
Discharge capacity WLTP (mAh)	18.658				
SOC reached considering the capacity at C/0.8	-15.3%				
SOC reached considering the capacity at C/5	35.2%				

Standard for material and battery testing

In order to allow the comparison of results between the different groups and sensors, integration material chemistry and electrolytes are common across the different WP. The material defined in this project is $\text{LiNi}_{0.6}\text{Mn}_{0.2}\text{Co}_{0.2}\text{O}_2$ (denoted NMC622 in the rest of this document), as a positive electrode, in combination with graphite, as negative electrode. To ensure reproducibility of results, electrode from only two suppliers will be used (Varta and LiFUN). The electrodes supplied by Varta are assembled at CEA to form a single-layer stacked pouch cell with a capacity of 29.6 mAh. LiFUN provides wounded pouch cell with a capacity of 1000 mAh. The cells geometry is highlighted in Figure 44. The electrolyte used throughout the project is a commercial mixture of Ethylene Carbonate (EC) and Ethyl Methyl Carbonate (EMC) in a weight ratio of 3:7 with 1M LiPF_6 conductive lithium salt and 2% of vinyl carbonate (VC) additive (denoted LP57+2% VC in the rest of this document) provided by Sol-Rite (Mitsubishi).

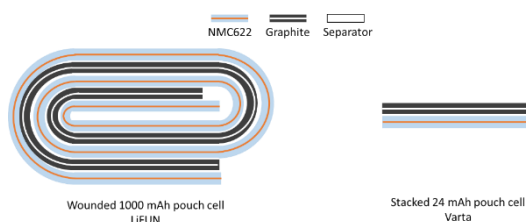


Figure 44 : Cells format used in INSTABAT project

Following the recommendations of the equipment supplier and the need of the partners for characterization and modeling, a list of protocols has been established within INSTABAT. Formation protocol is performed at 25°C following Varta's recommendation. After the formation cycles, a degassing step will be performed for LiFUN cells. This step is essential to achieve the maximum capacity of LiFUN cells but is not necessary for Varta cell due to their low mass of material producing a small amount of gas. Then capacity and internal resistance measurement protocol will be used by the modeling team to calibrate their model and a pulse test protocol will be used by CNRS to calibrate the thermal parameters such as the internal resistance (R_{in}), the external resistance (R_{out}) and the thermal capacity (c_p) to be able to solve the thermal model and to calculate heat and enthalpy. Then, C-rate test in charge and discharge will be performed at 25°C, 55°C and low temperature. The value at low temperature will be chosen according to the test results performed on instrumented pouch cells with LFP reference electrode at -10°C. For cell ageing, CEA has proposed a cycling protocol with a 2C (or 1C) charge and a discharge protocol based on the worldwide-harmonized test procedures for light vehicles (WLTP). This discharge profile is representative of a worldwide statistical study performed on real driving profiles. However, by choosing an excellent electrode material and electrolyte, the degradation of materials can take years. Consequently, a fast ageing protocol inspired by the work of Dahn et al. was proposed by CNRS [1]. By overcharging the cell and maintaining the voltage, heat generation, gas formation, and lithium plating are expected, which should be trackable by sensors. Detailed of the electrochemical protocol will be provided in deliverable D3.1.

Characterization of pristine cell

Pristine cells were tested according to the protocol defined between the partners. In addition, C-rate tests were performed at 25°C and 55°C in order to observe the degradation related to cycling in extreme conditions. As shown in Figure 45, the performances of the cells are impacted by both current density and temperature. The extreme condition being particularly detrimental during discharge.

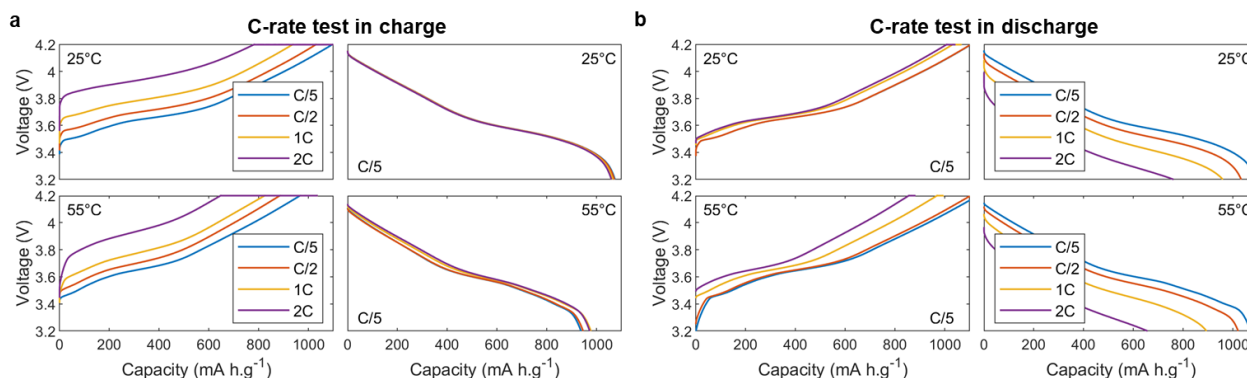


Figure 45 : C-rate test in charge (a) and discharge (b) at 25°C (top) and 55°C (bottom) of LiFUN cells.

Overview of FBG sensor tests

FBG sensors have been provided by UAVR University to CNRS in order to be implemented into pouch cell. To do so, firstly, a FBG sensor is protected with a stainless sheath to avoid contribution from strain and curvature. Then the sensor is attached to the pouch bag with a droplet of epoxy cured 24 hours. Inside glovebox, the sensor is placed in the middle of the jelly roll of LIFUN's cell previously dried at 55°C under vacuum overnight. Two sides of the bag are then sealed with a sealing machine at 180°C and the bag is filled with electrolyte and left for 12 hours. Finally, the bag is closed under vacuum. The pouch cell is connected inside an isothermal cabinet and two sensors (surface and ambient) are placed on top of the pouch and on top of the cabinet Figure 46c. The instrumented cell has been then cycled in the same condition as the pristine cell. As observed in Figure 46b and c, during the formation cycles and C-rate tests, the pristine and instrumented cells show exactly the same behaviour. Therefore, we can be confident that the sensor does not affect the electrochemical performance.

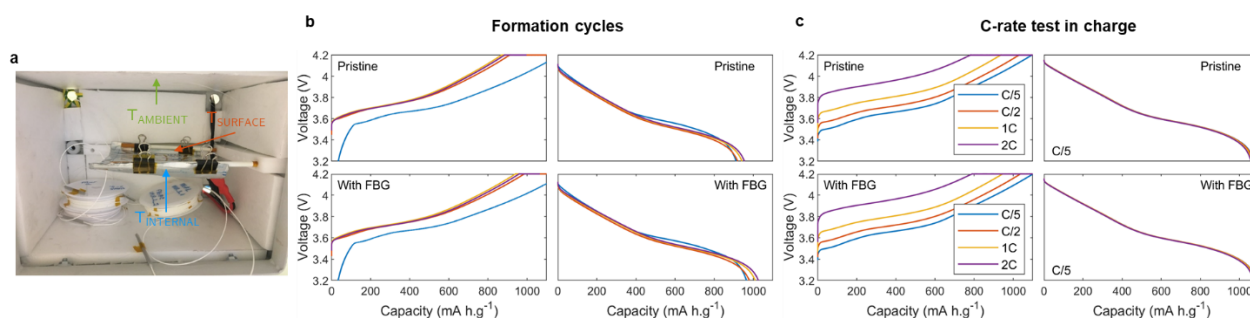


Figure 46 : (a) Picture of the isothermal cabinet instrumented with the pouch cell and sensor. The cabinet is placed in an oven to avoid any external temperature variation. Unless specified, the temperature of the experiments is maintained at 25°C. Formation cycles (b) and C-rate test in charge (b) at 25°C for pristine LiFUN cell (top) and LiFUN cell instrumented with FBG sensor.

Overview of strain sensor tests

The implementation of PANDA fiber is just beginning, but is worth mentioning because it has the potential to provide very important information about material degradation. Our strategy is to implement the fiber directly in the material of the positive electrode. To do so, the jelly roll need to be disassembled and the fiber can be pressed in the material and then covered with a new slurry. In this configuration the PANDA fiber should be able to detect changes in the volume of the electrode during cycling and its cracking or delamination during aging. However, during initial testing, the fiber came loose or broke, making it impossible to obtain robust results at this time.

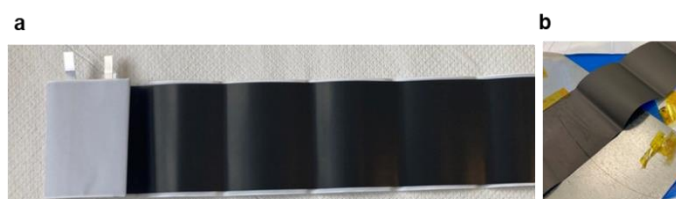


Figure 47: (a) Disassembled jelly-roll. (b) Panda fiber embedded in the positive electrode material.

TASK 3.2 IDENTIFICATION OF DEGRADATION MECHANISMS BY IN OPERANDO AND POST-MORTEM ANALYSIS

(Leader: CNRS; Participants: UAVR, CEA) (M6-M32)

Temperature variation during SEI formation

As we discussed above, FBG sensor can be implemented inside pouch cell to measure temperature without affecting the electrochemistry. Moreover, by using three sensors positioning inside, at the surface and far from the pouch we are able to solve the thermal model and calculate the heat. The explanation of the thermal model and its resolution will be described in Deliverable D3.2. The heat being directly connected to the amount of energy involve during the electrochemical reaction is very useful for comprehension of battery degradation.

To prove the ability of FBG to give valuable information on pouch cells during formation, we decided to realize three different instrumented cells with three different electrolytes: (i) the one of the project the LP57+2%VC which is expected to be the most stable thanks to VC additive, (ii) LP57 to investigate the influence of the additive during the first charge and (iii) LiPF₆ EC/DMC (1/1 v/v) (called LP30) an electrolyte well known in the literature but expected to be less stable than LP57. As provided in Figure 48, the heat released during the first cycle is proportional to the electrolyte decomposition. LP30 is known to decompose into various carbonates and alkoxides. In the case of LP57, decomposition is reduced as well as heat. Finally, the VC additive must decompose first to avoid solvent reduction. In agreement with this pathway in Figure 48 c, a small peak at the beginning of the charge and no further decay are observed.

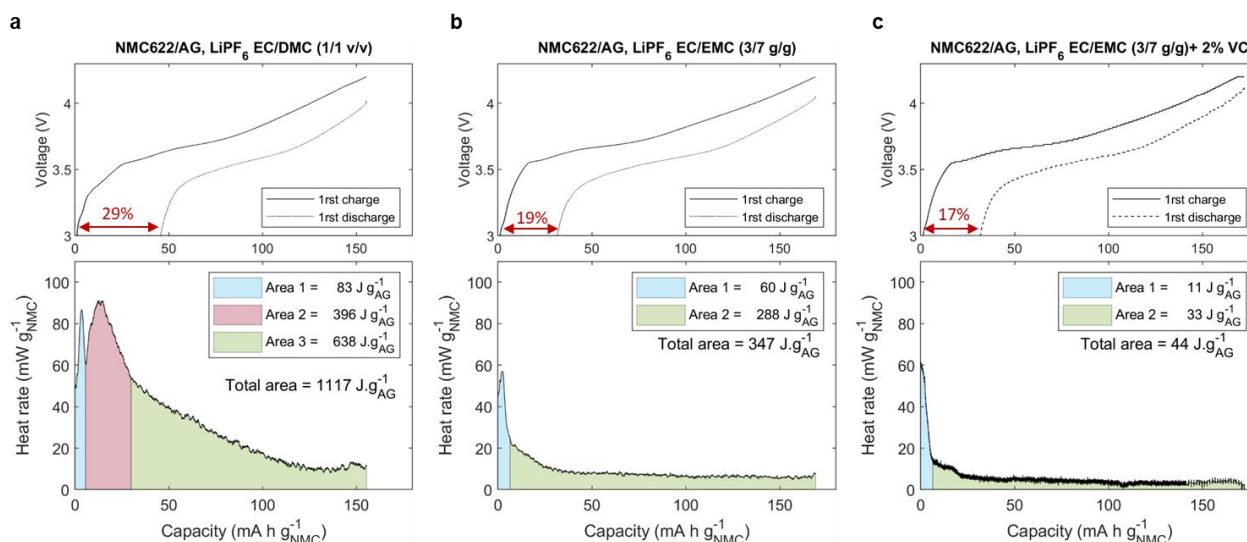


Figure 48: 1st formation cycle of NMC622/AG pouch cell instrumented with FBG and heat generated during the first charge with LiPF₆ EC/DMC (a) LiPF₆ EC/EMC (b) and LiPF₆ EC/EMC+2%VC (c).

Temperature variation during C-rate tests

The FBG sensing can also be helpful to study the influence of C-rate on the battery life. The Figure 49a give the maximum temperature reached during charging at different C-rates in charge for a NMC622/AG LiFUN cell instrumented with FBG. It is interesting to note that the surface temperature and the internal temperature are close, the design of the pouch-cell being favourable to the heat exchange with the outside. By looking at the Figure 49 b, at C/5, C/2 and 1C the voltage and heat profile appear as similar. However at 2C a significant decrease in capacity is observed as well as the appearance of a low voltage heat peak similar to that observed for SEI formation and which could correspond to a degradation of the electrolyte. Post-mortem characterization will be done on cells after high C-rate cycling to confirm the electrolyte degradation.

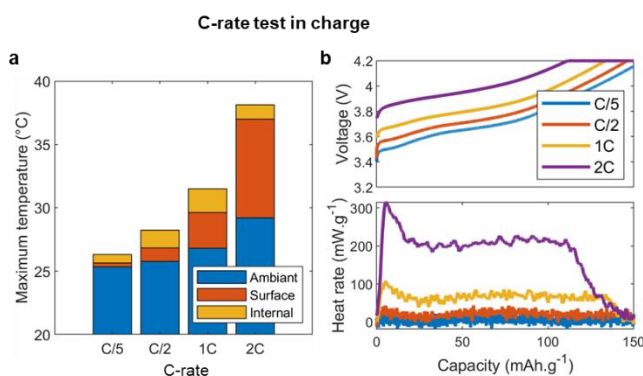


Figure 49. Study of the C-rate influence on charge. (a) Maximum temperature reached during charging at different C-rates. (b) Voltage profile and heat rate profile in charge in function of capacity at different C-rate.

Temperature variation during WLTP Cycling

Finally, we demonstrated the ability of FBG to provide information in real cycling conditions. As shown in Figure 50 a, temperature variation are obtained during C/2 charge and WLTP discharge. These variations are sensitive to the power profile. Indeed, during charging, a single temperature peak is observed, whereas during discharging, as observed in Figure 50 b, different temperature peaks exist. These peaks are characteristic of the different phases of braking or acceleration. In a real system where cell-level current and voltage cannot be accurately measured, the information provided by the sensors would be very useful in this case. Currently only dozens of cycles have been done with the WLTP profile and as observed the maximum temperature in discharge is stable. The cell correctly withstands the WLTP discharge.

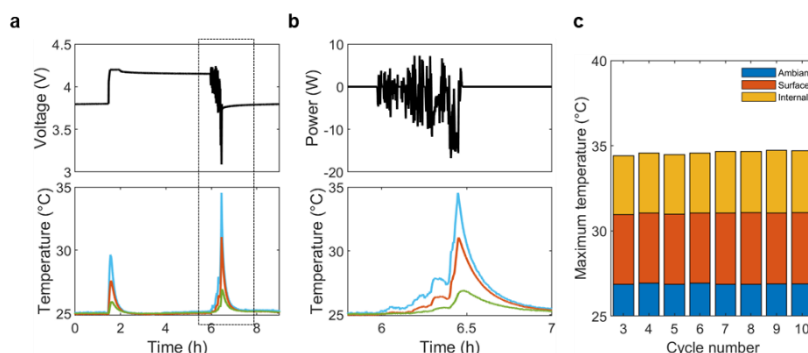


Figure 50. (a) Voltage and temperature profile of C/2 charge and WLTP discharge. (b) Power and temperature profile during WLTP discharge. (c) Maximum temperature during WLTP discharge in function of cycling.

Electrode potential measurement with reference electrode

The reference electrode sensor has been integrated in pouch cell as illustrated in the Figure 51. The piece of separator functionalized with coated LFP were added between the separator of the cell and the positive electrode as shown below. The coated side is facing the negative electrode. A square of hot-melt tape was placed around the separator film of the reference electrode face on the sealing area. No leakage has been observed during all the duration of the electrochemical test allowing to consider this method of implementation consistent. This way to proceed must be considered as a first approach to evaluate the response of the reference electrode on separator film. In the long term, the reference electrode will be on the separator on the cell and not added in addition to the separator of the cell.

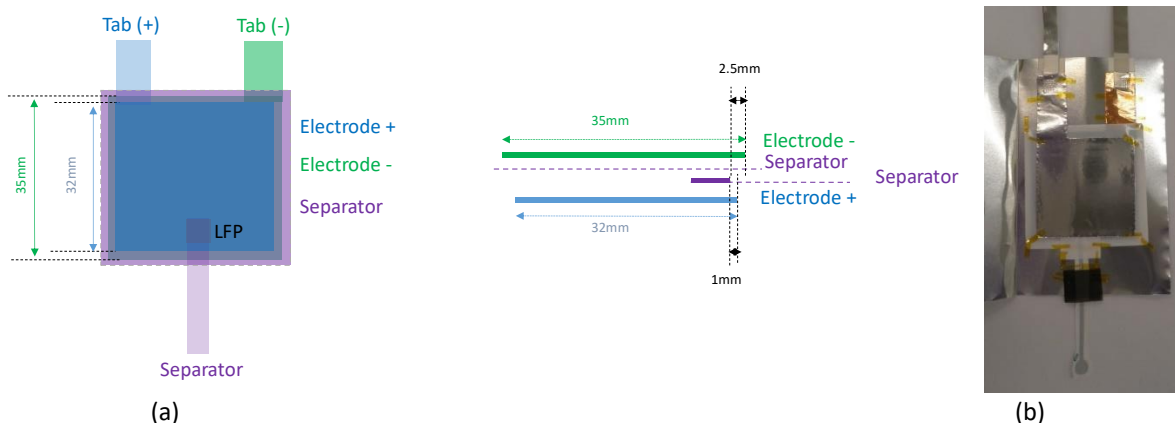
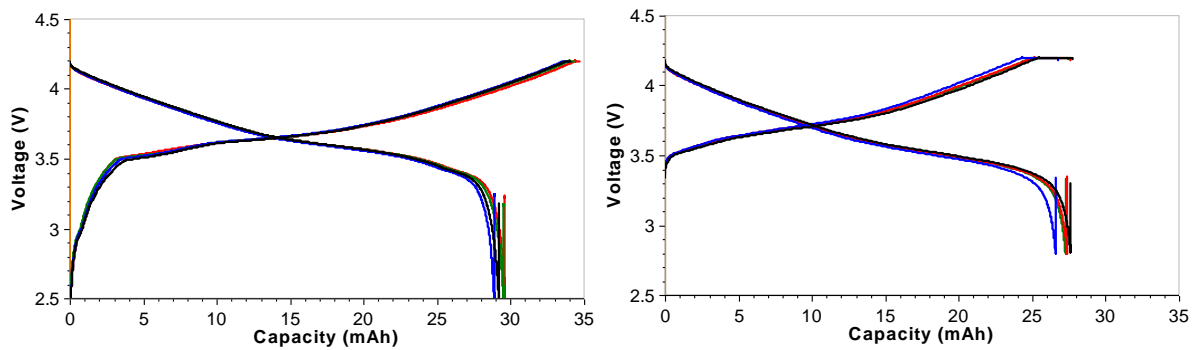


Figure 51. (a) Schematic illustration of the instrumented pouch cell, (b) picture of the cell assembled before activation

The Figure 52 and Table 12 gives the comparison of performances of 3 pouch cells instrumented with LFP reference electrodes with different patterns : folk or antenna, 300 nm thick Au. No significant difference is seen beyond the usual manufacturing scatter.



Pouch cell 1 non instrumented
 Pouch cell 2 + Reference electrode : Folk-300nm
 Pouch cell 3 + Reference electrode : Antenna 300nm
 Pouch cell 4 + Reference electrode : Antenna-300nm

Figure 52. Formation curves for the first cycle at C/20 and the third cycle at C/2 for pouch cells instrumented with LFP reference electrode (folk or antenna, 300 nm thick Au) and for a non-instrumented pouch cell.

Table 12. Comparison of the electrochemical results in formation for a non-instrumented cell and 3 cells instrumented with LFP reference electrode

	Discharge capacity (mAh)		%irreversible (1st cycle)	Discharge capacity (C/2) 3rd cycle	
	mAh	mAh/g NMC		mAh	mAh/g NMC
Pouch cell 1 non instrumented	29.21	157.2	14.2%	27.62	148.6
Pouch cell 2 + Reference electrode : Folk-300nm	28.88	155.4	14.9%	26.60	143.1
Pouch cell 3 + Reference electrode : Antenna 300nm	29.52	158.8	13.9%	27.26	146.7
Pouch cell 4 + Reference electrode : Antenna-300nm	29.62	159.4	14.5%	27.37	147.3

To compare the response of this innovative design for the reference electrode, we have instrumented two pouch cells with two reference electrodes (Figure 53):

- The reference electrode implemented on the separator film as developed in the project (The coated side is facing the negative electrode)
- The typical reference electrode used at CEA to perform electrochemical test in 3-electrode cell configuration.

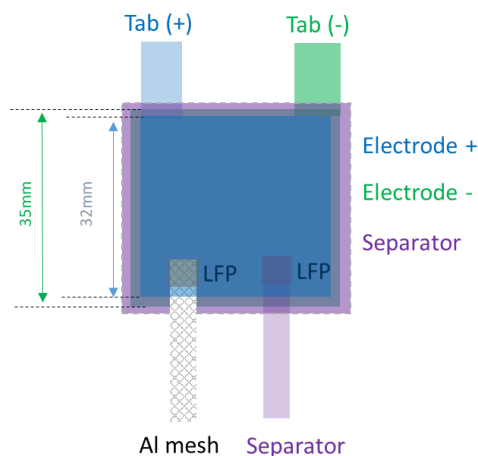


Figure 53. Schematic illustration of the double instrumented pouch cell

The respective design of the two reference electrodes is reminded in the Table 13. The total thickness for both is around 30µm but it will be possible to obtain thinner thicknesses for INSTABAT’s reference electrode by putting LFP ink by spray. For this moment, the LFP ink is simply applied with a brush.

Table 13. Respective design of the reference electrode developed in the project and the CEA’s typical reference electrode

	INSTABAT’s reference electrode on separator	CEA’s reference electrode on Aluminum mesh
Pouch cell 2 Design	Antenna : Au 100 nm Thickness coating LFP : 32 µm	Thickness : 30 µm

We have characterized the both pouch cells at different current rates (C/10, C/5, C/2, C, 2C) according to the C-rate protocol defined in the project. The cells were previously formed and the reference electrodes activated to place their potential in the middle of the plateau.

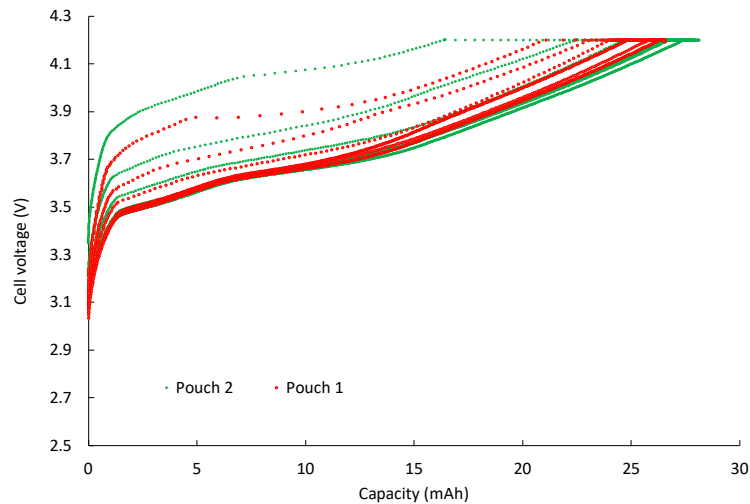


Figure 54. Electrochemical curves in charge at different current rates (C/10, C/5, C/2, C, 2C) for the pouch cells Nb1 and Nb2

Both cells showed not exactly the same performances. That difference of performance is more visible at high currents.

The Figure 55 and Figure 56 give the electrochemical profiles obtained in charge at different current rates (C/10, C/5, C/2, C, 2C) for the pouch cell Nb1 and Nb2 respectively. Contrary that it is observed for the pouch cell Nb1, we can see for the pouch cell Nb2 that the potential profiles provided by the INSTABAT’s or CEA’s reference electrode are very similar, allowing to confirm that the reference electrode design developed in the project is proper.

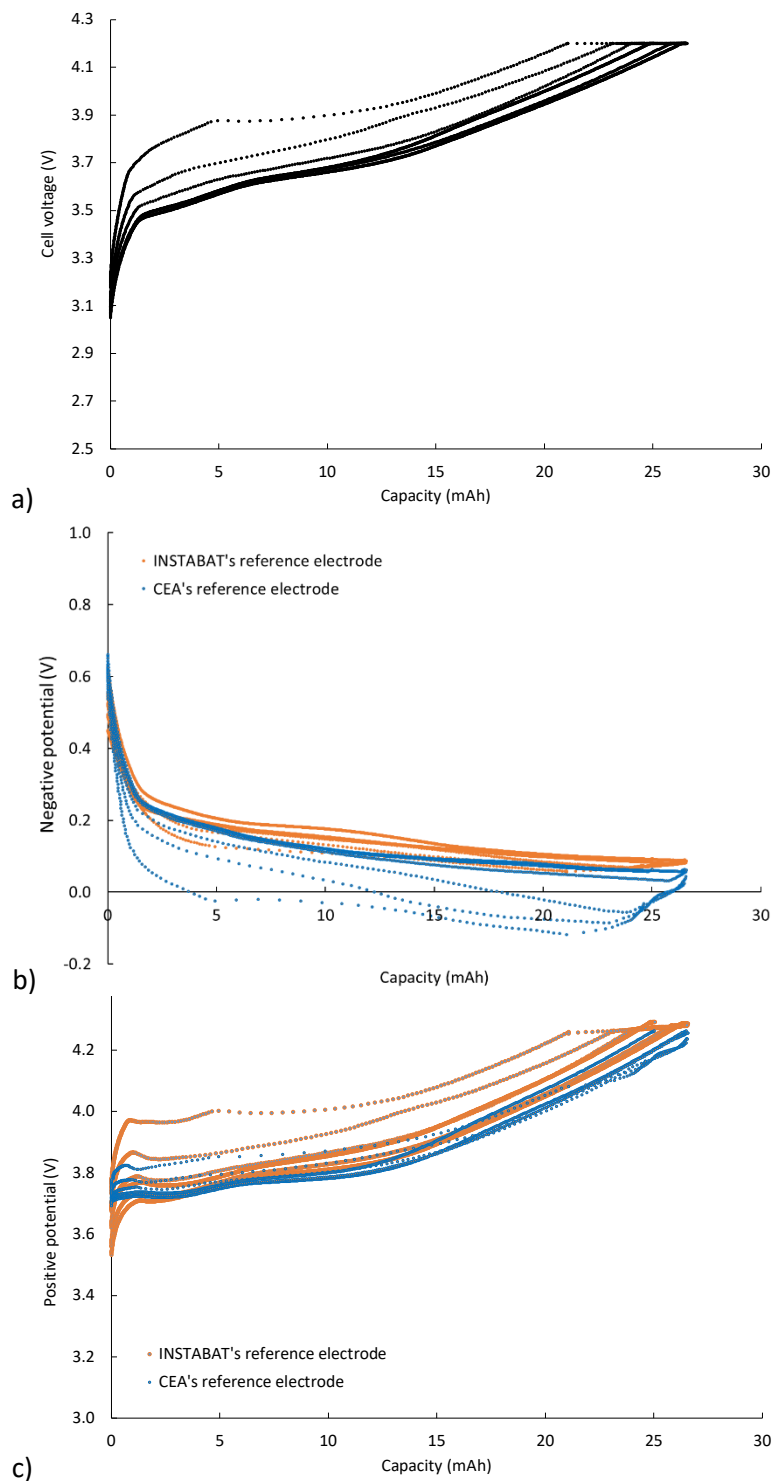


Figure 55. Electrochemical profiles of the pouch cell nb1 in charge at different current rates (C/10, C/5, C/2, C, 2C): (a) cell voltage, negative (b) and positive (c) electrode potential given by the INSTABAT's and CEA's reference electrode

Regarding the other pouch cell Nb1, the positive electrode potential provided by the INSTABAT's reference electrode is strongly polarized at high current rates whereas the profiles given by the CEA's reference electrode are less polarized. This is inverted for the negative electrode. The profiles given by the two reference electrodes are thus not correct and consequently not usable. We have started to analyse the two pouch cells by impedance measurements to compare the response given by the reference electrodes.

To conclude this part, we have demonstrated that the implementation of INSTABAT's reference electrode supported on separator film has been reached. However, because the performance of the monolayer format cell is relatively dispersed, the evaluation of the electrode potential profiles in function of the CEA's or INSTABAT reference electrodes is complicated.

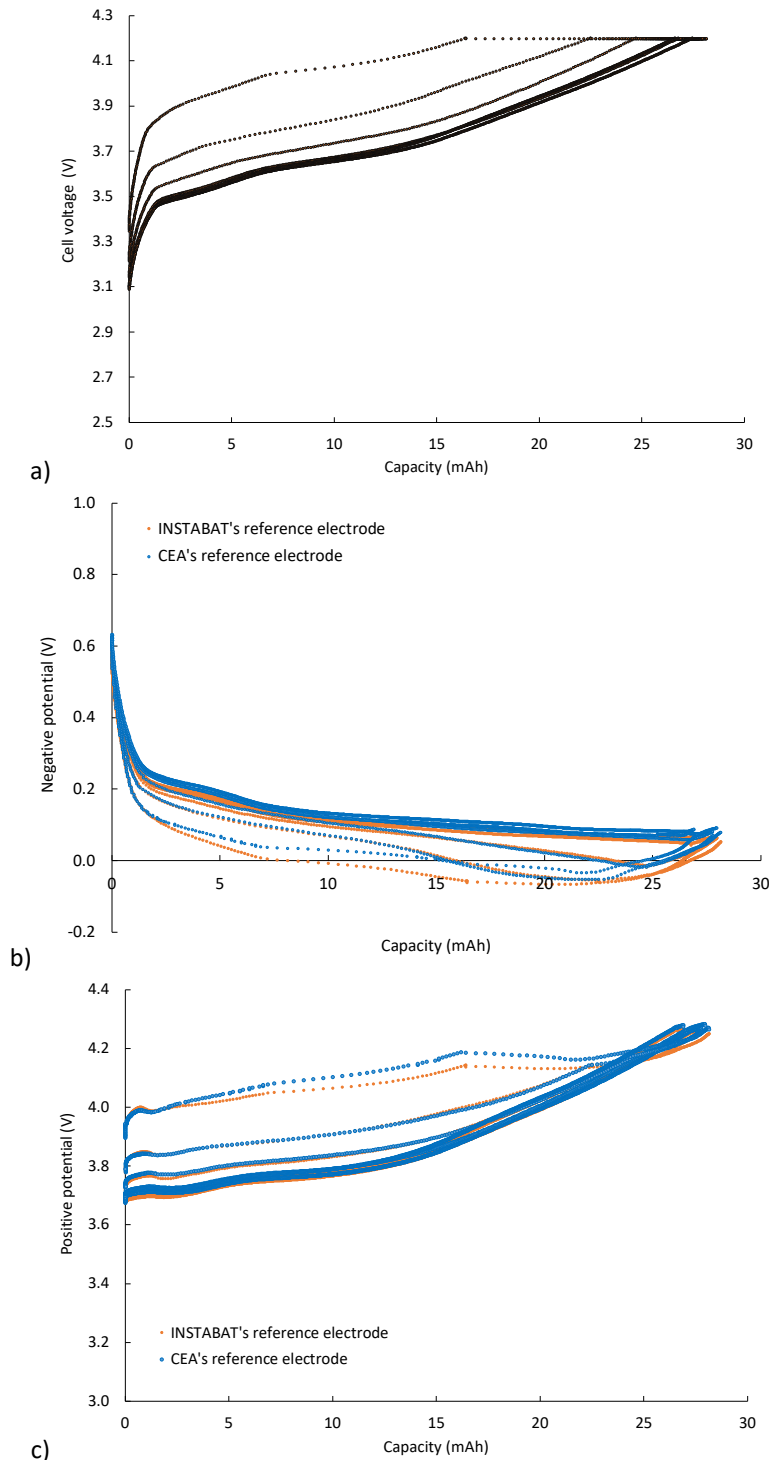


Figure 56. Electrochemical profiles of the pouch cell nb2 in charge at different current rates (C/10, C/5, C/2, C, 2C): (a) cell voltage, negative (b) and positive (c) electrode potential given by the INSTABAT's and CEA's reference electrode

Table 14. *List of deliverables WP3*

Deliverable Number	Deliverable Title	Lead beneficiary	Type	Dissemination level	Due date (in month)	Status
D3.1	Report electrochemical test results of instrumented cells	1-CEA	Report	Public	24	N/A
D3.2	Report on the correlation between physical/virtual sensor outputs and the identified physicochemical phenomena of the Li-ion batteries - V1	3-CNRS	Report	Public	24	N/A
D3.3	Report on the correlation between physical/virtual sensor outputs and the identified physicochemical phenomena of the Li-ion batteries - V2	3-CNRS	Report	Confidential	32	N/A

Table 15. *Relevant Milestones associate to WP3*

Milestone Number	Milestone Title	Lead beneficiary	Due date (in month)	Status
MS6	Correlation of at least one output signal from each sensor to a physico-chemical phenomenon of the Li-ion cell	3 – CNRS	32	N/A

WP4 - Development of virtual sensors and BMS SoX indicators algorithms

INSA LYON, CEA, FAURECIA, UAVR

Work package number	4	Leader			INSA				
Work package title	Development of virtual sensors and BMS SoX indicators algorithms								
Short name of participant	FAURECIA	CEA	UAVR	INSA					
Person months per participant	5	23	12	35					
Start month	M1			End month			M36		

Objectives

The aim of WP4 is to develop virtual sensors and BMS SoX indicators algorithms. The main objectives of this WP are the following:

- Develop numerical electro-chemical and thermal models and algorithms suitable for reference simulations (version 1 in D4.2, D4.3, D4.4 and version 2 D4.7, D4.8, D4.9);
- Reduce the models and develop virtual sensors (E-BASE and T-BASE) for electro-chemical and thermal physics-based models (D4.1, D4.5 and D4.6);
- Provide real-time SoX cell indicators estimation (D4.10);
- Provide real-time algorithms able to reconstruct the desired variables precisely enough at high charge/discharge rates and under different temperature conditions (D4.11).

Highlights of most significant results

The two main aspects of WP4 concern the development and exploitation (Task 4.1 and Tasks 4.2 and 4.3, respectively) of numerical models of the battery cell. Task 4.1 develops both electrochemical and thermal models for the battery cell, Task 4.2 exploits reduced-order models to reconstruct in real-time the internal state of the battery cell (i.e., develops virtual sensors for the system) and Task 4.3 utilizes the information provided by the physical and virtual sensors in the cell to obtain SoX indicators that inform the charge and discharge of the cell.

The results obtained thus far concern tasks 4.1 and 4.2 (Task 4.3 is scheduled to begin on month 23, even if coordination is ongoing between the different tasks to ensure integration of the data in the end).

The results obtained in Task 4.1 concern the development of version 1 of the electrochemical and thermal models for the battery cell used in this project (D4.2, D4.3 and D4.4). In particular:

- **An electrode (1D+1D) model based on Newman's porous electrode theory** has been developed by the CEA and fully parametrized based on available literature and material properties provided by VARTA. This is a first version, as the timeline of the project clearly indicates, and these parameters will be adjusted for further deliverables based on experimental results in the battery cell. This electrode model, implemented in COMSOL, is freely accessible to the partners in the consortium, to validate reduced order models in task 4.2.
- **A pseudo-3D (p3D) model of the cell** that solves both electrochemical and thermal equations in the different domains (positive and negative electrodes as well as separator) has also been developed by the CEA. As is the case with the 1D+1D model, this model has also been implemented using COMSOL and is accessible to INSTABAT partners for the validation of the electrochemical and thermal behaviour of the cell, for task 4.2
- **A 3D thermal model of the cell** has been developed by Faurecia and runs using a MATLAB® script. This model has been parametrized using project data as well as available data from the literature. The simulation is parametrizable with different cell dimensions/thermal properties/boundary conditions/electrical properties. The first simulations aim to reproduce the behaviour of the pouch cells used in the project, in both adiabatic and free convection.

The results obtained in Task 4.2 concern the development of reduced-order models and estimator design for the real-time reconstruction of internal variables, which will then be available to the BMS algorithms (D4.1 and, in the future D4.5). The models and estimation algorithms concerned are:

- **A reduced electrochemical electrode-electrolyte model** developed by INSA Lyon (D4.1) for state estimation purposes. This electrode model is based on a finite-volume scheme specifically developed for the project, considering the transport coefficient and porosity discontinuities at the interfaces of the different battery domains. This model has been validated against the references (1D+1D) model presented by the CEA in some charge/discharge scenarios.
- **An electrochemical “virtual sensor” (E-Base)** based on the reduced electrochemical model, developed by INSA Lyon (D4.1). This estimation structure allows some modularity (depending on the available physical measurements). It can consider as inputs current and voltage to the battery cell, as well as thermal information, Li⁺ concentration in the electrolyte and reference electrode information.

A reduced (2D) thermal model developed by UA based on an ANSYS-Fluent battery module with a Multi-Scale Multi-Dimensional model (not considering the microstructure of the battery). This model includes the solution of heat flux equations, as well as electrical field solution, as well as a simplified semi-empirical Newman-Tiedemann-Gu-Kim (NTGK) model parametrized based on experimental data and parameter estimation tools. Details and exploitation of any reduced thermal model will be presented in detail in D4.5, month 24 of the project.

Summary of progress towards objectives and details for each task

TASK 4.1 ELECTRO-CHEMICAL AND THERMAL MODELLING AND SIMULATION

(Leader: CEA; Participants: FAURECIA, INSA, UAVR) (M1-M18; M24-M29)

Task 4.1 is concerned with the development, implementation, and parametrization of reference numerical models of the different phenomena involved in the battery. In this section we will present some results of the different models developed in this task.

Electrode (1D+1D) model (D4.2)

The results of this sub-task consist of the development of a demonstrator version of a 1D+1D porous electrode (Newman) Model using COMSOL (D4.2). A Newman model consists of charge and mass conservation equations in both a liquid and a solid phase in 3 distinct domains, corresponding to the two electrodes and the separator region in the battery. A kinetic model for reaction rates at the particle-electrolyte interfaces is also included in the model. Both the solid and liquid phases are restricted to a 1D representation (thus the 1D+1D model designation). The modelled transport takes place along the thickness of the battery (for the electrolyte) and along the radial direction (for the electrode material particles). The particles in the active material are assumed spherical in this model (although variants with cylindrical particles exist).

By using this 1D+1D model, it is possible to simulate the potential of the lithium-ion battery and predict the cell capacity. Furthermore, internal variables are available in the model, such as local potentials, local lithium concentration, intercalation current, etc.

One of the main difficulties of the model developed here consists of the full parametrization of the Newman model, which requires good knowledge of the materials and the geometry of the cell. The main result of this subtask is, then, a fully parametrized Newman electrode model of the battery based on available properties in the literature, as well as information provided by INSTABAT partners, notably VARTA, for the cell used in the project. This model has further been validated by comparison to experimental results from WP2 in constant-current charge and discharge scenarios going from 0.1C to 2C charge/discharge rate. The comparisons show already good accuracy even before the parameter tuning that will be done for the V2 of the model.

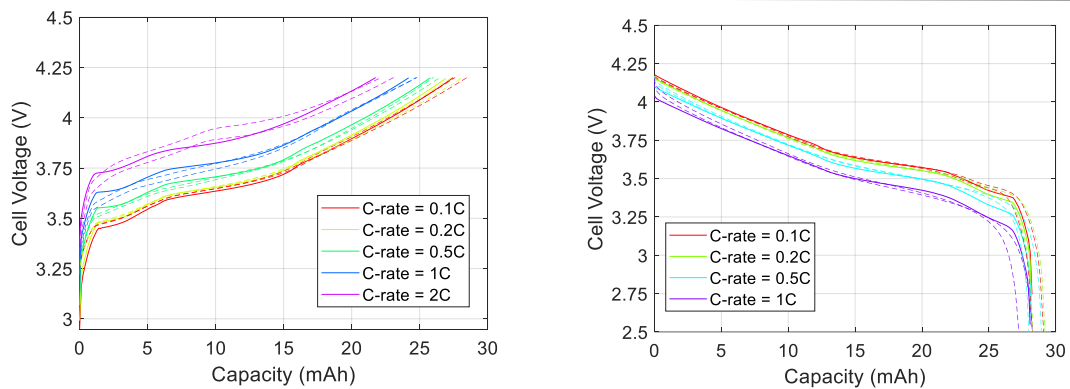


Figure 57: Comparison of charge and discharge profiles experimental (dashed lines) and in simulation (solid lines) for the 1D+1D model, version 1.

Pseudo-3D (p3D) model of the cell (D4.3)

The result of this task so far consists of a demonstrator code developed by the CEA and available to INSTABAT partners that implements, using COMSOL, a p3D model of the battery cell (D4.3). This demonstrator allows the validation and development of reduced order models, such as the electrochemical and thermal models developed in task 4.2.

The main addition in the p3D model of the cell, developed as well by the CEA, is the inclusion of in-plane heterogeneities along the cell plane (which are neglected in the 1D+1D model). As is the case of the 1D+1D model, the main challenge consists of the full parametrization of the model. In this case, the parametrization is done using the data of the 1D+1D model, which includes all the necessary transport parameters, except for those concerning the geometry and thermal characteristics of the p3D cell. The main difference in the phenomena modelled in this p3D model with respect to the 1D+1D model includes the in-plane transport of Li ions in the electrolyte phase, as well as a thermal model that was not included in the electrode model.

Besides the electrochemical information obtained with the p3D model (similar to that obtained with the 1D+1D model, except for the in-plane heterogeneities), this model provides thermal information on the cell, as seen in the next figure.

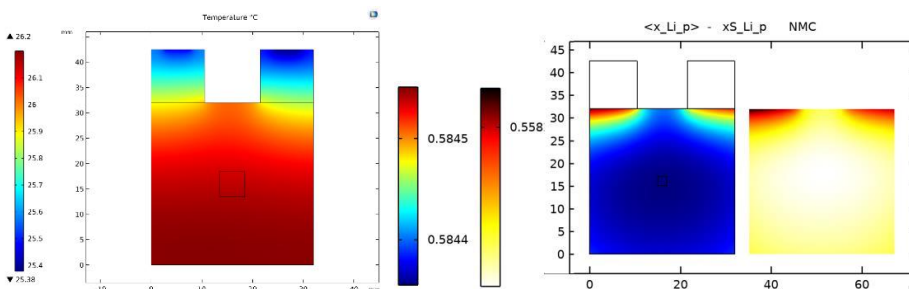


Figure 58: Example of thermal and stoichiometric information from p3D model of a sample cell for a constant-current charge profile.

3D thermal model of the cell (D4.4)

The main result in this subtask consists of the development of a parametrized 3D thermal model of a battery cell developed by VARTA (D4.4). In this case, the model is run using a MATLAB® script that can be parametrized according to the specific cell geometries and thermal characteristics. Unlike the p3D model previously presented, this includes more specific material properties, as well as a full 3D heat transfer model. As was the case in the previous models, the main difficulty consists of fully parametrizing such a model. This was done based on available material properties from the literature and adapted to the INSTABAT pouch cell under consideration.

Unlike the other models in this Task, this is a purely thermal model, based on a thermal diffusion model with parametrizable boundary conditions representing different scenarios, such as adiabatic conditions or operation with cooling on a particular boundary.

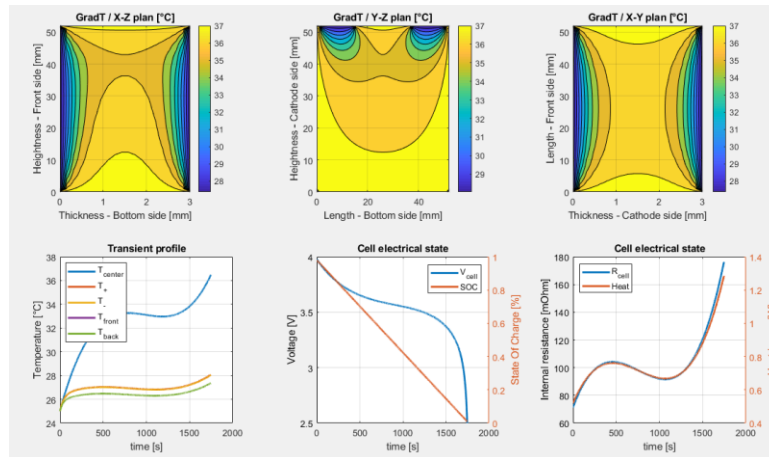


Figure 59: Example of thermal information obtained from the 3D model of a sample cell for a constant-current discharge profile.

TASK 4.2 VIRTUAL SENSORS DEVELOPMENT AND IN SILICO TEST

(Leader: INSA; Participants: UAVR, CEA) (M1-M29)

Reduced Electrochemical electrode-electrolyte model and E-BASE virtual sensor

The main result in this subtask is the development of a reduced electrode-electrolyte model based on the 1D+1D model developed in task 4.1 and oriented towards the development of real-time reconstruction of internal electrochemical states. The main challenge of this reduced-order model consists of obtaining a modular design where the compromise between model complexity and execution time can be chosen depending on the needs of real-time execution and available resources.

A finite-volume based model reduction, using MATLAB and specifically developed polynomial interpolants was developed to obtain fast and accurate representation of the system. An example showcasing the modularity of the approach is shown in the figure below. All the phenomena in the Newman model can be included (or excluded) from the reduced order model based on the complexity requirements. For instance, a fast simulation (around 5ms per second of real-time) can be obtained by neglecting lithiation heterogeneity in the solid phase.

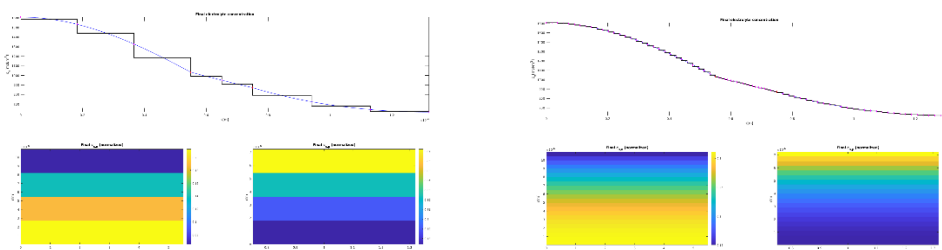
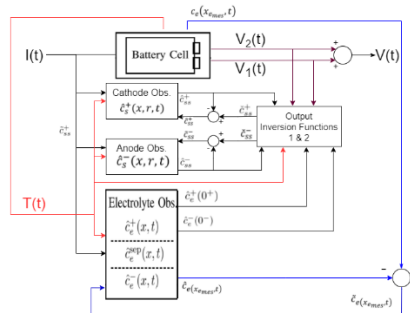


Figure 60: Example of electrochemical information obtained from the reduced order model of a sample cell for a constant-current discharge profile with very low complexity model (left) and high-resolution model (right). In this case, the lithiation heterogeneities are neglected to reduce the computational cost, and a second of simulation in the low complexity model can be simulated in 5ms on average.

Furthermore, this model has been implemented in such a way as to be able to generate C code and compile to generate a DLL library for integration with WP5.

This model was then integrated into a state estimation scheme (E-BASE) detailed in deliverable D4.1 and represented schematically in the next figure:



Block diagram of the observer with inclusion of Temperature, Feedback Injection and Reference electrode

Reduced 2D thermal model

The main result in this subtask was the development by University of Aveiro of a 2D simulation model using ANSYS Fluent battery modules and the parametrization of a Semi-empirical Newman, Tiedemann, Gu and Kim (NTGK) model where the coefficients are identified using experimental data. The model requires the reconstruction of the electric field inside the battery (or electric potential) and uses Arrhenius-type dependencies on the kinetic parameters. An energy conservation equation solved in the domain is used to estimate the heat exchanges and evolution.

The proposed reduction and parameter identification methods were tested based on experimental data using a commercial cell and an example of the available information provided by this model is presented in the following figure:

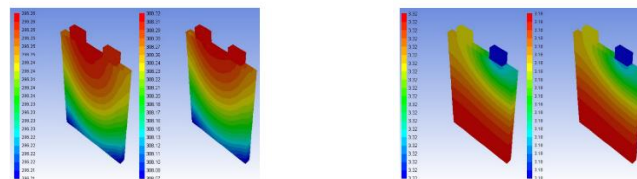


Figure 61: Sample results of the simplified 2D thermal model for different discharge rates. Temperatures on left figure, positive potential on the right figure.

The development of a thermal virtual sensor will be included in the next deliverable for this task (M24).

TASK 4.3 DESIGN OF STATE OF CHARGE, HEALTH, POWER, ENERGY AND SAFETY CELL INDICATORS ALGORITHMS

(Leader: CEA) (M23-M36)

Task 4.3 will begin in M23 of the project. Nevertheless, coordination with T4.2 is ongoing to be able to integrate the information of the virtual sensors to the BMS indicator algorithms.

Table 16. *List of deliverables WP3*

Deliverable Number	Deliverable Title	Lead beneficiary	Type	Dissemination level	Due date (in month)	Status
D4.1	Report on generic structure of electrochemical virtual sensor algorithm	6-INSA LYON	Report	Confidential	12	Submitted
D4.2	Version 1.0 of the 1D+1D electrode model	1-CEA	Demonstrator	Confidential	18	Submitted
D4.3	Version 1.0 of the p3D cell model	1-CEA	Demonstrator	Confidential	18	Submitted
D4.4	Version 1.0 of the 3D thermal cell model	4-FAURECIA	Demonstrator	Confidential	18	Submitted
D4.5	Report on temperature dependent electrochemical virtual sensor algorithm (E-BASE and T-BASE)	6-INSA LYON	Report	Public	24	N/A
D4.6	Report on adapted electro-chemical/thermal virtual sensor algorithms compatible with BMS	6-INSA LYON	Report	Public	29	N/A
D4.7	Version 2.0 of the 1D+1D electrode model	1-CEA	Demonstrator	Confidential	29	N/A
D4.8	Version 2.0 of the p3D cell model	1-CEA	Demonstrator	Confidential	29	N/A
D4.9	Version 2.0 of the 3D thermal cell model	4-FAURECIA	Demonstrator	Confidential	29	N/A
D4.10	Preliminary design report of BMS SoX indicators algorithms architecture	1-CEA	Report	Confidential	24	N/A
D4.11	Final design report of BMS SoX indicators algorithms architecture	1-CEA	Report	Confidential	29	N/A
D4.12	Performance analysis report on the BMS SoX estimation algorithms	1-CEA	Report	Public	36	N/A

Table 17. *Relevant Milestones associate to WP4*

Milestone Number	Milestone Title	Lead beneficiary	Due date (in month)	Status
MS2	Coupled electro-chemical and thermal models for state estimation (virtual sensing) ready for validation	6 - INSA LYON	12	Submitted
MS4	BMS SoX algorithms and virtual sensors ready	6 - INSA LYON	29	N/A
MS7	Performances of “lab-on-acell” platform available	1 - CEA	36	N/A



WP5 - Proof of concept multi-sensor platform

CEA, CNRS, FAURECIA, IFAG, INSA LYON, UAVR, VMI

Work package number	5	Leader	CEA						
Work package title	Proof of concept multi-sensor platform								
Short name of participant	UAVR	CNRS	IFAG	FAURECIA	VMI	INSA	CEA		
Person months per participant	10	9	4	1.5	9	4	13		
Start month	M4			End month			M36		

Objectives

The objective of WP5 is the implementation of a proof of concept of the multi-sensor platform. The main objectives of this WP are the following:

- Integrate successfully the sensors into the cell prototype;
- Develop a functional proof of concept of the multi-sensor platform that, combined with appropriate BMS, is able to improve the accuracy of the SoX cell indicators.

Highlights of most significant results

An accurate and reliable knowledge of the operando key parameters of a Li-ion battery is essential to its optimal use, safety and extended lifespan. The WP5 must use and combine previous WPs results to achieve the implementation of a proof of concept of the multi-sensor platform. First, the knowledge acquired in the WP2 will help for integrating each innovative sensor into an instrumented prototyped cell.

A multi-physics instrumentation platform is necessary to exploit the signals of these sensors and to analyse and process them in real time. Indeed, the INSTABAT multi-sensor platform will not only acquire signals from various sensors developed in WP2 but also embed models and algorithms developed in WP4 thanks to WP3 characterization results and finally record all the produced data (raw and processed). Models and algorithms use cross information obtained from different sensors but corresponding to a common phenomenon, which will enrich the correlation analysis with the physico-chemical phenomena happening inside the cell.

Once the platform built and the cell prototypes manufactured, we will be able to perform lab-scale tests on the assembled testbench. Two types of tests are planned, standard cycle based on EV use cases and abusive test. First type is used to evaluate the behaviour of the prototype cell during classical operating conditions and during limited stresses (cycling at extreme conditions and high-power) in an EV context. Abusive tests are used to find out if the innovative sensors can provide early detection of hazardous events or if, on the contrary, they damage the cell.

The database collected by the platform will be used to analyze the relevance of physical/virtual sensors by correlating them with internal electro-chemical phenomena but also by evaluating the impact on the performance of BMS and safety indicators.

As can be noticed in the previous description, much of the activities are closely linked to the tasks performed in the other WPs. However, during this first half of the INSTABAT project, we have worked hard to ensure that we will properly interface and integrate outcomes from previous work packages. To this end, the work undertaken last year has consisted of:

- keeping a strong link with sensors developers in WP2 to take into account integration techniques and requirements for Li-ion battery cell
- specifying the sensors interfaces and the required instruments to access measurements
- specifying a way to interface the processing of algorithms and models
- building the platform hardware/software architecture to acquire, process and store signals and data
- Validating platform hardware/software components integration step by step

This preparatory work led to the realization of instrumented cells (with 2 INSTABAT sensors) and a Beta version of the multi-sensor platform that we were able to use during a campaign of characterization tests under X-rays at the ESRF to follow in situ and operando behaviour of Li-ion cells.

Ahead of schedule, a first batch of non-instrumented reference battery cells based on VMI components will soon be produced and characterized to be compared later to the prototype cell.

Summary of progress towards objectives and details for each task

TASK 5.1 CELL PROTOTYPE FABRICATION AND MULTI-SENSOR HARDWARE INTEGRATION

(Leader: CEA; Participants: CNRS, UAVR, VMI, IFAG) (M4-M36)

As a reminder, the goal of this task is to fabricate a prototype cell that simultaneously integrates multiple INSTABAT sensors in a large pouch cell with a capacity target between 0.3 and 4 A.h based on a chemistry used in WP2, to be delivered Month 24.

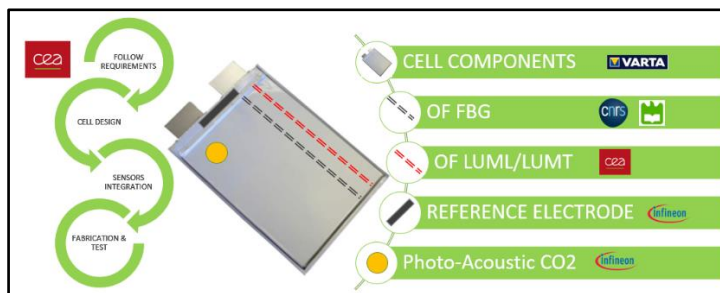


Figure 62: Multi-sensor cell prototype structure

At this time, the work of WP2 is still in progress to optimize sensors integration. VARTA VMI and CEA follow closely WP2 to be ready to transpose the process. However, for the needs of the experiment at ESRF in February 2021, we developed a first prototype of cell which integrated 2 sensors of the project, namely the reference electrode and the thermoluminescence optic fiber. This experiment was planned in collaboration with the BIGMAP project (see Task 7.3). We based our prototype on non-activated commercial LiFun cells used in WP2 which has the NMC-Graphite electrodes couple as targeted in the project. The original cell was disassembled and stacked to obtain a 1.1A.h Li-ion cell equipped with reference electrode and thermoluminescence optic fiber.

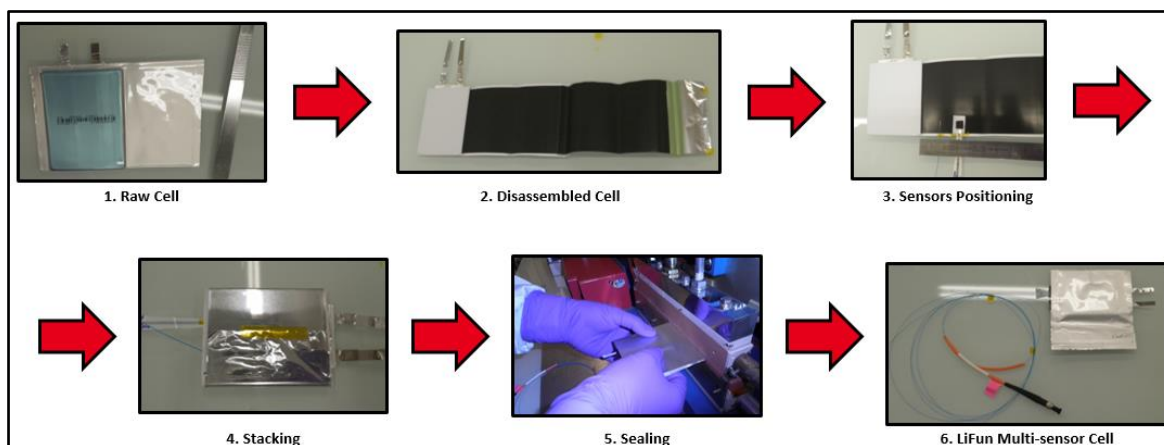


Figure 63: Multi-sensor cell ESRF prototype Process

After activation, we were able to demonstrate that the prototype cell worked even at high speeds without being damaged or disturbed by the integration of sensors and that it had an equivalent nominal capacity over the few cycles of use.

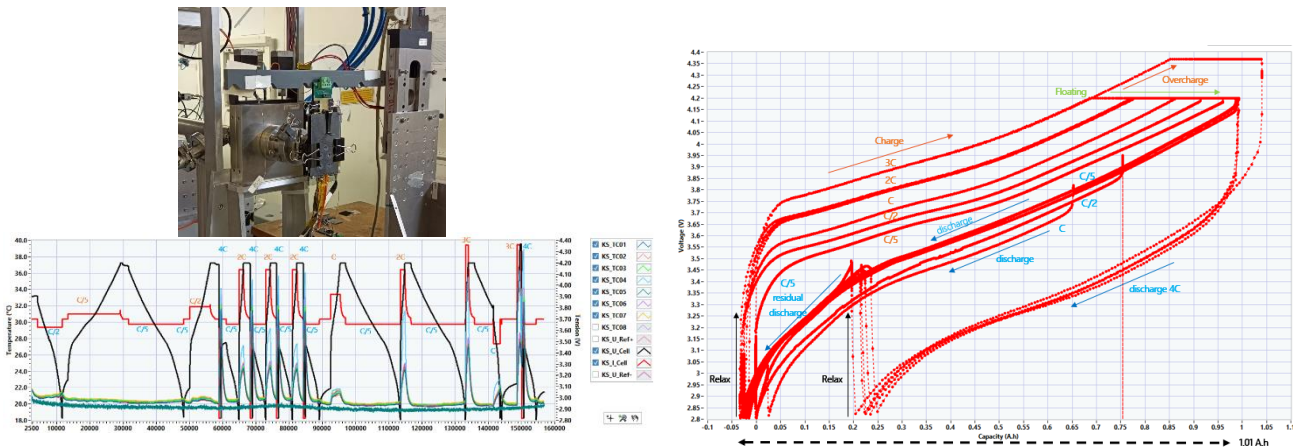


Figure 64: Electrochemical parameters of multi-sensor prototype cell performing cycle during ESRF experiment

Further on, the challenge will be to realize successfully a cell based on the VMI components by adding the Bragg fiber with partner's requirements to have a complete prototype. As we mentioned earlier, reference cell design with these components will be produced and characterized soon (next month) to be compared to the final prototype.

TASK 5.2 DATA POST-PROCESSING AND DATA LOGGING

(Leader: IFAG; Participants: CNRS, UAVR, CEA, FAURECIA, INSA) (M4-M36)

5.2.1 Platform architecture 5.2.1.1 Hardware

To realize the proof of concept of the multi-sensor platform, it is necessary to find a hardware target able to measure the signals coming from our sensors but also to process them to feed the virtual sensor models and the battery state estimation algorithms. Most of the INSTABAT sensors are of low TRL and require specific non-integrated instrumentation and equipment to acquire their signals. In addition, we did not want to impose strong constraints on algorithm and model developers in terms of computational or memory resources. Consequently, we decided to build a platform based on an instrumentation computer rather than a rapid prototyping target.

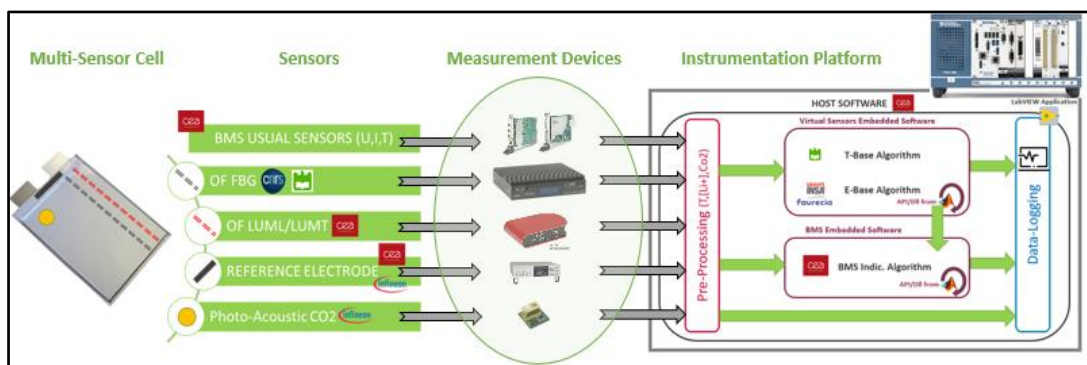


Figure 65: POC multi-sensor platform architecture

The instrumentation computer allows a better connectivity with various equipment I/O and less constraints for software developers. The host software will use the LabVIEW environment to perform the following functions:

- Control/command measurement devices to acquire usual BMS sensors and INSTABAT sensor signals
- Pre-process signal to extract battery parameters (ex: temperature from OF spectrum)
- Operate virtual sensors algorithm (E-Base, T-Base) and BMS state indicators calculation compiled in a library
- Synchronize and log all the data produced by the platform

5.2.1.2 Software

The software architecture is built around periodic process loops that exchange data by FIFO or Events. Each measuring instrument has its own process with a predefined period to refresh values. In the same way, the processing algorithms are executed in parallel and read/write respectively input/output from and to the data manager at the frequency assigned to them. Additionally, the loop of the data recording process requests the last value in the data manager at the recording period to store them in a secure database. The user interface (HMI) also uses this data stream to refresh visuals and graphics. The loops are synchronized with each other on a common clock but the measurements made by the instruments are not because some of them do not allow it. The data used by the other processes are based on the last value stored in the data manager. Thanks to the low dynamics of the underlying phenomena, this solution is sufficiently efficient. Indeed, the system is limited here by some measuring instruments whose acquisition frequencies cannot be reduced (for example luminescence spectrum could require 1 second of integration to be acquired). We target to refresh and record data manager content at 1 second period to feed algorithms for a proper execution. The adjustment of this timing will be possible as the platform software will evolve.

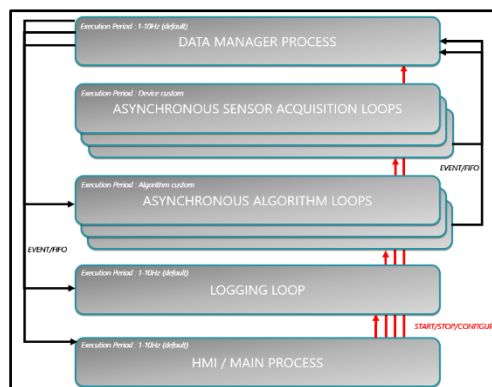


Figure 66: Software architecture

5.2.2 Sensor interface

A preliminary work consisted in interfacing the LabVIEW environment together with the various instruments necessary to measure the signals of the INSTABAT sensors. The photo-acoustic CO2 sensor has an UART communication interface developed by Infineon. The luminescence optical fiber and Bragg optical fiber requires respectively a compact spectrometer (CSS100 from Thorlabs) and an interrogator (Hyperion Si255 or similar). Both have LabVIEW driver available to control and command them through USB or Ethernet link. Reference electrode and usual BMS measurement such as cell voltage, current and skin temperature is performed by Keysight precision multimeter 34970A which also has LabVIEW drivers. So far, all sensors, except for the Bragg fiber, have been successfully integrated into the software environment.

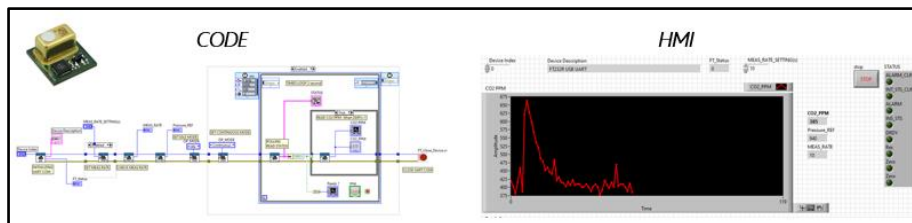


Figure 67: Interface of PAS CO2 sensor with LabVIEW software environment

5.2.3 Beta version

For the needs of the ESRF experiment, we have implemented the hardware and software architectures described in the previous chapter integrating the usual BMS and thermoluminescence measurements and pre-processing. It was a good opportunity to validate on a reduced scale our system design. Coupled with the cell prototype, this beta version of the proof of concept of the multi-sensor platform has successfully completed a 90-hour in-situ operando cycling test.

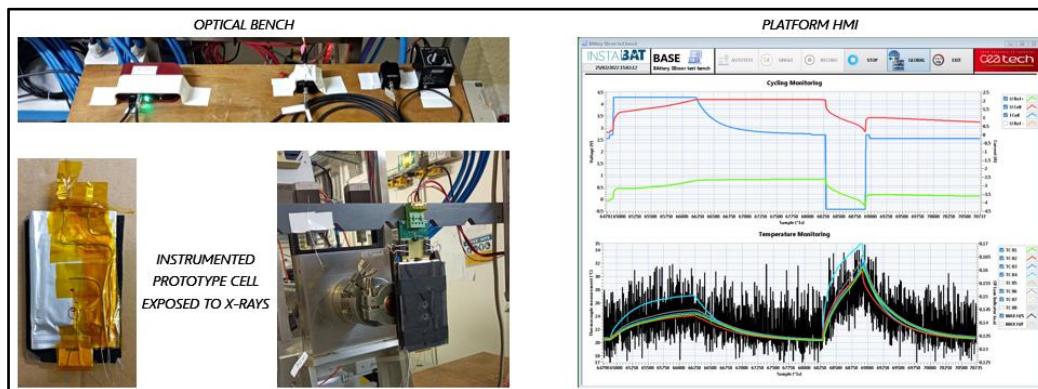


Figure 68: Beta version of multi-sensor platform used for ESRF experiment session

There is still work to be done, especially to interface the Bragg fiber interrogator but also to embed the WP4 algorithms and models into the platform.

TASK 5.3 ADVANCED BMS ALGORITHM INTEGRATION AND OPERATION

(Leader: CEA, Participants: INSA, IFAG) (M24-M36)

As we mentioned before, it will also be necessary to embed the virtual sensor E-Base and T-Base as well as the BMS estimator algorithms. Both are developed using MATLAB® software. Our solution to implement these algorithms on the software platform is to use automatic code generation to create a Windows library (*.dll) that can be executed by the LabVIEW engine. In this context partners involved in algorithms development must:

- reduce models to minimize the use of computer resources
- adapt algorithm to be time based (executed at each time step)
- define format and datatype of inputs/outputs
- use MATLAB® Coder code generation function to convert MATLAB® code to operable library

The work of WP4 is still in progress and we have not had the opportunity to test the integration of one of the algorithms of the INSTABAT project so far. However, an initial version of the BMS algorithm estimating SOC/SOH, using the usual cell measurements (voltage, current and temperature) and based on Kalman filter processing was converted to test successfully the connectivity of the LabVIEW environment with the generated library.

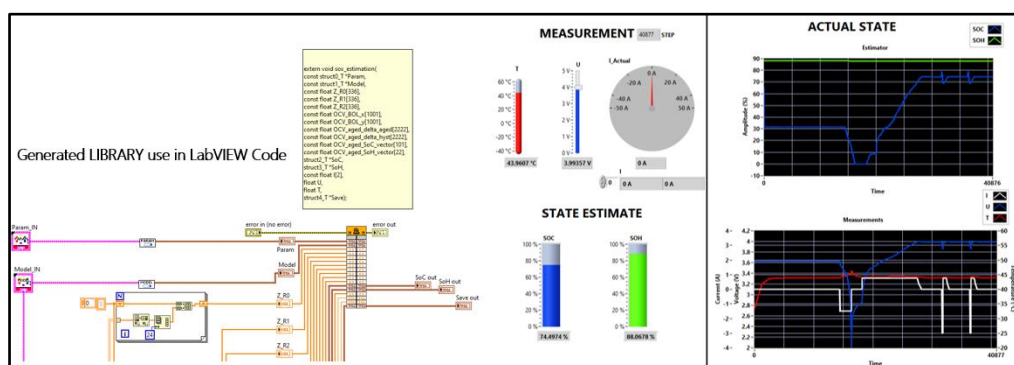


Figure 69: Execution of BMS indicators algorithm library converted with Matlab Coder in the LabVIEW environment

On the other hand, detailed specifications relative to algorithm I/O has been approved and constructed by all partners. The aim of this document was to define what the properties of I/O processing blocks are and how they are supposed to be linked with sensors measurement values. Among required processing blocks inputs, there are physical or structural parameters with configurable values relative to battery cell or sensors. An essential work will be to prepare algorithms integration when a first version would be ready even if it remains still some requirements to be defined.

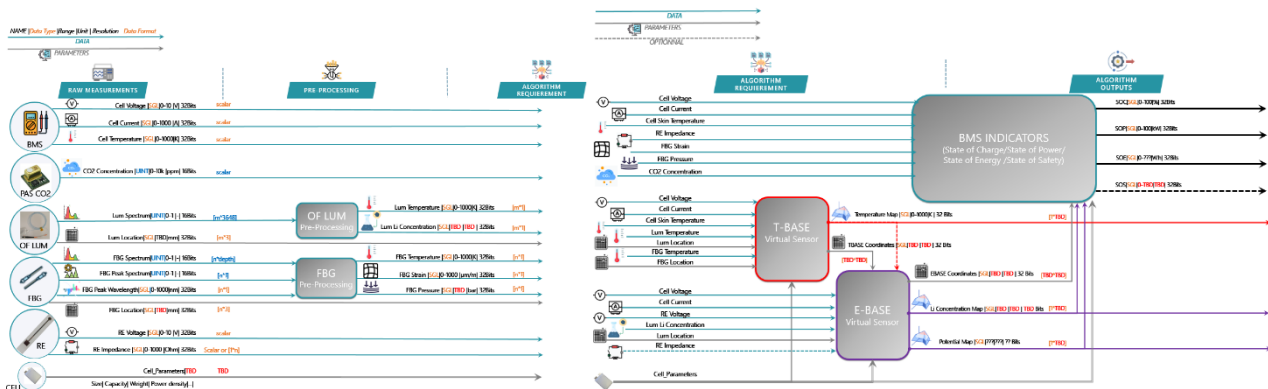


Figure 70: Algorithm integration specification block diagram

TASK 5.4 LAB-SCALE TESTS ON CELL PROTOTYPE

(Leader: CNRS; Participants: UAVR, CEA) (M24-M36)

This task didn't start yet. A detailed test plan for cycling and abusive test would be submitted to partners next months to be validated around M24 (June 2022). This plan will be based on test already performed during the WP2 and WP3.

Table 18. *List of deliverables WPS*

Deliverable Number	Deliverable Title	Lead beneficiary	Type	Dissemination level	Due date (in month)	Status
D5.1	At least 12 cell prototypes, and report on cell prototype manufacturing	1 - CEA	Demonstrator	Public	28	N/A
D5.2	Strategy for data logging on a multi-sensor cell	5 - IFAG	Report	Confidential	24	N/A
D5.3	Communications between physical sensor platform, virtual sensors and BMS established	5 - IFAG	Report	Confidential	29	N/A
D5.4	Proof of concept multisensor platform / "lab-on-a-cell"	1 - CEA	Demonstrator	Public	30	N/A
D5.5	Performance analysis of the BMS algorithms in the context of the defined two use cases for EV applications	1 - CEA	Report	Public	36	N/A
D5.6	Report about cell prototype performance	3 - CNRS	Report	Public	36	N/A



Table 19. *Relevant Milestones associate to WP5*

Milestone Number	Milestone Title	Lead beneficiary	Due date (in month)	Status
MS5	“Lab-on-a-cell” platform ready (cell prototype equipped with physical/virtual sensors, and associated BMS algorithms providing SoX indicators in real-time)	1 - CEA	30	N/A
MS7	Performances of “lab-on-a-cell” platform available	1 - CEA	36	N/A

WP6 - Techno-economic feasibility, adaptability to other cell markets and environmental considerations

VMI ,FAURECIA, CEA, BMW GROUP, CNRS, IFAG, INSA LYON, UAVR,

Work package number	6	Leader	FAURECIA							
Work package title	Techno-economic feasibility, adaptability to other cell markets and environmental considerations									
Short name of participant	BMW	VMI	CNRS	UAVR	IFAG	CEA	INSA	FAURECIA		
Person months per participant	2.6	6	0.5	0.5	0.5	0.5	0.5	6		
Start month	M24			End month			M36			

Objectives

The aim of WP6 is to establish the steps necessary to ensure a successful commercialisation of the multi-sensor platform. WP6 will:

- Carry out an industrialisation and scalability study and a preliminary design for an industrial multi-sensor platform.
- Assess manufacturability and techno-economic feasibility.
- Study adaptability to other cell technologies and use cases.
- Provide an environmental assessment, focusing on traceability, second life and recyclability.

Highlights of most significant results

This task didn't start yet. Any progress report is necessary for this report.

Summary of progress towards objectives and details for each task

TASK 6.1 INDUSTRIALISATION STUDY

(Leader: VMI; Participants: All) (M24-M30)

This task didn't start yet. Any progress report is necessary for this report.

TASK 6.2 TECHNO-ECONOMIC ANALYSIS INCLUDING ENVIRONMENTAL CONSIDERATIONS AND ADAPTABILITY TO OTHER CELL TECHNOLOGIES AND USE CASES

(Leader: FAURECIA; Participants: All) (M28-M36)

This task didn't start yet. Any progress report is necessary for this report.

Table 20. *List of deliverables WP6*

Deliverable Number	Deliverable Title	Lead beneficiary	Type	Dissemination level	Due date (in month)	Status
D6.1	Market research on components and manufacturing processes for industrial multisensory platform	8- VMI	Report	Public	30	N/A
D6.2	Environmental assessment and recyclability analysis	4- FAURECIA	Report	Public	33	N/A
D6.3	Techno-economic feasibility	4- FAURECIA	Report	Confidential	36	N/A
D6.4	Adaptability of the multi-sensor platform to different cell formats, future cathode, anode and electrolyte chemistries	4- FAURECIA	Report	Confidential	36	N/A

Table 21. *Relevant Milestones associate to WP6*

Milestone Number	Milestone Title	Lead beneficiary	Due date (in month)	Status
MS8	Industrialisation and future of the multi-sensor platform assessed	4- FAURECIA	36	N/A

WP7 - Dissemination, communication and exploitation

CEA, BMW GROUP, CNRS, FAURECIA, IFAG, INSA LYON, UAVR, VMI

Work package number	7	Leader	CEA							
Work package title	Dissemination, communication and exploitation									
Participant number										
Short name of participant	BMW	VMI	CNRS	IFAG	FAURECIA	UAVR	INSA	CEA		
Person	months	per	4	1	0.5	0.5	0.5	0.5	0.5	4.5
participant										
Start month	M1		End month				M36			

Objectives

WP7 aims to implement the dissemination, communication and exploitation strategies of INSTABAT. The work under this WP will be carried out at two levels: (1) under the umbrella of the EU large-scale research initiative on Future Battery Technologies102, led by LC-BAT-15 successful consortium and in cooperation with LC-BAT-12 and LC-BAT-14; (2) at INSTABAT individual level. WP7 will be divided into the following complementary activities:

- Dissemination and communication activities to show the attractiveness of the results achieved and their impact towards a target audience composed of already identified key stakeholders;
- Exploitation actions will establish the main pillars for a future market uptake plan of the most promising and mature results generated in the project, thus maximising the opportunities for innovation and business development.
- Implementation of an IPR and Knowledge Management Plan based on the background of each partner and the expected foreground produced in the project. This plan will bear in mind the progress of foreign IP by a continuous observatory of existing and new patents/utility models to ensure freedom to operate.

Highlights of most significant results

This part outlines the most important results from WP7. During the first period of the project, the materials and tools for communication were developed (website, visual identity, etc.). The dissemination and communication strategy was established (deliverable D7.1) during this first period. The Key exploitation results are identified and the exploitation plan was decided. The coordination with other projects was done through the BATTERY2030+ initiative with active participation to the related activities.

TASK 7.1. Implementation of dissemination and communication strategy

(Leader: CEA; Participants: All) (M1-M36).

The communication and dissemination strategy was defined at the beginning of the project and detailed in the deliverable D.7.1. During the first period of the project, we achieved some planned actions. The web site and the visual identity of the project was developed. The detail of the web site and the content was detailed in the D7.2. The communication supports such as poster, flyer and booklet were also developed to share the INSTABAT objectives and promote the project. A detailed view of the dissemination and communication activities since the project started were given in the D7.6.

TASK 7.2. Exploitation plan

(Leader: VMI; Participants: All) (M12- M36)

During the 1st reporting period, a methodology was developed (please refer D 7.4 report) for the identification and evaluation of potential KERs based on the processes shown in the following figure.

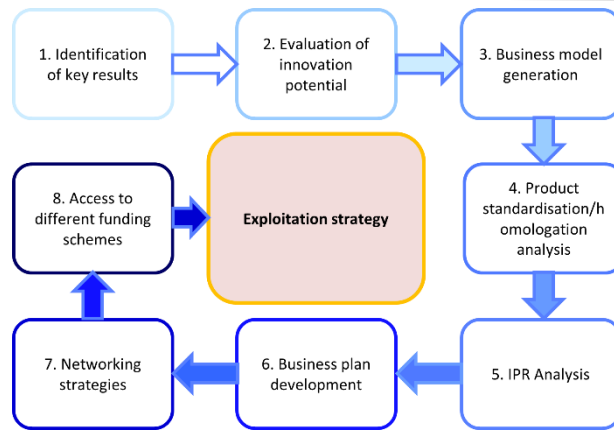


Figure 71: Global overview of the INSTABAT exploitation plan

This general approach in this respect within the INSTABAT project was codified in the D7.4 delivery report. Based on this methodology, preliminary KERs could be identified by month 18, as shown in the following table.

Table 22 Preliminary Key Exploitable Results (KERs) identified during INSTABAT Project by M18

KER-Item	Type of Key Exploitable Result (KERs)	Type of Exploitation CE/SAT	Ownership	Title	Confidential (YES/No)
KER01	Education	SAT	UAVR	PhD thesis	No
KER02	Innovation	SAT	UAVR	Custom fiber sensor fabrication platform	No
KER03	Research	SAT	Consortium	Lab-on-a-battery cell demonstrator	No
KER04	Societal impact	SAT	Consortium	Industry/Academy collaboration	No
KER05	Economic impact	CE	Consortium	Industry/Academy Services	No
KER06	Methodology	SAT	INSA Lyon	Methodology for development of estimation-oriented (fast) electrochemical models	No
KER07	Software	SAT	INSA Lyon	E-BASE, state estimation algorithm implementation	Yes
KER08	Methodology	SAT	INSA Lyon	Methodology for development of state estimators ("virtual sensors") for reduced electrochemical models	No
KER09	Software	SAT	INSA Lyon	Fast Finite-Volume Electrochemical Battery Model implementation	Yes
KER10	Software	SAT	CEA	Software integrating physical models in charge of predicting internal state of battery cells at electrode and cell scale	Yes
KER11	Patent	CE	CEA	Methodology for current collector connection of thin metallic layer supported by polymer film	Yes
KER12	Research	SAT	CEA	Results on stability study of integrated reference electrode	No
KER13	Research	SAT	CEA	Comparison methodology for in-situ operando characterisation of multi reference electrodes.	No
KER14	Equipment/Software	SAT	CEA	Multi-sensor cell bench for in-situ operando measurements with embedded processing (BMS)	No
KER15	Research	SAT	Consortium	Methodology for manufacturing multi-sensor Lithium-Ion cell	Yes
KER16	Research	SAT	Consortium	In-situ operando characterization database on Lithium-ion cell for cycling and abusive tests	No
KER17	Software	SAT	CEA	Software Library integrating reduced order physics based model together with online sense data to produce improved SOX estimation at BMS Level	Yes
KER18	Research	SAT	CEA	Luminescent probe for temperature and Li-ion concentration measurement	Yes

TASK 7.3. Coordination with others EU projects

(Leader: CEA; Participants: All) (M1- M36)

INSTABAT project is on the umbrella of BATTERY2030+ initiative, however natural links were created under the other projects from this initiative such as BIGMAP⁹, HIDDEN¹⁰, BAT4EVER¹¹, SPARTACUS¹² and SENSIBAT¹³ (see Figure 72).

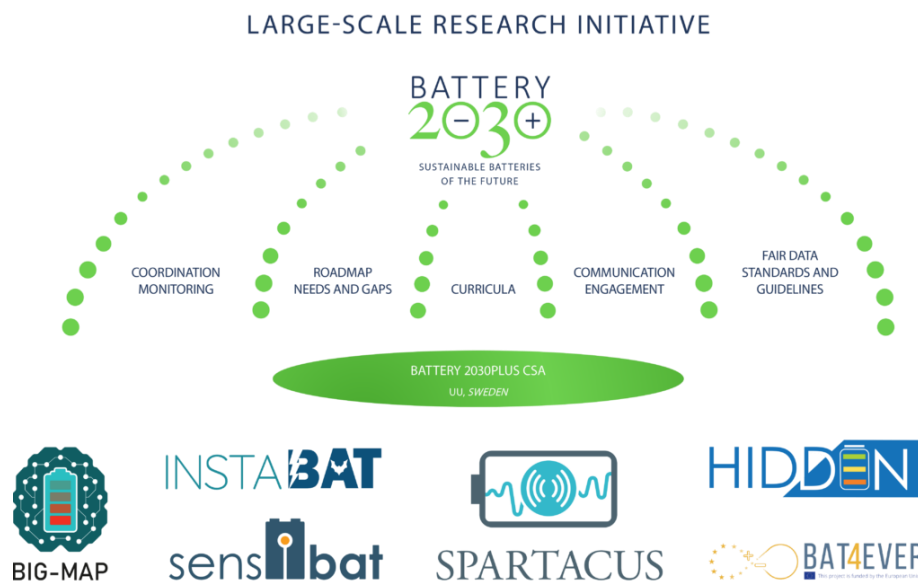


Figure 72: BATTERY2030+ largescale initiative and related projects (LCBAT13 and LCBAT14)

Participation to the BATTERY2030+ collaboration board meeting

Coordinator or deputy coordinator of the INSTABAT project was involved in the collaboration board BATTERY2030+ meeting. This biweekly meeting organized by the BATTERY2030+ board is the place for all the stakeholder activities and initiative between partners. During these meetings, a status of the progress of all the projects were presented. We also discussed of the results and cooperation subject between the projects. Some information of workshop and others collaborative activities were presented and discussed. This information is communicated to the INSTABAT consortium after each BATTERY2030+ collaborative board meeting.

Participation to the BATTERY2030+ communication board meeting

INSTABAT coordinator participates regularly to the communication board meeting of BATTERY2030+. The objective is to disseminate the results from INSTABAT to the BATTERY2030+ initiative and participate to the joint communication activities. During the first period of INSTABAT project:

- 1- A contribution from INSTABAT to the BATTERY2030+ Poster for the Advanced Battery Power Conference (March 29-30, 2022) in Münster.
- 2- A presentation of INSTABAT key results during the internal BATTERY2030+ workshop organized by Lormann Henning the February 14th, 2022 (online).

⁹ <https://www.big-map.eu/>

¹⁰ <https://www.hidden-project.eu>

¹¹ <https://www.bat4ever.eu/>

¹² <https://www.spartacus-battery.eu/>

¹³ <https://sensibat-project.eu>

Collaboration between INSTABAT and BIGMAP project

Within BIGMAP, an experimental portfolio of complementary techniques is developed towards the implementation of a multimodal and multiscale characterization platform. Operando synchrotron experiments were realized and analysed according to BIGMAP standards and protocols on INSTABAT pouch cells instrumented with different types of sensors.

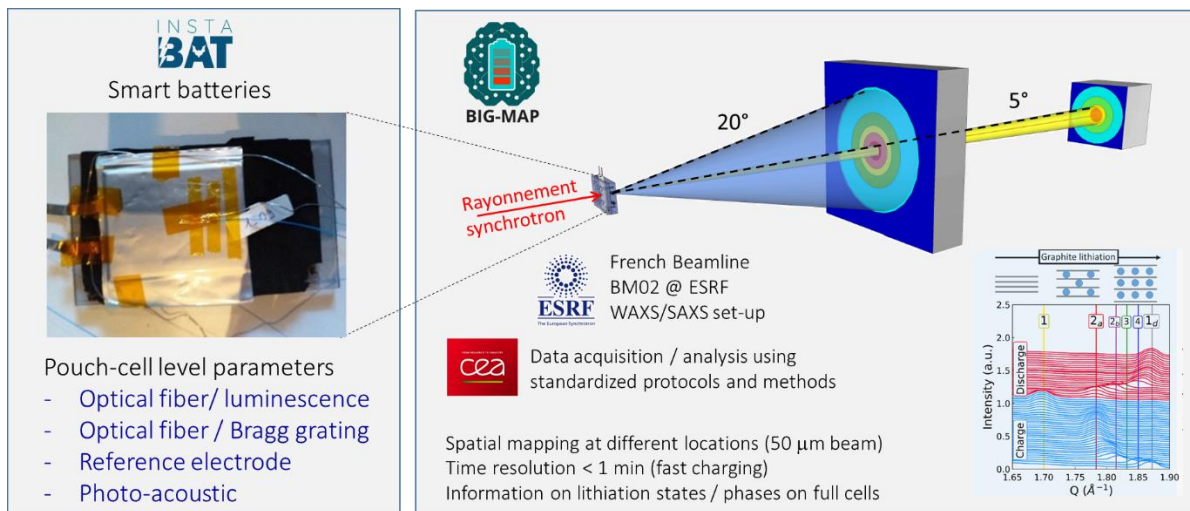


Figure 73: Joint experiment between INSTABAT and BIGMAP project

In the frame of WP2 and WP3 work, Lifun1,1Ah cells were used for this experimental campaign. CEA has instrumented these cells with OFLumT and RE sensors. Reference cells without sensors were also prepared with one moncell and one multilayer cell to study the effect of the number of layers on the XRD measurement. 3 instrumented cells were prepared from Lifun cell (1.1Ah). One with only OFLumT sensor inside the cell and two with OFLumT and RE sensors inside the cell. Cells are tested in BM02 line at ESRF in operando condition. This work is a collaboration with INSTABAT partners (CEA) and BIGMAP partners (CEA, LEPMI, ESRF)¹⁴.

The spatially-resolved real-time structural data obtained by X-rays diffraction (phase transitions, strain, local lithiation mechanism) will be cross-correlated to the various sensing data (temperature, local electrode potential), allowing to monitor the potential perturbations of reaction mechanisms due to sensor integration and to correlate micro-to-macro scale performance related to parameter variations along cycling.

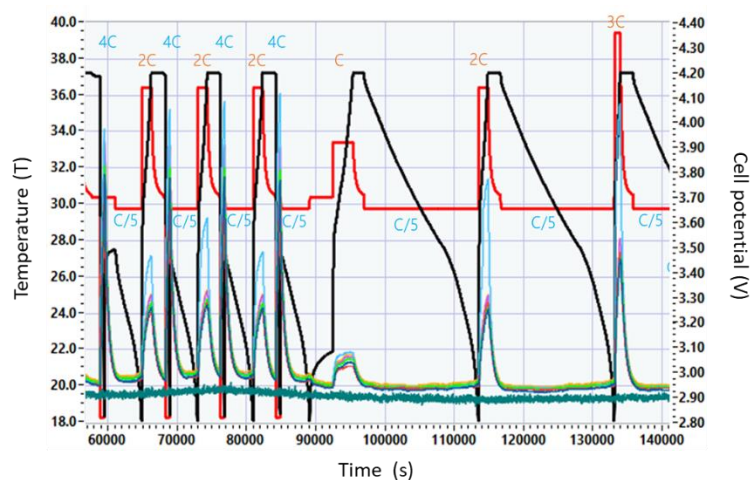


Figure 74: Multi instrumented measurement on LiFun cell (1.1Ah) during ESRF experiment. Cell potential (black), cell current (red), external temperature (blue = Tab+, green, purple, yellow = cell surface, dark green = ambient)

¹⁴ List of collaborators by partners. CEA: E. Villemin, S. Genies, C. Septet, M. Guillon, O. Ponelet, S. Desousa-Nobre R. Franchi, S. Tardif, S. Lyonard, O. Raccurt ; LEPMI CNRS: C. Villevieille, ESRF : N. Blanc

The instrumented cells and reference cells are tested in charge and discharge at various rates (from 0.5 to 3 C and from 0.5 to 4 D). Surface temperature was monitored during the experiment with K-type thermocouples. The signal from sensors giving the internal temperature of the cells (OF LUM-T) and the electrochemistry potential of each electrode (RE) are also recorded.

Figure 74 and Figure 75 show two examples of results from this experiment.

During this experiment we have validated the following steps:

- The instrumentation of cells with 2 sensors (OF LUM-T and RE).
- The cell performance was not modified by the integration of the sensors.
- The setup for, data acquisition and real-time treatment is functional with these 2 sensors
- The measurement of the internal cell parameters with sensors (Temperature, Electrochemistry).
- The local impact of sensor on the cell functioning can be characterized with operando XRD measurements.

A lot of data was collected during the experiment. We are currently analysing the data to correlate the signals from sensors, XRD measurements and electrochemistry phenomena. We will also study the impact of sensors on the cell behaviour.

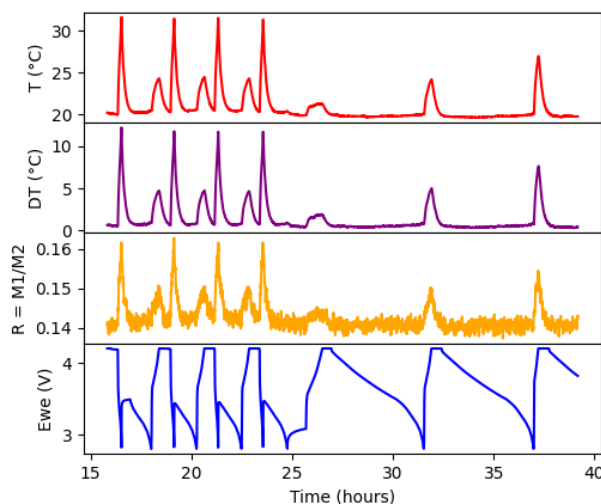


Figure 75: Response of the OF Lum-T sensor inside the cell over the time (orange) compared to the surface cell temperature (red), surface heating (purple) and cell potential (blue) during the 4D/1C and 0.5C,1C,2C/0.5D cycle.

This collective work between INSTABAT and BIGMAP and the results will be valorised through publications.

[Participation to the revision of the BATTERY2030+ roadmap](#)

From the beginning of INSTABAT project, Olivier RACCURT participates to the working group of BATTERY2030+ for the roadmap revision. During the years 2021 and beginning of the year 2022 several meetings driven by Jana Kumber (Battery2030+) were organized to discuss and revised the roadmap. The results of this meeting for roadmap revision were shared to the INSTABAT partners for comment and inputs.

Table 23. *List of deliverables WP7*

Deliverable Number	Deliverable Title	Lead beneficiary	Type	Dissemination level	Due date (in month)	Status
D7.1	Dissemination, Communication and Exploitation Plan	1- CEA	Report	Public	3	Submitted
D7.2	INSTABAT website	1- CEA	Other	Public	3	Submitted
D7.3	Data Management Plan	1- CEA	Report	Public	6	Submitted
D7.4	IPR survey and INSTABAT knowledge management strategy	2- BMW GROUP	Report	Confidential	18	Submitted
D7.5	Exploitation strategy	2- BMW GROUP	Report	Confidential	36	N/A
D7.6	Report on communication and dissemination activities - V1	1- CEA	Report	Public	12	Submitted
D7.7	Report on communication and dissemination activities -V2	1- CEA	Report	Public	24	N/A
D7.8	Report on communication and dissemination activities - V3	1- CEA	Report	Public	36	N/A



WP8 - Project Management

CEA, BMW GROUP, CNRS, FAURECIA, IFAG, INSA LYON, UAVR, VMI

Work package number	8	Leader	CEA							
Work package title	Project Management									
Participant number										
Short name of participant	BMW	VMI	CNRS	IFAG	FAURECIA	UAVR	INSA	CEA		
Person	months	per	0.5	0.5	0.5	0.5	0.5	0.5	7	
participant										
Start month	M1			End month			M36			

Objectives

The main objective of WP8 will be to adequately manage and coordinate the project. The WP will also be focused on executing the following specific objectives:

- monitor activities and ensure that the anticipated project outcomes will be in time and in line with the expected results;
- comply with the legal, contractual, financial and reporting requirements of H2020 and EC;
- organise and lead coordination meetings on a regular basis;
- adequately manage the funds of the partners.

Highlights of most significant results

The project management structures have been set-up and the cooperative work between partners work very well. The consortium working in close cooperation and the interaction between work packages are effective. Project is globally on track to achieve its goals within given contractual timeframe & budget.

The coordination of the project suffered from an overload of work for the coordinator (Maud Priour) due to the impact of COVID on CEA activities and the delay of several other projects. The priority has been made for the technical work and the coordination between partners. Nevertheless, this situation impacted the delivery of several management deliverables. Corrective action was taken by CEA to reinforce the coordination by appointing Olivier RACCURT as the new coordinator in February 2022, M. Priour becoming the new deputy coordinator. This action enabled the documents delivery before the date set for the mid-term review.

TASK 8.1. Project administration and management

(Leader: CEA; Participants: All) (M1-M36).

This task lead by CEA covers the activity of administration and management of the project. The description of the “Project Management Handbook” is given on the deliverable D8.1. CEA has also produced a gender equality plan detailed in the D8.2. The coordinator was organised the monthly meeting and general assembly to manage the progress of work. The management of the consortium agreement at the beginning of the project was made on time. During the first period the coordinator is the central contact point for all project partners and monitoring the action with a global view of the project.

To support the collaboration and communication between partners a working space (sharepoint) has been created. For the daily communication between INSTABAT partners and/or the project coordinator tools like email, phone, skype or teams are intensively used.

Monthly meeting with all WP leaders are organized to exchange together on the progress of each WP and coordinates the action. The information from Battery2030+ initiative was shared to the consortium by the coordinator during these meetings.

Online meeting are also organized on WP level by the WP leader.

Following Management Board & General Assembly meetings took place in Period M18:

- 1- Kick-off meeting 29/09/2020 and 02/10/2020 (online)
- 2- Kick-off meeting on Battery 2030+ initiative 14/10/2020 (online)
- 3- General assembly of Battery 2030+ initiative 07-08/10/2021 (online)
- 4- General assembly of INSTABAT: 23/11/2021 (Grenoble, France)

The coordination of the project suffered from an overload of work for the coordinator (Maud Priour) due to the impact of COVID on CEA activities and the delay of several other projects. The priority has been made for the technical work and the coordination between partners. Nevertheless, this situation impacted the delivery of several management deliverables. Corrective action was taken by CEA to reinforce the coordination by appointing Olivier RACCURT as the new coordinator in February 2022, M. Priour becoming the new deputy coordinator. This action enabled the documents delivery before the date set for the mid-term review.

TASK 8.2. Governing bodies meetings and interaction with the EC

(Leader: CEA; Participants: All) (M1-M36)

The project coordinator has been in close contact with the project officer and providing regular updates on the progress of the project via email or phone call. One of the first administrative action items at the beginning of the project was the preparation of the consortium agreement. The coordinator is responsible to the communication with the project officer and with the partners.

The coordinator was coordinated the whole process for collecting all information needed for the periodic report (technical and financial) in close cooperation with WP leaders.

The project coordinator also prepared the project review meeting which is planned on 20th April 2020 (online meeting) with the PO and the expert.

TASK 8.3. Risk management and contingency plan monitoring

(Leader: CEA; Participants: All) (M1-M36).

The list of risk was established at the beginning of the project and was based on initial risk determine during the proposal preparation (Table 24). This list was discussed during the monthly meeting and during the general assembly. At this time no new risk was identified from original list from the beginning of the project. The status of each risk was detailed in the (Table 24). Many of these risks have not been encountered or are not considered since they do not correspond to the current advancement of the project. From this list R1 related to the WP1 don't appear and the WP1 is now finished. The R1 is closed. The R2 related to WP2 not appear at this time. From WP2 only R3, R6, R7 and R8 was appear during the first phase of the project. We detail below each of this risk and the risk mitigation measure and results.

Table 24: Risk list, risk mitigation measure and status

Risk	DESCRIPTION OF RISK AND LEVEL OF LIKELIHOOD	WP	PROPOSED RISK-MITIGATION MEASURES	DID YOU APPLY THE RISK-MITIGATION MEASURED (YES/NO)	DID THE RISK MATERIALIZED? (YES/NO)	IF THE RISK-MITIGATION MEASURES COULDN'T BE APPLIED, PLEASE EXPLAIN WHY
R1	Requirements for integration of the multi-sensor platform are not well identified. / Low	WP1	Use partners' (VMI, CEA, and CNRS) valuable expertise on the integration of components such as sensors in the cells.	N/A	NO	Not applicable
R2	Some of the key parameters are not capable	WP2	Possible strategies are improving the sensor capabilities, exploring	N/A	NO	Not applicable

to be acquired through the sensors. / Medium

commercial solutions, tuning sensors to measure other parameters.

R3	Signal output from the sensor (any sensor) is too low for detecting key parameters. / Medium	WP2	Routes for amplifying the signal of the sensor will be considered, e.g. by increasing the size of the measurement probes, implementing a higher number of sensing points per probe or multiple sensing probes per sensor.	YES	YES	Not applicable
R4	Implementation of a sensor (any sensor) in a cell disrupt the cell functioning (accelerated degradation, lower performances, etc.). / Medium	WP2	Work towards further miniaturisation and reduction of chemical reactivity of components. Explore different positioning. Increase efforts on other sensor types.	(1)	(1)	(1)
R5	These risks apply to OF/FBG sensor 1. Short lifetime of sensor (fast degradation of polymer fiber). 2. Fibers fragility on handling could make cell assembling process too difficult. / High	WP2	1. Test different polymer materials. 2. Test different structuring strategies such as coating or reinforcement of the fibers.	(1)	(1)	(1)
R6	These risks apply to RE sensor 1. Coating of reference electrode degrades too fast to reach acceptable number of cycles. 2. Parameters signal not stable enough because of electro-chemical instability of the reference electrode material. / High	WP2	1. Manage the coating resistance by improving material stability and/or chemistry. 2. Improve in situ repair strategy and diagnostic by external electro-chemical methods.	YES	YES	Not applicable
R7	This risk applies to OF/Lum sensor Luminescent probes cannot be implemented or do not correctly detect the expected parameters. / High	WP2	Explore other luminescent molecules and deposition techniques; explore different strategies of probe positioning (surface, inside porous protective coating); manage and adapt probe	YES	YES	Not applicable



			chemistry to electrolyte species.			
R8	This risk applies to PA sensor 1. Sensing functionality of the CO ₂ sensor cannot be confirmed in the battery cell environment 2. Adaption to the battery cell environment of CO ₂ sensor cannot be fully implemented. / Medium	WP2	Explore other IR-absorbing gases. Increase efforts on other sensor types.	YES	YES	Not applicable
R9	Physico-chemical phenomena cannot be properly characterised by the mentioned characterisation techniques./Low	WP3	Use of other characterisation techniques not already described in the proposal.	(1)	(1)	(1)
R10	Physico-chemical phenomena cannot be properly correlated to any of the sensors' outputs./ Medium	WP3	Investigate if the physico-chemical phenomena can be indirectly deduced from another sensor output signal.	(1)	(1)	(1)
R11	Post-mortem analysis reveals a negative impact of the sensors on the cell degradation. / High	WP3	Improve integration of sensors and development of sensors materials and chemistry (retroaction on WP2 for sensor development).	(1)	(1)	(1)
R12	Low correlation between virtual sensors outputs and actual values./ Medium	WP3	Perform more validation against models and characterisation tests to improve the virtual sensors.	(1)	(1)	(1)
R13	Interplay between thermal dynamics and electro-chemical parameters might reduce reconstruction accuracy at some points in the battery./ Low	WP4	A modular approach is considered (not beginning with fully coupled dynamics between electro-chemical and thermal models).	(1)	(1)	(1)
R14	Spatially inhomogeneous behaviour may not improve quality of reconstruction when only extremely localised measurements are available./ Medium	WP4	FBG sensor adds previously unavailable information.	(1)	(1)	(1)
R15	Flat open-circuit potential curves and low-sensitivity of other outputs to variable	WP4	Data from reference electrode available, as well as measurements	(1)	(1)	(1)

	and parameter variation may have a negative impact on sensitivity of the algorithms to measurement and model uncertainties./ High		in the electrolyte coming from Li ⁺ concentration sensor.			
R16	Implementation of multiple sensors in a single cell disrupt the cell functioning (accelerated degradation, lower performances, etc.)./ High	WP5	Integrate sensors gradually. Discard defaulting sensor.	(1)	(1)	(1)

(1) Tasks are not sufficiently advanced, the risk could not appear and is not evaluated.

R3: Signal output from the sensor (any sensor) is too low for detecting key parameters.

This risk appeared during the work in WP2 for three sensors: OF/FBG, OF/Lum and PAS-CO₂. For each of these sensors the signal from the first version was too low to give the required accuracy. The mitigation procedure applied was to work on the technical aspect of the sensor to increase some of parameters and improve the sensitivity. In the case of OF/FBG sensors reflectivity had to be increased. For the OF/Lum the sensitivity was improve by study alternative optical probe and by improve the coating procedure on the fiber. For the PAS-CO₂ sensor technical improvement of the electronics was used to improve the sensitivity. The detection limited was reduce from 50 to 2 ppm. This improvement for the three sensors removes the risk and we can say the mitigation procedure gives effective results.

R6: These risks apply to RE sensor: low stability of RE material.

This risk appeared at the beginning of work with RE developed in the project with gold coating. The mitigation procedure was applied to identify a solution to protect this material or to change the composition of RE material. Finally, the solution to used LFP coating as reference electrode show a very good stability. The good results from stability test closed this risk and demonstrate the efficiency of the mitigation procedure.

R7: This risk applies to OF/Lum sensor- Luminescent probes cannot be implemented or do not correctly detect the expected parameters.

This risk appeared during the work on Li⁺ optical probe. Several molecules were studied to find the right candidate for Li⁺ detection and can be working into the electrolyte. The mitigation procedure was applied by study alternative way to find best optical probe. Based on a deeper study of the state of the art and with the expertise of CEA, a promising optical probe was synthesized and successfully tested in carbonate medium for lithium detection. These good results show that the mitigation procedure was efficient.

R8: This risk applies to PA sensor: Sensing functionality of the CO₂ sensor cannot be confirmed in the battery cell environment, Adaption to the battery cell environment of CO₂ sensor cannot be fully implemented.

This risk appeared during the WP2 work. The first test of PAS CO₂ sensor into pouch cell does not give conclusive results. The mitigation procedure was applied to understand the reason of this behaviour. It appears that the protocol used to integrate the sensor was not adapted to the sensor specificity. The protocol used damaged the sensor due to vacuum phase. Alternative way to integrate the sensors was propose and will be applied during the next phase of the project.



Table 25. *List of deliverables WP8*

Deliverable Number	Deliverable Title	Lead beneficiary	Type	Dissemination level	Due date (in month)	Status
D8.1	Project management Handbook	1-CEA	Report	Public	1	submitted
D8.2	Gender equality action plan	1-CEA	Report	Public	6	submitted
D8.3	Periodic report to the EC	1-CEA	Report	Public	20	submitted
D8.4	Periodic report to the EC	1-CEA	Report	Public	36	N/A

1.3 Impact

Back in 2017, the EC warned about the serious risk for Europe to become irreversibly dependent on battery cells imports, for the rollout of clean mobility, the industry and the stabilisation of power grids integrating high shares of variable renewable energy sources. According to the views of the European Battery Alliance (EBA), if Europe does not act fast, catching up with Asia will become impossible¹⁵. Just in the field of mobility, given the size of the EU automotive sector (13.3 million jobs, or 6.1% of the total workforce¹⁶) it is a strategic imperative to reach the EBA's target of 200 GWh/year manufacturing capacity by 2025. The EU could capture a battery market up to €250 billion per year from 2025 onwards to cover an estimated EU need of at least 10-20 Gigafactories. To reach this goal, the EU must bring innovative batteries to the market to attract potential end-users and make them adopt EU batteries. INSTABAT aims at bringing innovation to batteries by including a smart multi-sensor platform into the battery cell ("lab-on-a-cell"). This embedded platform will allow a more effective battery use and control over lifetime through high-accuracy SoX cell indicators. INSTABAT will also advance EU knowledge, by developing/adapting new sensors and reducing the current lack of knowledge about cell internal behaviour. This will prepare the grounds for a highly innovative new generation of batteries. In addition, by prolonging battery life and facilitating battery second life, INSTABAT will have a positive impact on costs and environmental aspects.

1.3.1 General impacts

INSTABAT will contribute to an improvement of performance and strongly force the development of sustainable battery storage solutions for Li-ion batteries at a more competitive price. The "lab-on-a-cell" approach will be used to develop a new generation of Li-ion and post-Li-ion batteries in the future, which is aligned with the objectives of the Work Programme¹⁷. Moreover, INSTABAT will contribute to a successful mass introduction of batteries for mobility, allowing for substantial improvements leading to an ultra-high performance. The INSTABAT project is also well aligned with the specific impacts set out in the call LC-BAT-13. The list of 6 general impacts of the project as described below

Impact 1: Increased quality, reliability and life (QRL) of the battery system by maximizing the performance and safety of the complete battery system over its lifetime, including forecasting the remaining lifetime under different use cases, especially the suitability for possible "second life" usage.

INSTABAT will allow maximising the QRL of Li-ion batteries via a substantial improvement of the monitoring of battery key parameters¹⁸ during operation. The consortium's ambition is to develop cell SoX indicators (States of Charge, Health, Power, Energy and Safety) with unprecedented accuracy. For this purpose, battery parameters will be monitored with high accuracy (temperature ($\leq 0.1^\circ\text{C}$), pressure ($\leq 0.03\text{ MPa}$), strain ($\leq 0.1\ \mu\epsilon$), Li^+ concentration ($\leq 0.1\text{ mmol/l}$) and CO_2 concentration ($\sim 10\%$)).

Obtaining accurate SoX cell indicators will allow for a more effective battery use and control over lifetime by means of (1) reducing battery safety margins, thus allowing less over design and less inefficient use of capacity; (2) increasing battery functional performance thanks to feedback loops from the BMS, based on the SoX indicators, adapting the management of the battery in real-time; (3) forecasting the evolution of SoX through time, including forecasting of the remaining lifetime of the battery; (4) providing triggers for battery self-healing or replacement of defective components; (5) recording data about the cell, granting more efficient second life usage. Therefore, better battery management and wiser use of the battery will be possible. The smart sensors integrated in the battery will act as tools to record the performance, ageing and safety of Li-ion batteries during operation by measuring precisely the degradation phenomena in the core of the cells.

¹⁵ <https://energypost.eu/the-european-battery-alliance-is-moving-up-a-gear/>

¹⁶ https://ec.europa.eu/growth/sectors/automotive_en

¹⁷ http://ec.europa.eu/research/participants/data/ref/h2020/wp/2018-2020/main/h2020-wp1820-cc-activities_en.pdf

¹⁸ Temperature and heat flow; pressure; strain; Li^+ concentration and distribution; CO_2 concentration; "absolute" impedance; potential; polarization

Better thermal management of batteries will be enabled by identifying critical zones for the appearance of hot spots thanks to thermal profiles recognition through multi-point and multi-layer monitoring.

The “second life” usage aspect will be ensured, based on a solid and structured lifetime characterisation and data logging. By continuously recording the information generated from the multi-sensor platform, a complete data logging covering the entire life of the battery will be created, granting a more efficient second life usage. The data generated from the battery first life will be key to determine its second life capabilities. In short, our foreseen ambition is to establish the health record of the battery, analogous to personal health records for human beings to estimate its degree of fatigue.

During INSTABAT project, focus will be made on two use cases: “High-power charging” and “Cycling at extreme conditions”. The expected results of these selected use cases for EV applications are to acquire high-power charging profiles and understand how they could be better adapted by monitoring the SoX in real-time. These profiles will consider extreme temperatures to take full advantage of the power and capacity of the cell without any degradation. Cycling at extreme temperatures will be similarly studied.

Impact 2: Assured best possible performance and lifecycle for a range of applied cell types at lowest cost

The extra cost of the sensors’ materials, assembly, integration and wiring will be compensated and even reduced by the increase of the total number of cycles (estimated increase of 20% over the battery lifecycle), which is linked to a slower ageing in fast charging (see KPI 13) and better recycling possibilities. In addition to all the improvements in terms of performance and lifecycle already explained in “Impact 1” above, the following aspects have to be considered:

- A more efficient use of the cell capacity will lead to a need for a lower total installed battery capacity to reach the same performance, which will contribute to decrease the cost of the battery.
- A safer use of batteries will contribute to decrease the hazards, e.g. associated with battery usage in EVs and energy storage system applications (thermal runaway, etc.). When a hazard takes place, the cell could be damaged, making the whole battery pack unusable. The costs for replacing battery packs being very high, it is expected that the end-users will consider paying for the “lab-on-a-cell” platform to reduce their exposure to those risks.
- An increase of the lifetime of batteries (due to a more efficient and safer use of batteries) could widen the potential for a second life usage, which means a reduction of the effective cost per cycle as well as a positive impact on environmental aspects.
- Real-time monitoring of key cell parameters with high time and spatial resolution will allow detecting sources of potential problems early on. This could act as a trigger for defective components replacement and self-healing, which would also contribute to increase battery life and thus, reduce its cost.
- The cost of the “lab-on-a-cell” platform could also significantly be reduced in the mid-term as it provides more validation datasets for the models (thanks to the data collected from the sensors). Higher-accuracy and precise models will reduce the need for physical sensors, which will also contribute to reduce the cost of the “lab-on-a-cell” platform.
- The application of the “lab-on-a-cell” will also be considered for different cell types in the techno-economic analysis conducted as part of Task 6.2.

Impact 3: Industrial opportunities for exploiting new concepts and technologies for integrating multifunctional sensor capabilities in the battery cells and for optimizing the performance of the complete battery systems

INSTABAT will advance EU knowledge by developing/adapting sensors, enabling in-cell sensing capabilities and reducing current lack of knowledge about internal cell behaviour. This will pave the way for a highly innovative new generation of batteries manufactured by the EU industry.

All the technologies developed during INSTABAT project will be validated at lab scale at the end of the project (at least TRL 3), with the aim of reaching a higher TRL when possible. After the project (INSTABAT-EXPANSION), the new technologies will be demonstrated at module and pack level, ensuring the scalability of manufacturing concepts to the features of large battery production lines (TRL 8-9). Some activities, such as new manufacturing processes, new machines and adapted cell and module set-up will be necessary, to ensure the market uptake of these technologies. Therefore, the demonstration at a TRL 8-9 of the technologies and results obtained in INSTABAT (physical sensors, virtual sensors, validated thermal and electro-chemical models, BMS algorithms, multi-sensor platform or “lab-on-a-cell”

approach) will allow generating business opportunities for the exploitation of the new concepts and technologies obtained as a result of this project:

- **Business opportunities for physical sensors manufacturing:** the partners involved in the sensor development will transmit the know-how to industrial partners in order to manufacture the sensors at a larger scale and study all their commercial applications such as: (1) their integration in INSTABAT multi-sensor platforms for mobility applications; (2) their use in other sectors where the safety aspect is important, such as the aeronautics and naval sectors where battery failure can lead to dramatic consequences (in this sense, a letter of interest has been signed by SAFRAN); (3) new applications needing further developments, e.g. adaptation to other cell chemistries and geometries or adaptation of sensors monitoring CO₂ to the monitoring of other gases;
- **Business opportunities for the “lab-on-a-cell” concept:** many battery manufacturers (VMI, who is an INSTABAT partner, but also Lithops and Leclanché who signed letters of interest for the project) would be interested in adopting new solutions for characterising new cell materials and formats, understanding the phenomena taking place at cell level and understanding the interaction between the cell components (anode, cathode, electrolyte, etc.). The lab-on-a-cell could indeed be used as a material characterisation platform. The knowledge obtained at cell level in terms of thermal and chemical behaviour could open the door to new cell designs and materials.
- **Business opportunities for battery manufacturers:** many battery manufacturers are interested in this project due to the improvement opportunities offered in terms of performance and safety of batteries. Indeed, the “lab-on-a-cell” approach would bring them an added value compared to the products offered by their competitors. In this project, the battery manufacturer partner (VMI) will focus on the battery requirements for the mobility applications. However, the multi-sensor platform concept could reach many other applications in the future: (1) aeronautics and naval sectors where safety aspects are critical; (2) stationary applications, such as renewable energy generation or energy storage solutions for industrial plants and household energy storage, where lifetime and performance are fundamental; (3) Industry 4.0., where a higher performance, increased efficiency and lifetime are needed.

INSTABAT will bring a technological competitive advantage to the EU battery industry and will open the door to an innovative new generation of batteries.

Impact 4: Better identification of defective cell components, allowing replacement of components or introduction of local targeted repair mechanisms, such as self-healing, in future cell design and chemistry generations.

INSTABAT “lab-on-a-cell” can also serve to identify defective components and local spots in the cell that would need repairing. The spatially and temporally resolved monitoring of cell key parameters and their correlation with the degradation phenomena will provide the BMS with a detailed knowledge of the cell so that it could trigger self-healing capabilities or predict the replacement of components if needed.

The sensing technologies developed in INSTABAT could allow to: (1) identify defective components that must be repaired; (2) develop mechanisms within the battery for the on-demand administration of molecules that can e.g. solubilize a resistive deposit such as Solid Electrolyte Interphase; (3) restore a faulty electrode within the battery. This constitutes a transformational change in battery science, as it supposes a great potential for developing supramolecular architectures, which could be physically or chemically cross-linked to heal the electro-chemically driven growth of cracks/fissures in electrode materials. An intimate synergy between intelligent BMS and self-healing capabilities will further secure success and enable EU to lead the world in sustainable technology development.

Collaboration with the LC-BAT-14 consortia on this topic will be fundamental for INSTABAT. The “lab-on-a-cell” approach is the first step towards our long-term ambitious vision of combining sensing and stimulus-driven self-healing functionalities within the cell for developing smart cells.

Impact 5: Improved knowledge on different factors (use patterns, ambient temperature etc.) impacting on battery performance and characteristics.

The INSTABAT “lab-on-a-cell” will allow to gather a vast knowledge on the thermal and physico-chemical degradation phenomena (SEI growth, dendritic formation, etc.) taking place at the cell level. The physical and virtual sensors to be developed in INSTABAT will bring in real-time data that today is not possible to collect. The monitoring of the evolution

of the cell key parameters will produce large amounts of data that will be correlated to battery cell degradation phenomena and that will be useful to study more in depth the impact of the use of the battery (cycling patterns, external temperature, etc.) on the battery performance and ageing.

Large amounts of data will be collected on Li-ion cells through the characterizations and the tests carried out for the two INSTABAT use cases. The data will be logged and made accessible to the research community. A large quantity of cells equipped with “lab-on-cell” will mean even more data available and will allow using statistical approaches e.g. to obtain a higher precision for calculating safety limits (higher accuracy for thermal runaway detection...).

Impact 6: Provide foundations for collecting large amounts of data that can be used for autonomous discovery of future battery chemistries and for development of advanced modelling approaches to improve current chemistries with a view of optimising cell performance for mobility applications (link with topic LC-BAT-6-2019)

As already mentioned previously, the “lab-on-a-cell” can also be used as an in operando characterisation platform for battery materials. INSTABAT physical and virtual sensors as well as models and BMS algorithms will be designed keeping in mind that they should be adaptable to other cell geometries and chemistries (for that matter, one test dedicated to another cell chemistry and a broader paper study will be conducted during the project).

Already in INSTABAT, large amounts of data will be collected on Li-ion cells through the characterisations and the tests carried out for the use cases. This data will be correlated with the physico-chemical degradation phenomena taking place in the cell. The INSTABAT consortium will share their battery key parameters datasets with the LC-BAT-6 and LC-BAT-12 consortia.

Further tests could provide even larger amounts of data from the heart of battery cells, to allow studying new materials and discovering new cell chemistries beyond Li-ion. In this way, INSTABAT aims at contributing to autonomous material findings and interphase engineering. This would also open the door to develop advanced modelling approaches to improve current chemistries, contributing to a future cell development for mobility applications, in line with the topic LC-BAT-6. The INSTABAT consortium will therefore collaborate with other consortia to provide the foundations for collecting large amounts of data to be used for autonomous discovery of advanced battery chemistries (LC-BAT-12) and for development of advanced modelling approaches to improve current chemistries (LC-BAT-6) with a view of optimizing the cell performance for mobility applications.

1.3.2 Impact on the project partners

The project creates a collaborative environment for consortium to accelerate the development of INSTABAT technologies. All the partners of the consortium will improve their own innovation capacities and will consolidate their positioning in the battery sector.

CEA

The outcomes of this project will contribute to explore new technologies (e.g. luminescence (OF/Lum)) and increase CEA know-how and knowledge in the following areas: reference electrode (RE), cell assembly and testing, battery modelling and BMS. This will allow CEA to increase their innovation capacity and consequently gain competitiveness to create more industrial partnerships. Thanks to this project, CEA will also be able to gain more visibility in the academic community, by publishing the obtained results at conferences or in scientific publications and to open the door to new projects (H2020 cooperations, etc.).

CNRS

The present project will help CNRS to create a vast knowledge about the characterisation of commercial battery cells, increasing their innovation capacity in cell design for future battery technologies. For CNRS, this project will also contribute to an increase of the understanding and control over batteries, ultimately contributing for extending the lifetime of such systems and enabling more reliable second life applications. The collaborative work developed under this project will also favour the development of a network of companies and research institutions engaged in technologies for instrumenting batteries.

INSA

INSA's participation to INSTABAT will contribute to develop the basis for future R&D in the area of electro-chemical model exploitation for advanced BMS with potential application to novel chemistries, increasing INSA's visibility in the field and allowing for its participation in new R&D projects. In addition, this project has financed a PhD position in Control Systems and allowed for further development of collaborations in the area of modelling and estimation for electrochemical energy storage systems.

UAVR

The INSTABAT project will allow UAVR to increase their innovation capacity by facilitating the creation of new partnerships in the future and opening the door to new research projects in the field of INSTABAT. The project will have a positive impact on UAVR's visibility, allowing an increase of their presence at conferences and other events. The collaborative work with relevant industrial partners will facilitate further research in the field of INSTABAT and produce innovative patents related to fiber sensing and battery virtual sensors, creating new market opportunities for industries. In addition, thanks to this project, UAVR will create 4 jobs (3 MSc and 1 PhD thesis in Physical Engineering program).

IFAG

For IFAG, the success of the INSTABAT project will open the access of its microelectronic and –mechanical technologies for CO2 sensing to the battery cell market. Furthermore, the partnership with BMW and VMI from previous collaborations will be strengthened, which will contribute to the growth of the company. With IFAG as WP leader and both, BMW and VMI, being responsible for the deliverables, the collaboration in WP1 provided an excellent opportunity to strengthen the partnership between these three companies. This encompassed in particular a better mutual understanding of the respective requirements and constraints.

FAURECIA

This project is well aligned with FAURECIA's goal to adopt "zero emission vehicles" mobility. Being one of the largest automotive equipment suppliers, FAURECIA is highly concerned by the batteries environmental performances at the lowest cost in order to offer their customers the most competitive products. This project will contribute to improve FAURECIA's innovation capacity.

BMW

This project will allow BMW to provide better battery packs to customers, at lower cost and with improved functionality, which will lead a stronger market position with increased sales. This effectively impacts a wide range of jobs at BMW, from worker level to highly skilled experts.

VMI

The outcome of INSTABAT will significantly support future material and cell development activities. Using these new methods, a considerable reduction in product development times is expected.

2 Update plan of the exploitation and dissemination results

The plan for exploitation and dissemination of results as described in the DoA and detailed in the D7.1 is still relevant.

3 Update of data management plan

The data management as described in the deliverable D7.3. For the period cover by this report, no modification of the data management plan is required.

4 Fellow-up of recommendations and comments from previous review(s)

The deviation of annexe for uses resources are explain for each partners in paragraph 5.2

5 Deviation from Annex 1 and Annex 2

Overall, INSTABAT is on track and there are no deviations from the DoA with important consequences. It is expected that the INSTABAT project will be completed within the scheduled timeframe, reaching the initially set objectives, without requiring more than the allocated resources.

Regarding the identified implementation risks, status and corrective actions are reported in the Task8.3 of this report and in the critical risks section of the Participant Portal.

In the next part, more details are given on deviations at the level of Tasks and at the level of Resources. For all information related to Resources, see **Appendix 1 “Periodic Financial Report”**.

5.1 Tasks

Partners	Task	Deviation explanation	Impact on other tasks, on the available resources and the planning
CEA	WP8, WP7	Internal difficulties at CEA was impact the coordination of the project. The impact of COVID on the global activities of CEA and the charge from others project to the coordinator (Maud Priour) was impact the work in WP8 and induce delay on the delivery of numbers of Deliverables in WP8 and WP7.	The impact of this deviation was essentially on the WP8 and in a little bit on the WP7 activities. This lake of resources for coordination impact the following and deliverance of a number of deliverable of the project (see Table 26). The change of coordinator by CEA in February 2022 made it possible to catch up and provide all the deliverables for the midterm review.
CEA, CNRS, UAVR, IFAG	WP2	The development of sensors and they adaptation to the cell environment taking more time than initial planning (OF-Lum, OF-Li and PASCO2).	This deviation of the planning impact the WP3 for the implementation of sensors in cells for ageing study and correlation between sensors signal and degradation mechanisms.
CEA, CNRS, UAVR	WP3	Due to the time shift on the development of sensors the ageing campaign on instrumented cell was shifted in the planning	This deviation will be impact the WP4 and the WP5 for validation of the ageing model, the development of virtual sensors and the development of SOx (WP4 and WP5). This deviation is not critical at this time due to the recent results on the development of sensors and the validation of the multiplatform in WP5 (see results from WP3, WP5 and the collaboration work with BIGMAP project: ESRF experiment)
All	WP5	From the first considerations on the multi-sensor platform, we quickly realized that it would be challenging to interface sensors and algorithms with a rapid prototyping platform. It's absolutely necessary to choose a target with a wide variety of physical and communication I/O to interface sensors but also without strong memory or computation resource limitations to interface all processing blocks. Consequently, we decided to base our platform on a flexible, reconfigurable and high performance target hardware such as an instrumentation computer. This architecture is more in line with the level of maturity of the sensors and	It's noteworthy that WP5 advanced faster than expected on the proposal planning. The multi-sensor platform validated functional blocks developed for the WP5 have already been used during the experiments at the ESRF and to obtain results for the WP2 and WP3.

		<p>algorithms developed within the framework of INSTABAT, whose primary objective is to demonstrate the relevance of these technologies rather than their integrability. All the partners have validated the changes compared to initial proposal. There is no impact on the distribution of resources allocated to the WP5.</p>	
--	--	--	--

Table 26: List of deliverable already delivery with due date, delivery date and delay

Deliverable	WP	Due date	Delivery date	Delay (J)
D1.1	1	31/01/21	12/03/21	40
D1.2	1	28/02/21	12/03/21	12
D2.1	2	30/11/20	04/01/21	35
D2.2	2	31/08/21	30/08/21	-1
D2.3	2	30/11/21	20/01/22	51
D4.1	4	31/08/21	30/08/21	-1
D4.2	4	28/02/22	28/02/22	0
D4.3	4	28/02/22	28/02/22	0
D4.4	4	28/02/22	02/03/22	2
D7.1	7	30/11/20	22/03/22	477
D7.2	7	30/11/20	11/02/22	438
D7.3	7	28/02/21	11/02/22	348
D7.4	7	28/02/22	14/03/22	14
D7.6	7	31/08/21	31/03/22	212
D8.1	8	30/09/20	06/04/22	553
D8.2	8	28/02/21	11/02/22	348

5.2 Use resources

The paragraph below gives the explanation about the deviation of use resources for each partners.

5.2.1 CEA

EC comment:

For CEA: Total costs: budgeted € 575.128,13; claimed in this period € 458.025,76. Deviation -20.36%. Effort in person-months: budgeted PM 51,46 ; claimed in this period PM 35,92. Deviation -30.20%. Please explain.

Justification:

Sensors development in the WP2 took more time than initial planed. The consequence is a shift in the planning for the WP2 and WP3 task. Task dedicated to the integration of sensor in cells and test campaign was shifted and explain the deviation of the budget and person-month at lower value.

5.2.2 BMW GROUP

EC comment:

For BMW: Total costs: budgeted € 98.943,13; claimed in this period € 127.407,83. Deviation +28.77%. Please explain.

Justification:

BMW's project contribution within the duration of project is not distributed linearly between all funding periods/quarters.

Therefore, a cost overrun (here: +28.77%) within one funding period may occur.

The duration of WP1 „Definition of requirements“ according to the description within GA lasted 6 months (from PM 01 to) PM 06.

As described within BMW's part of the proposal, the main part of the BMW contribution for Project INSTABAT takes place in WP1 (6.0 PM out of 11.1 PM in total = 54,0% of contribution).

Therefore, the amount of € 100.225,88 out of the total of € 127.407,83 for Period 1 are the costs for WP 1 (claimed effort: 6,5 PM).

The difference of € 27.181,95 (= 27,8 % of the remaining project budget of € 97.660,38) is claimed for contributions to WP 7 (1,28 PM) and WP 8 (0,46 PM).

5.2.3 CNRS

EC comment:

For CNRS: Total costs: budgeted € 263.786,88; claimed in this period € 115.626,15. Deviation -56.17%. Effort in person-months: budgeted PM 39,36; claimed in this period PM 20,88. Deviation -46.95%. Please explain.

Justification:

Owing to the pandemic, decision was made to postpone by few months the hiring of Dr. Fu Lui knowing that he was the best candidate for this position with a very strong background in handling optical fibers as well as the physics of optical signal associated with these sensors. This delay thus led to some delay in buying consumables. Finally, and again owing to the pandemic situation, most of the meetings were held virtually, and thus the money previously budgeted for missions was not used as planned.

5.2.4 IFAG

EC comment:

For IFAG:

1. There are personnel costs declared as unit costs, which were not foreseen in the budget. This should have been put under deviations in the Periodic Report. Please explain the reason of this transfer.
2. Average personnel costs: budgeted € 11.061,00; claimed in this period € 6.010,66. Deviation -45.66%. Please explain.

3. Please also provide details about external colleagues reported under other direct costs. Anyway, these costs were not foreseen as other direct costs in Annex 1. Therefore please correct the Use of Resources.

Justification:

1. It was our mistake having applied the personnel cost with category a) as actual personnel cost, IFAG uses average hourly rate for personnel cost calculation, the right category should be b) as unit personnel cost. According to Annotated Grant Agreement for cost transfer between category a) and b) there is no amendment required, but if it's wished then we can change the cost category within next amendment run.
2. We have planned the personnel cost of internal and external employees both as personnel cost, total Plan PMs were also for internal and external colleagues. But in last EU audit in 2021 we learned from the EU auditor that the cost for external colleagues in our case should be reported with category other direct cost for service. Therefore, in financial statement we separated the personnel cost for internal and external colleagues in two cost categories, I decided to report also actual PMs for external colleagues in financial statement, as their PMs are also in the Plan PMs. Therefore, the actual average personnel cost in comparison to plan average personnel cost should be calculated in this way: The sum of actual personnel cost and other direct cost /actual PMs
 → Average personnel costs: budgeted € 11.061,00; claimed in this period € 10.447,54; Deviation is 5% not 45%.

Cost for external colleagues was foreseen as personnel cost in Annex 1, if it's required we can divide the budget of personnel cost into two cost categories.

5.2.5 FAURECIA

EC comment:

- for FAURECIA: Total costs: budgeted € 46.500,00; claimed in this period € 12.500,00. Deviation - 73,12%. Effort in person-months: budgeted PM 3,18; claimed in this period PM 0,80. Deviation - 74.84%.
- for Faurecia Ger (Third party of beneficiary FAURECIA): There are personnel costs declared as unit costs, which were not foreseen in the budget. This should have been put under deviations in the Periodic Report. Please explain the reason of this transfer. Total costs: budgeted € 69.750,00; claimed in this period € 20.132,08. Deviation -71,14%. Effort in person-months: budgeted PM 1; claimed in this period PM 1,22. Deviation +22.00%.

Justification:

1. Faurecia's contribution within the duration of the project is not distributed linearly between all funding periods. Therefore, the deviations of -74.84% for Faurecia and -71,14% for Faurecia Ger were occurred.
 - a. As it is described within INSTABAT proposal, the main part of the Faurecia contribution for INSTABAT project takes place in WP6 and WP6 will start on the third year of the project which has a total effort in person-months as 6 PM (out total of 14 PM for Faurecia).

- b. Like WP6, our main contribution for WP5 will also start only on second half of the project which corresponds to 1.5PM for 14 PM (Currently, we used only 0.05 PM for the meetings we have attended for WP5).
- c. We have used the budget for following work packages.
 - i. 0.5 PM for WP1 (out of 0.5 PM) which has been finished after first 6 months of the project.
 - ii. 1.2 PM for WP4 (out of 5 PM): 1.2 PM was used to give the first version of the 3D thermal model and the rest of the budget will be used to give a final version of the 3D thermal model.
 - iii. 0.17 PM for WP8 (out of 0.5 PM): The project will require more program management from Faurecia side, when the workload is higher on second half of the project.
 - iv. 0.10 PM for WP7 (out of 0.5 PM): Similar to WP8, we will require more budget for second half of the project for dissemination, communication and exploitation of the data that we will produce within INSTABAT project.

Since our workload will be higher on the second half of the project, we believe the deviations are normal for each work package.

2. Faurecia and Faurecia Ger use average hourly rate for personnel cost calculation, so the right category should be b) as unit personnel cost. We apologize for our mistake having applied for the personnel cost with the category a).
3. The team of Faurecia for INSTABAT project has changed after INSTABAT proposal submission. During the proposal stage, we have defined Faurecia France taken the management and main workload of this project, however after the proposal, it was decided to give more workload and management of the INSTABAT to Faurecia Ger (third party of beneficiary Faurecia). Due to this reason, the effort in person-months for Faurecia Ger (third party of beneficiary Faurecia) is higher than Faurecia.

5.2.6 INSA LYON

EC comment:

For INSA LYON: Total costs: budgeted € 142.961,88; claimed in this period € 88.785,58. Deviation -37.90%. Average personnel costs: budgeted € 5.079,00; claimed in this period € 3.317,53. Deviation -34.68%. Please explain.

Justification:

The average PM cost of € 5.079,00, given in the initial budget, was calculated based on the salaries of senior researchers and junior researchers, and on an estimation of time for each person. During this first period, most activities have been carried out by the junior researcher (PhD employed to work in the action), who has declared 17 PM on a total of 20.96 PM.

Mian Asif, the junior researcher, has worked on the development of a reduced-order electrochemical model for state-estimation of the battery; as such, the code development and testing process has been carried out in a large percentage by him.

As the salary of the junior researcher is lower than the cost of senior researchers, the declared average personnel cost of this first period is lower than € 5.079,00. This could also explain that the personnel costs we are claiming for this mid-term reporting is lower than half of the personnel budget.

The activities in the second half of the project will concern the fine-tuning of the developed state estimators to obtain the required performances for the specific cell chemistry used in the INSTABAT project. This will undoubtedly require more work by more senior researchers in order to explore new optimized strategies applied to the model and prepare publication of novel results.

Moreover, claimed costs for “other direct costs” are lower than initially planned for two reasons: Due to COVID context, it was not possible to travel. As a consequence, we only declared € 1 493,00 while we initially budgeted € 14 500 for travels.

The budget foreseen to buy consumables will only be used in the second period of the project. The budget for consumables will help with the validation of the real-time code using a small microcontroller to test the required computational capabilities in order to illustrate the tradeoff between accuracy of state reconstruction and computational cost of the developed estimators. This cannot be carried out before the production of a code-generation ready version of the code, which will be done in parallel with the demonstrator development by CEA in the second half of the project.

5.2.7 UAVR

EC comment:

Effort in person-months: budgeted PM 37,42 ; claimed in this period PM 17,21. Deviation -54,01%. Average personnel costs: budgeted € 3.115,00; claimed in this period € 4.635,90. Deviation +48.83%. Please explain.

Justification:

"The deviations of -54.01 % in Person-Months were due to delays that could not be avoided in the signings of the contracts of Post-Doc and PhD student. The processes, in COVID19 context, took much longer than expected and required a higher effort of the Senior Researcher, originating a deviation of +48.83% in average personnel costs during reported period. In any case, in the end of the project, no significant deviations are expected in total number of person months and personnel costs".